APPLICATION OF PHOSPHORUS LIGANDS IN RHODIUM-CATALYZED ASYMMETRIC HYDROFORMYLATION AND HYDROGENATION

By

RENCHANG TAN

A dissertation submitted to the

Graduate School-New Brunswick

Rutgers, The State University of New Jersey

In Partial Fulfillment of the Requirements

For the degree of

Doctor of Philosophy

Graduate Program in Chemistry and Chemical Biology

Written under the direction of

Professor Xumu Zhang

And approved by

_____

_____

_____

_____

New Brunswick, New Jersey

May, 2017

ABSTRACT OF THE DISSERTATION

APPLICATION OF PHOSPHORUS LIGANDS IN RHODIUM-CATALYZED ASYMMETRIC HYDROFORMYLATION AND HYDROGENATION

By RENCHANG TAN

Dissertation Director:

Professor Xumu Zhang

Asymmetric catalysis has been playing an important role in modern synthetic chemistry. In the past decades, chiral ligands especially phosphorus chiral ligands, have demonstrated their power in transition metal catalyzed asymmetric reactions. New chiral ligands with high efficiency, selectivity and generality are always the key for the campaign of asymmetric reactions. In this dissertation, we will focus on design of new chiral phosphorus ligands and their applications in rhodium-catalyzed asymmetric hydrogenation and hydroformytation.

In chapter 1, the air stable bisphosphole BIBOP ligand was applied in asymmetric hydroformylation, the new rhodium based catalytic system was demonstrated to be very effective for vinyl acetate, allyl alkenes and styrene

derivatives. A new synthetic route for a chiral δ-lactone via asymmetric hydroformylation was established. Computational studies were conducted for a deeper insight of the reaction mechanism.

In chapter 2, a ligand library was screened for achieving rhodium catalyzed asymmetric hydroformylation of challenging 1,1-disubstituted alkenes. The BIBOP ligand successfully hydroformylated 1-(trifluoromethyl)-ethenyl acetate into a very useful precursor for drug synthesis, with good enantioselectivity. A branched product favoring approach was discovered for hydroformylation of *α*-(trifluoromethyl) styrene. Up to 68% ee was achieved with DuanPhos .

Chapter 3 discussed the application of a novel cooperative catalyst system in asymmetric hydrogenation. Indole derivatives were hydrogenated via hydrogen bonding, with excellent enantioselectivity. The mechanistic studies supported a proton mediated tautormerization-hydrogenation sequence. Dimerization of ZhaoPhos was proposed for explaining the observed nonlinear effect.

ACKNOLEDGEMENTS

I express my sincere gratitude to my supervisor, Professor Xumu Zhang, for his encouragement, guidance, advices, valuable comments and support during my graduate research career. His deep understanding of organometallic and organic chemistry and passion towards chemistry research have inspired us to come out with many interesting ideas. Besides chemistry, his always optimistic attitude is another valuable treasure I learn from him. It will keep guiding me to overcome any challenges in the future.

I wish to thank my committee members, Professor Alan Goldman, Professor Leslie Jimenez, Professor Kai Hultzsch and Professor Longqin Hu for their time and valuable discussions.

I want to thank Dr. Qingyang Zhao and Dr. Kexuan Huang for their help and guidance when I joined the Zhang group at Rutgers more than 4 years ago. I want to thank Dr. Shaodong Liu and Dr. Jialin Wen for countless exciting discussions about chemistry we had together, also Jialin and I composed chapter 3 together. I would like to thank Dr. Chris H. Senanayake and Dr. Bo Qu from Boehringer Ingelheim for offering the cooperation and summer intern opportunities. I wouldn't be able to finish works in chapter 1 and 2 without their helpful suggestions. I want to thank all other former and current group members in the Zhang group for their help and great suggestions in the past five years, including Dr. Xin Zheng, Dr. Tanglin Liu, Dr. Shengkun Li, Mr. Bin Qian, Dr. Lin Yao, Mr. Yang Hu, Mr. Jun Jiang, Dr. Hao Xu, Dr. Hongfei Lu and

Dr. Tao Zhang. I would also like to thank undergraduate students Mr. James Liu and Mr. Kenneth Jenkins for sharing some wonderful time doing research on Chemistry.

Last and most importantly, I want to dedicate this dissertation to my parents Lianhui Tan, Zhenxiang Zhou, and my wife Yanru Yu. Their endless love has always been the solidest support for me to overcome challenges I encountered during my journey of doctoral research.

Table of Contents

Abstract ii

Acknowledgments iv

List of Tables ix

List of Figures x

1. Application of BIBOP Ligands in Rhodium-Catalyzed Asymmetric Hydroformylation 1

1.1. Introduction 1

1.2. Synthesis of BIBOP ligands and their applications in asymmetric hydrogenation 6

1.3. Application of BIBOP ligands in asymmetric hydroformylation 10

1.3.1. Asymmetric hydroformylation of vinyl acetate derivatives with BIBOP ligands 10

1.3.2. Asymmetric hydroformylation of allylic substrates with BIBOP ligands 15

1.3.3. Asymmetric hydroformylation of styrene substrates with BIBOP ligands 18

1.3.4. Synthesis of chiral lactone via AHF of styrene derivatives 20

1.4. Conclusion 21

1.5. Experiment Section. 22

1.5.1. General remarks. 22

1.5.2. General procedure for the preparation of amide substrates. 22

1.5.3. General procedure for the asymmetric hydroformylation. . . 23

1.5.4. GC and HPLC analysis of the chiral aldehydes. 26

1.5.5. ^{1}H NMR spectra of crude AHF reaction mixtures. 40

1.6. References. 48

2. **Asymmetric Hydroformylation of 1,1-Disubstituted Alkenes**. 50

2.1. Introduction. 50

2.2. Asymmetric hydroformylation of 1-(trifluoromethyl)-ethenyl acetate. 55

2.3. Asymmetric hydroformylation of α-(trifluoromethyl) styrene. 58

2.4. Conclusion 62

2.5. Experiment Section. 62

2.5.1. General remarks. 62

2.5.2. General Procedure for the Asymmetric Hydroformylation. 63

2.5.3. GC and HPLC analysis of the chiral aldehydes. 63

2.5.4. ^{1}H NMR spectra of crude AHF reaction mixtures. 64

2.6. Reference 66

3. **Rhodium-Catalyzed Asymmetric Hydrogenation of Indoles via Anion Binding** 68

3.1. Introduction 68

3.2. Asymmetric hydrogenation of indoles with ZhaoPhos 75

3.3. Mechanistic study 83

3.4. Nonlinear effect 86

3.5. Conclusion 89

3.6. Experiment Section 90

3.6.1. Synthesis of indole substrates 90

3.6.2. General procedure for asymmetric hydrogenation of indoles 92

3.6.3. Deuterium labeling experiments 93

3.6.4. Characterization data for chiral indolines 94

3.7. References 110

List of Tables

1.1. AHF screening of vinyl acetate. 12

1.2. AHF of vinyl acetate derivatives. 13

1.3. AHF of the allylic substrates. 16

2.1. Ligand screening for AHF of 1-(trifluoromethyl)-ethenyl acetate. 56

2.2. Ligand/Rh ratio screening for AHF of 1-(trifluoromethyl)-ethenyl acetate. 57

3.1. Condition optimization for 2-methylindole. 76

3.2 Brønsted acid screening for 2,3-disustituted indole. 77

3.3. Substrate scope for asymmetric hydrogenation of indol. 82

3.4. Control experiments and ligand evaluation. 84

3.5. Counterion effect. 85

3.6. Nonlinear effect for asymmetric hydrogenation of indole. 86

List of Figures

1.1. General reaction equation for hydroformylation. 2

1.2. Current mechanistic description for the rhodium-catalyzed hydroformylation of alkenes. 3

1.3. Transformations of chiral aldehydes. 4

1.4. Chiral phosphorus ligands for asymmetric hydroformylation. 5

1.5. Application of DuanPhos in asymmetric hydroformylation of 1,1-disubstituted olefin. 7

1.6. Synthesis of Chiral 3-tert-Butyl-2,3-dihydrobenzo[d][1,3]oxaphosphol-4-ol Oxide ((R)-12). 8

1.7. Syntheses of BIBOP Ligands. 9

1.8. Asymmetric hydrogenation with Rh-BIBOP complex. 10

1.9. BIBOP ligands for asymmetric hydroformylation. 11

1.10. DFT (UB3LYP/LanL2DZ for Rh; UB3LYP-gCP-D3/6-31G(d) for all other atoms) calculated transition state for the Rh-hydride olefin insertion and stereochemical model. 15

1.11. AHF of the simple styrene. 18

1.12. AHF of the styrene derivatives. 19

1.13. Synthesis of chiral δ-lactone via AHF. 20

1.14. Synthesis of amide substrates. 21

2.1. Asymmetric hydroformylation of 1,1-disubstituted alkenes. 51

2.2. Asymmetric hydroformylation of N-(1-alkyl)vinyl phthalimide. 47

2.3. Asymmetric hydroformylation of α-alkylacrylates and potential applications. 53

2.4. Asymmetric hydroformylation of 1-(trifluoromethyl)-ethenyl acetate and example application. 54

2.5. Asymmetric hydroformylation of 1,1-disubstituted allylphthalimides and potential applications. 55

2.6. Asymmetric hydroformylation of 1,3-dichloro-5-(3,3,3-trifluoroprop-1-en-2-yl)benzene. 59

2.7 Ligand screening for asymmetric hydroformylation of α-(trifluoromethyl) styrene. 59

2.8. Linear aldehyde favored ligands for AHF of α-(trifluoromethyl) styrene. 60

2.9 Branched aldehyde favored ligands for AHF of α-(trifluoromethyl) styrene. 62

3.1. A novel thiourea-bisphosphine ligand: strategy of hydrogen bonding and cooperative catalysis. 69

3.2. Synthetic route for ZhaoPhos. 70

3.3. Asymmetric hydrogenation of nitroalkenes with ZhaoPhos. 71

3.4. Chiral Brønsted acid catalysis versus thiourea anion binding with simple Brønsted acid. 72

3.5. Asymmetric hydrogenation of unprotected indole. 73

3.6. ZhaoPhos and cooperative catalysis of transition metal, Brønsted acid and thiourea anion binding. 74

3.7. Leveling effect of HCl in solutions. 79

3.8. Origin of stereoselectivity in the hydrogenation of disubstituted indoles. 81

3.9. Deuterium labeling experiments. 86

3.10 Equilibrium scheme for nonlinear effect. 89

Chapter 1

Application of BIBOP Ligands in Rhodium-Catalyzed Asymmetric Hydroformylation

1.1 Introduction

Hydroformylation was accidently discovered by Roelen in 1938,[1] during his investigations of Fischer–Tropsch process using cobalt catalyst, which is also called 'oxo process'. It has become one of the largest homogenous catalytic processes in industry. Today, over 10 million tons of oxo products are produced per year worldwide. As a metal-mediated process, Cobalt catalysts dominated in the early age, despite their low reactivity and harsh reaction condition. In 1968,[2] Wilkinson and co-workers reported the first rhodium-catalyzed hydroformylation, they demonstrated the much higher reactivity and milder condition with phosphine binded Rh complexes comparing to those with cobalt catalysts. Ever since then, other metals (Ir, Ru, Fe etc.) have been widely studied for hydroformylation. The following series of the activities of the unmodified metal is generally accepted:[3]

Rh >> Co > Ir, Ru > Os > Pt > Pd >> Fe > Ni

Due to the major advantages of Rh complexes in hydroformylation, regarding reactivity and condition, Rh quickly dominates the area, by 1995, ~80% of hydroformylation was conducted with rhodium.[4]

Hydroformylation of alkenes normally generates a mixture of branched and linear aldehyde products (Figure 1.1). Experimental results imply that ligand properties play a pivotal role in the regioselectivity during the formation of aldehydes.

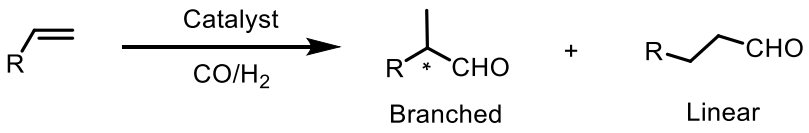

Figure 1.1 General reaction equation for hydroformylation

In the early 1960s Breslow and Heck were the first to propose a mechanism for the cobalt-catalyzed hydroformylation.[5] The so-called *dissociative mechanism* is widely accepted and is applied with little modifications also to the phosphine and phosphite modified rhodium-catalyzed hydroformylation (Figure1.2).[6] Thus, starting from different Rh(I)-sources under syngas pressure and in the presence of donor ligands L such as phosphines, phosphites or carbon monoxide, trigonal bipyramidal complex **A** is formed (18 valence electron species) as a key intermediate. Dissociation of one ligand L from this complex generates the coordinatively unsaturated and hence, catalytically active 16 valence electron species **B**. The main catalyst cycle starts with the coordination of alkene preferably in the equatorial position thus furnishing trigonal bipyramidal hydrido olefin complex **C**. Alkene insertion into the Rh-H bond (*hydrometallation*) takes place to form isomeric tetragonal alkyl rhodium complexes **D** and **E**. Subsequent coordination of carbon monoxide (IV) yields trigonal bipyramidal complexes **F** and **G**, respectively.

Migratory insertion of the alkyl group to one of the coordinated carbon monoxide ligands generates tetragonal acyl complexes **H** and **I**. Oxidative addition of molecular hydrogen forms tetragonal bipyramidal rhodium(II) complexes **J** and **K**. Subsequent reductive elimination liberates the isomeric linear and branched aldehydes and regenerates the catalytically active species **B** (**Figure 1.2**)

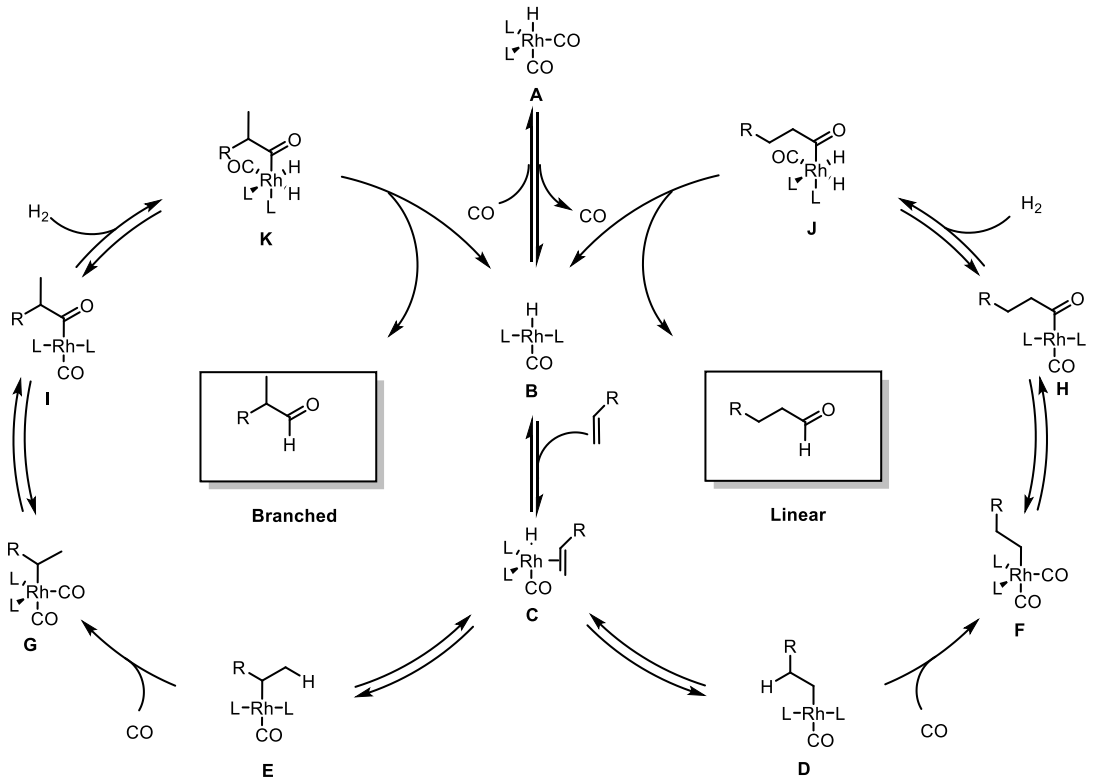

Figure 1.2 Current mechanistic description for the rhodium-catalyzed hydroformylation of alkenes

Kinetic studies of the unmodified rhodium catalyst suggest that, the oxidative addition of dihydrogen is the rate determining step for linear alkenes.[7] This is in accord with computational studies for the unmodified cobalt catalyst[8] as well as for a $[HRh(CO)_2(PH_3)_2]$ catalyst system.[9] However, kinetic

studies of the triphenylphosphine modified rhodium catalyst indicate that even for sterically less demanding alkenes, the rate determining step is early in the catalytic cycle, may be either the alkene addition or insertion step.

Asymmetric hydroformylation is most efficient and direct approach for constructing chiral aldehydes.[10] Chiral aldehydes are important building blocks for modern organic synthesis, which can be easily transform into chiral amines, alcohol, carboxylic acid, alkenes etc (Figure 1.3).

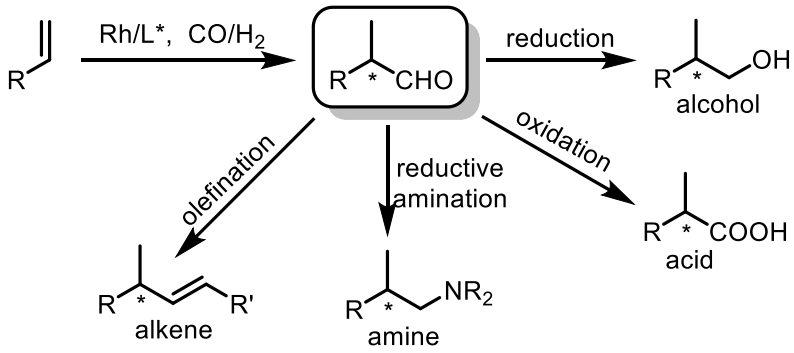

Figure 1.3 Transformations of chiral aldehydes

In contrast to the finely developed linear selective hydroformylation reaction, the asymmetric hydroformylation has not been studied extensively until the early 1990's. Asymmetric hydroformylation suffers from the difficulty of controlling chemoselectivity (hydroformylation, hydrogenation and isomerization), resioselectivity (branched and linear) and enantioselectivity (ee value), whittling its potential in industry application. Thus far, only a few of the chiral phosphorus ligands have been applied to asymmetric hydroformylation with decent results (Figure 1.4).

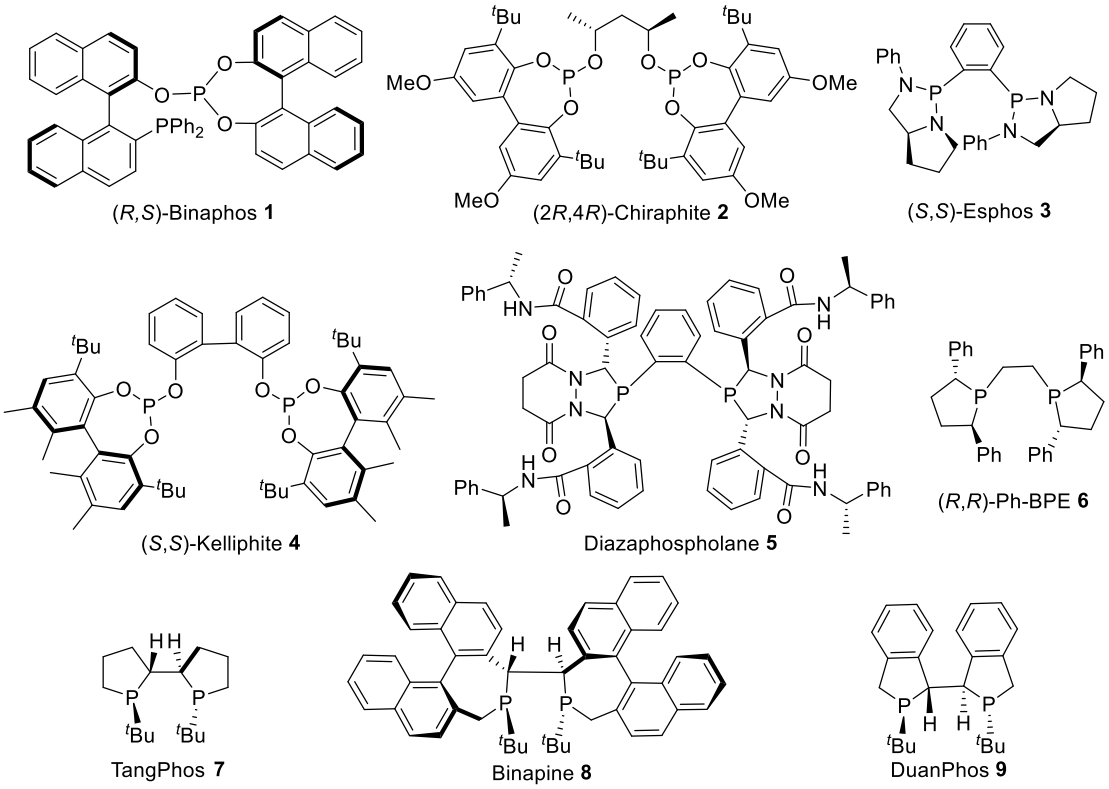

Figure 1.4 Chiral phosphorus ligands for asymmetric hydroformylation

In 1997, Takaya and coworkers reported the milestone chiral phosphine-phosphite ligand (*R*,*S*)-Binaphos **1** for highly efficient and enantioselective asymmetric hydroformylation, which is capable to hydroformylate styrene derivatives, ethyl acetate and allyl cyanide when combined with rhodium complexes, with moderate to good regioselectivity favoring branched aldehyde products, and good to excellent enantioselectivity.[11] Meanwhile, Babin and Whiteker at Union Carbide reported the so called Chiraphite **2**, this ligand was prepared from a chiral (2R,4R)-pentane-2, 4-diol backbone. It was the first successful diphosphite

ligand that achieved over 90 % ee in the asymmetric hydroformylation of styrene under mild reaction conditions.[12] In 2000, Esphos **3** and related ligands were developed by Wills and co-workers and successfully tested for asymmetric hydroformylation of vinyl acetate.[13] In 2004, Klosin and co-workers at Dow Chemical reported a diphosphite ligand, known as Kelliphite **7**,[14] with a non-chiral 2,2-biphenol backbone and chiral phosphite moieties, for asymmetric hydroformylation. Significantly enhanced efficiency for the asymmetric hydroformylation of a wide range of substrates was achieved with a series of bisphospholane ligands discovered by Dow Chemical group in cooperation with Landis's group in 2005. In particular Diazaphospholane **5** and its enantiomer, belonging to a family of ligands called BDP, is now one of the most efficient chiral ligands for hydroformylation of ethyl acetate, styrene and allyl cyanide.[15]

Interestingly, (*R,R*)-Ph-BPE **6**, which an excellent ligand for asymmetric hydrogenation of various substrates, performs very decently in asymmetric hydrogenation as well,[16] implying potential applications of chiral ligands for hydrogenation in the more challenging area of asymmetric hydroformylation. Indeed, Huang and coworkers from Amgen had proved that TangPhos **7** (developed by our group for asymmetric hydrogenation) can hydroformylate cyclic alkenes with over 90% ee, which was better than the famous Binaphos.[17] Binapine **8** was found to be having moderated reactivity and excellent enantioselectivity in hydroformylation of the three classic types of

alkene substrates.[18] Recently, Buchwald group has successfully applied other famous ligands for hydrogenation DuanPhos **9** in the hydroformylation of a challenging 1,1-disubstituted olefin, in which the precursor of an important building block for many active pharmaceutical ingredients 2-trifluoromethyllactic acid was obtained (Figure 1.5).[19]

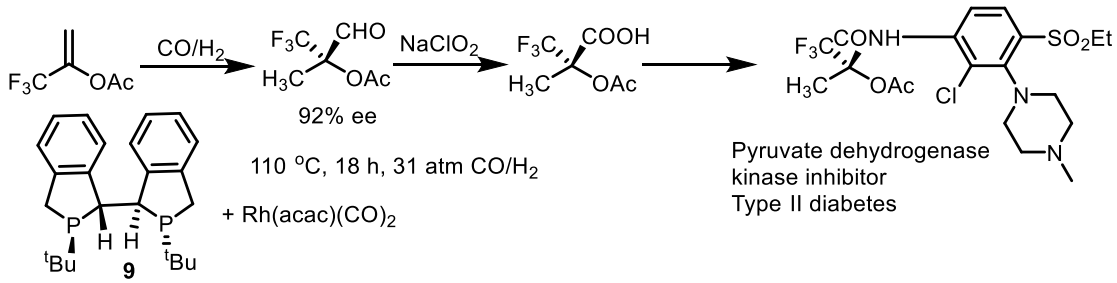

Figure 1.5 Application of DuanPhos in asymmetric hydroformylation of 1,1-disubstituted olefin

1.2 Synthesis of BIBOP ligands and their applications in asymmetric hydrogenation

In the field of transition metal catalyzed asymmetric reactions, the development of efficient chiral ligands for wide range of substrates plays an very important role. The *C-2* symmetric, *P*-chiral TangPhos **7**[20] and DuanPhos **9**[21] developed by our group have been demonstrated to be very powerful ligands for asymmetric hydrogenation of extensive substrates. However, there are some drawbacks for these two ligands preventing them from even boarder applications in practical processes: (1) they are very sensitive to air, due to their strong electron donating property on the phosphorus centers; (2) modifications on these two ligands are barely possible, due to the unique

starting materials or process for their synthesis. Inspired by the successes of TangPhos and DuanPhos in industry, Tang[22] and coworkers from Boehringer Ingelheim designed and synthesized a new family of *P*-chiral bisdihydrobenzooxaphosphole BIBOP ligands, which are air-stable and highly tunable regarding electronic and stereo properties. The synthetic routes for BIBOP ligands are as follow (Figure 1.6 and 1.7):

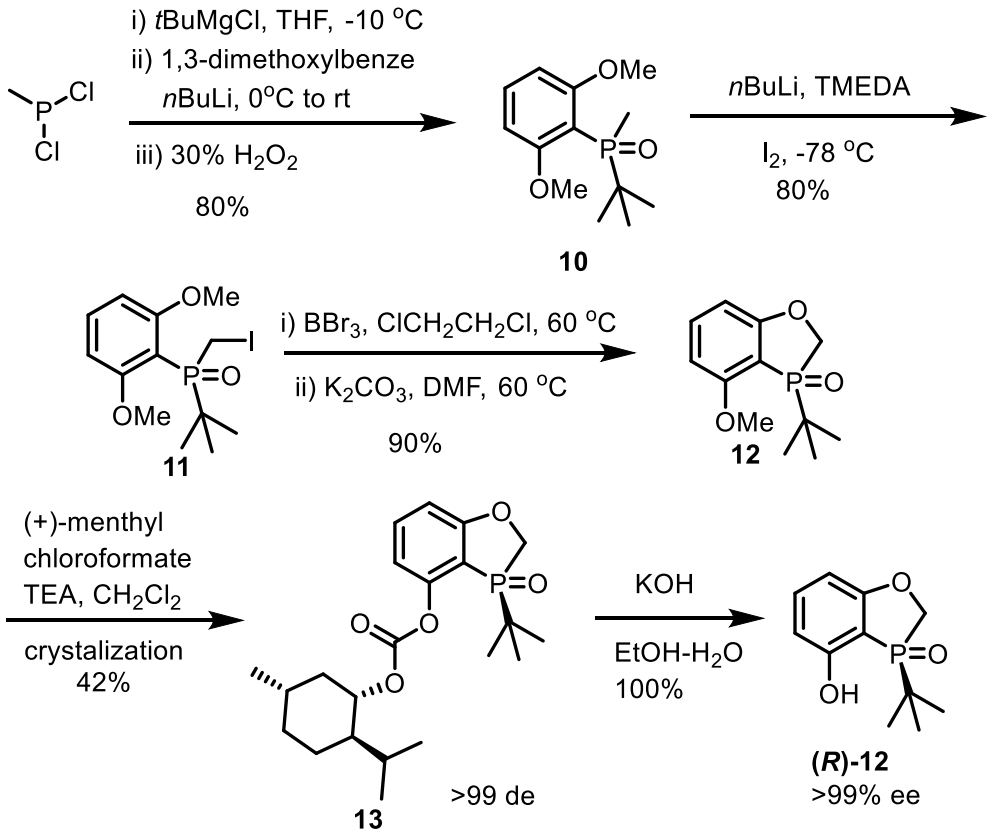

Figure 1.6 Synthesis of Chiral 3-*tert*-Butyl-2,3-dihydrobenzo[*d*][1,3]oxaphosphol-4-ol Oxide ((*R*)-**12**)

Preparation of racemic **12** was accomplished from methyldichlorophosphine in four steps. Reaction of methyldichlorophosphine with *t*-butylmagnesium chloride and 2,6- dimethoxyphenyllithium followed by oxidation with H_2O_2 provided phosphine oxide **10** in 80% yield. Iodination of **10**

was accomplished by deprotonation with *n*BuLi followed by addition of I2 to form iodo compound **11** in 80% yield. Demethylation with boron tribromide as the reagent followed by cyclization with K_2CO_3 as the base in DMF afforded racemic **12** in 90% yield over two steps. Efficient resolution of **12** was successfully accomplished by converting to its menthyl carbonate. The diastereomerically pure isomer **13** was isolated in 42% yield after single crystallization. Basic hydrolysis of carbonate **13** afforded enantiomerically pure compound (*R*)-**12** quantitatively.

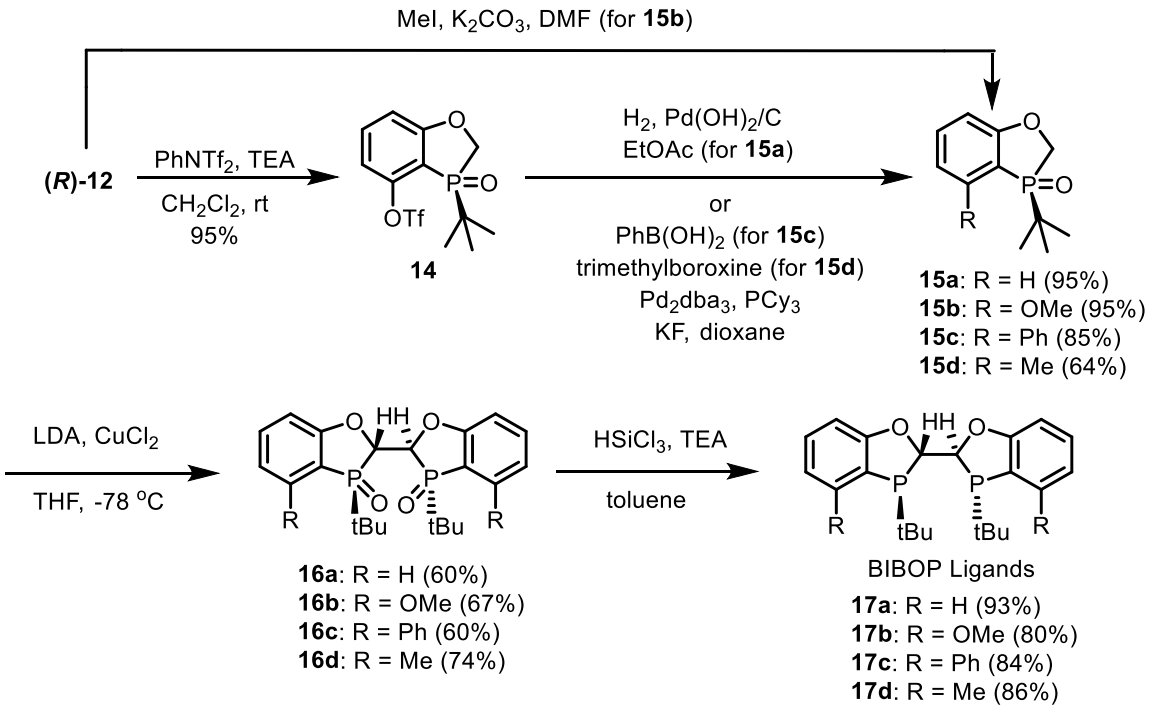

Figure 1.7 Syntheses of BIBOP Ligands

From (*R*)-**12** different substituents (H, OMe, Ph, or Me) were installed at the 4 position of the benzene ring (Figure 1.7). Then, **15a** was obtained by converting (*R*)-**12** to its triflate **14** followed by hydrogenolysis in 90% overall yield. Methylation of (*R*)-3 using MeI and potassium carbonate provided **15b** in

95% isolated yield. The phenyl-substituted product **15c** was formed by Suzuki coupling from **14** and phenylboronic acid in 85% yield. Similarly, the methyl-substituted compound **15d** was prepared in 64% yield from the triflate and trimethyl boroxine. Homocouplings of **15a**-**d**, mediated with LDA and $CuCl_2$ as the reagents afforded **16a**-**d** in 60-74% isolated yields as single isomeric coupling products. Reduction of **16a**-**d** with $HSiCl_3$ provided a series of BIBOP ligands **17** as white solids in high yields.

The BIBOP series ligands showed excellent performance for Rh catalyzed asymmetric hydrogenation of *α*-Arylenamides and *α*- (Acylamino)acrylic Acid Derivatives:[22]

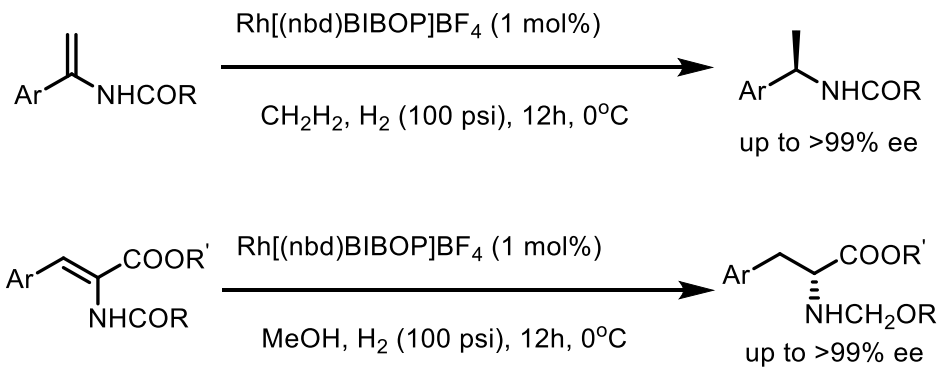

Figure 1.8 Asymmetric hydrogenation with Rh-BIBOP complex

1.3 Application of BIBOP ligands in asymmetric hydroformylation

1.3.1 Asymmetric hydroformylation of vinyl acetate derivatives with BIBOP ligands

As mentioned in **section 1.1**, there have been a few examples of application of bidentated chiral phosphorus ligands (which normally used for

asymmetric hydrogenation) in asymmetric hydroformylation. Realizing the tunable potential, suitable electronic property and stereo rigidity of BIBOP ligands, we envisioned that these ligands could be effective for rhodium catalyzed asymmetric hydroformylation. Thus, cooperating with researchers from Boehringer Ingelheim, we initiated our exploration of applying the BIBOP ligands (Figure 1.9) in asymmetric hydroformylation (AHF).

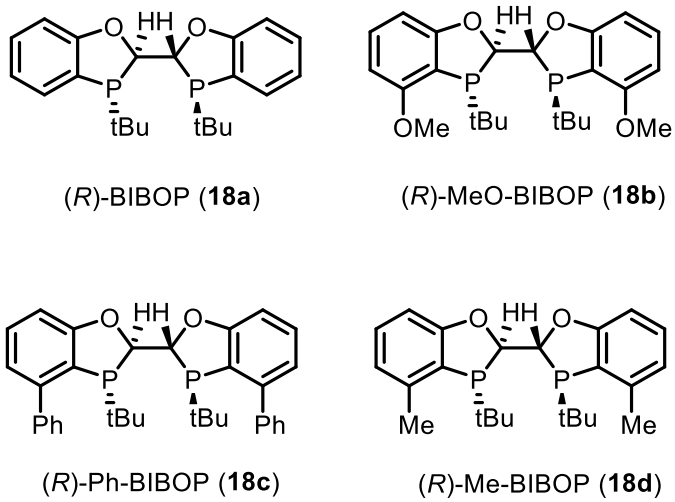

Figure 1.9 BIBOP ligands for asymmetric hydroformylation

Our initial investigation started with the classic vinyl acetate (**19**) as the model substrate. Excess ligand with high L/Rh ratio was commonly required to stabilize the catalytically active complex under high temperature conditions in hydroformylation reactions to maintain catalyst activity and enantioselectivity.[23] The Rh/L ratio of 1:3.0 was applied at 60 ℃ for 20 h in toluene in the presence of 1.0 mol% of $Rh(acac)(CO)_2$ and 3.0 mol% of (*R*)-BIBOP (**18a**) under 20 bar syngas (CO/H_2 = 10/10). To our delight, vinyl

acetate was fully hydroformylated with 25:1 branch to linear regio-isomeric ratio and 91:9 er of the branched isomer. Furthermore, the ligand was found to be stable under the reaction conditions and no access ligand is required. Same conversion and enantioselectivity were obtained with a slight excess ligand loading at Rh/**1a** ratio of 1:1.2 (Table 1.1, entry 3).

Table 1.1 AHF screening of vinyl acetate 19[a]

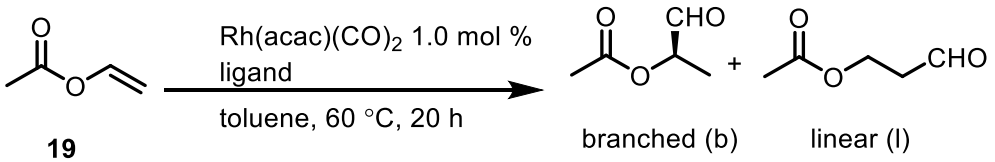

entry	L	Rh/L	CO/H_2	conv (%)[b]	b:l[b]	er[c]
1	18a	1:3.0	10 / 10	>99	25:1	91.0:9.0
2	18a	1:2.0	10 / 10	>99	20.6:1	91.3:8.7
3	18a	1:1.2	10 / 10	>99	20:1	91.5:8.5
4	18a	1:0.9	10 / 10	>99	13:1	72.5:27.5
5	18a	1:1.2	5 / 15	>99	27:1	91.2:8.8
6	18a	1:1.2	15 / 5	>99	27:1	91.0:9.0
7	**18b**	**1:1.2**	**10 / 10**	**>99**	**>200:1**	**95.3:4.7**
8	18c	1:1.2	10 / 10	28	12:1	71.0:29.0
9	18d	1:1.2	10 / 10	96.4	20:1	51.0:49.0

[a] Reaction conditions: **19** (1.0 mmol) catalyzed by Rh-ligand in toluene (0.5 mL) at 60 ℃ for 20 h under syngas pressure of 20 bar. [b] Conversions and branch to linear ratio (b:l) of the products were determined by ^{1}H NMR spectroscopy. [c] Determined by Chiral GC.

Next, CO partial pressure was varied since it affects both the conversion and regio- and enantioselectivity of AHF.[23] The catalyst system turns out to be robust towards the CO pressure. Decreasing the partial CO pressure in CO/H_2

from 10/10 to 5/15 (Table 1.1, entry 5) or increasing the CO pressure to 15/5 (Table 1.1, entry 6), conversions remained >99%. Both the b:l ratios and the enantiomeric ratios are the same under different CO pressures (entries 3, 5 and 6). Syngas pressure of CO/H_2 = 10/10 was selected for further studies.

Among the BIBOP ligands, the Ph substituent (**18c**) led to low conversion and enantioselectivity (Table 1.1, entry 8). The Me substituent (**18d**) also led to low enantiomeric ratio although providing almost full conversion (Table 1.1, entry 9). To our delight, (*R*)-MeO-BIBOP (**18b**) provided an increased regioselectivity at the b:l ratio of >200:1 and higher enantioselectivity at 95.3:4.7 er (Table 1.1, entry 7). On the other hand, the structural related Duanphos and Tangphos ligands produced poor reactivity and enantioselectivity.

With the optimized reaction conditions in hand, AHF of vinyl acetate derivatives was explored in the presence of MeO-BIBOP ligand (Table 1.2). The conditions are applicable to both the aliphatic and aromatic substituents. All the substrates were successfully converted to the desired aldehydes with excellent enantioselectivities of up to 95.3:4.7 er. It is noteworthy that the regioselectivities are outstanding with the branch to linear aldehyde ratio (b:l) of up to 415:1 (entry 4).

Table 1.2 AHF of vinyl acetate derivatives

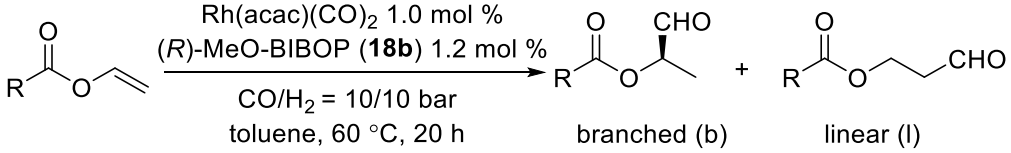

entry	substrate	product	conv (%)[a]	b:l[a]	er[b]
1	R = CH_3 (20)	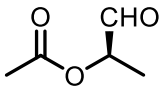 **21**	>99	285:1	95.3:4.7
2	R = *t*-Bu (22)	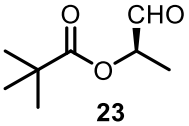 **23**	>99	127:1	95.2:4.8
3	R = *n*-C_7H_{15} (24)	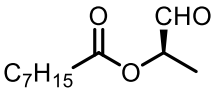 **25**	>99	269:1	94.5:5.5
4	**R = *n*-C_9H_{19} (26)**	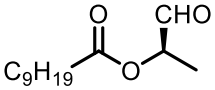 **27**	**>99**	**415:1**	**94.4:5.6**
5	R = Ph (28)	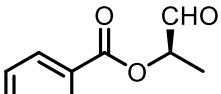 **29**	>99	37:1	95.0:5.0

[a] Conversions and branch to linear ratio (b:l) were determined by ^{1}H NMR spectroscopy, see the Supporting Information. [b] Determined by Chiral GC.

For better understanding of the origin of enantioselectivity, computational studies were conducted for the hydroformylation process of vinyl acetate in the presence of (*R*)-BIPOP ligand (**18a)** (Figure 1.10). All calculations were performed with Gaussian 09[24] at the DFT level of theory employing UB3LYP[25] and the LANL2DZ basis set with ECP for Rh[26] and UB3LYP-gCP-D3/6-31G(d) for all other atoms. The geometrical counterpoise (gCP)[27] and dispersion (D3)[28] corrections of Grimme et al. were applied to all stationary points to correct for basis set superposition error with 6-31G(d) and missing VDW

dispersion in B3LYP, respectively. Based on the reported mechanism,[29] the calculated rate-determining transition state of the stereochemically defining Rh-hydride olefin insertion shows that the vinyl group binds to the rhodium center to position the acetate away from the bulky *tert*-butyl group of the BIBOP ligand. In this orientation the *Si*-face of the olefin is bound to the rhodium center and ultimately receives the carbonyl functionality, generating the *R*-configuration of the aldehyde. This result is in consistence to the experimental data.

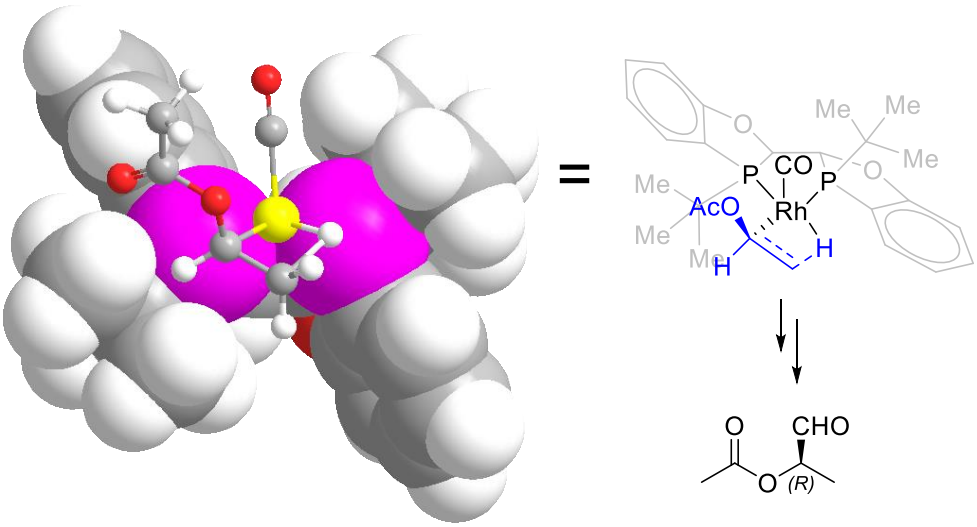

Figure 1.10 DFT (UB3LYP/LanL2DZ for Rh; UB3LYP-gCP-D3/6-31G(d) for all other atoms) calculated transition state for the Rh-hydride olefin insertion and stereochemical model.

1.3.2 Asymmetric hydroformylation of allylic substrates with BIBOP ligands

Encouraged by the successes of AHF of vinyl acetate derivatives with BIBOP ligands, AHF was tested on a series of allylic derivatives (Table 1.3). Allylic compounds are particularly challenging for AHF due to the potential of

double bond migration[30] and difficulty of regioselectivity control.[31] To our glad, for benzoyl-, phthaloyl-, and *p*-MePhSO$_2$- protected allylic amines **30**, **32** and **34**, enantiomeric ratios of 89.2:10.8, 87.3:12.7 and 92.2:7.8 were obtained respectively in the presence of (*R*)-BIBOP ligand (Table 1.3, entries 1, 2 and 3). The resulting amide-protected chiral β^2-amino aldehydes are useful synthons that can be transformed into important building blocks such as chiral β^2-amino acids and amino alcohols.[32] The protecting groups can then be removed according to the known procedures.[33] Encouraged by the success of the AHF of *N*-functionalized allyl substrates, Ph- and O-functionalized allylic substrates were also evaluated. For the aryl allyl substrates **36** and **38** that are lack of directing groups, 93.0:7.0 er and 88:12 er were obtained for aldehydes **37** and **39**, nevertheless modest b:l ratios. Allyl acetate **40** gave excellent enantioselectivity at 93.3:6.7 er and good regioselectivity of b:l at 7.7 (Table 1.3, entry 6).

Table 1.3 AHF of the allylic substrates

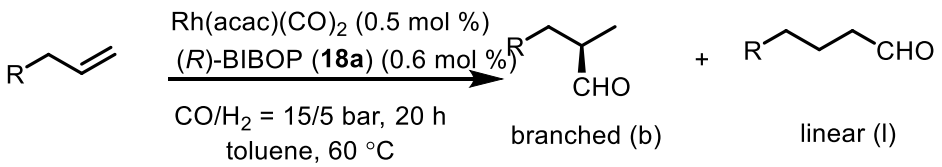

entry	substrate	product	conv (%)[a]	b:l[a]	er[b]
1	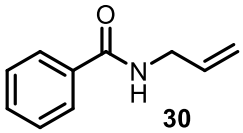 **30**	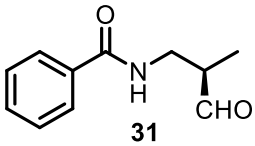 **31**	>99	8.0:1	89.2 : 10.8
2	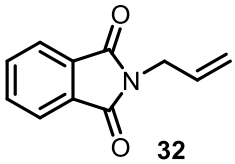 **32**	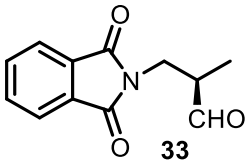 **33**	>99	11.2:1	87.3:12.7
3	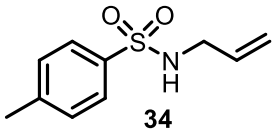 **34**	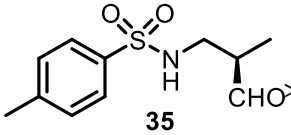 **35**	>99	3.0:1	92.2:7.8
4	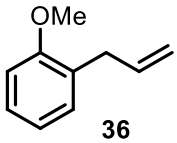 **36**	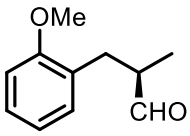 **37**	>99	1.2:1	93.0:7.0
5	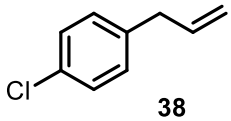 **38**	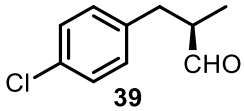 **39**	>99	1.1:1	88.1:11.9
6	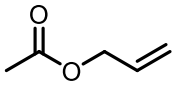 **40**	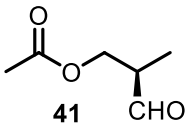 **41**	>99	7.7:1	93.3:6.7
7	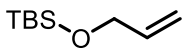 **42**	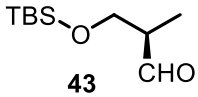 **43**	>99	2.0:1	88.8:11.2
8	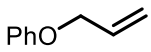 **44**	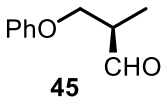 **45**	>99	4.1:1	86.8:13.2

[a] Conversions and branch to linear ratio (b:l) were determined by ^{1}H NMR spectroscopy. [b] Determined by Chiral GC and HPLC.

1.3.3 Asymmetric hydroformylation of styrene substrates with BIBOP ligands

Simple styrene is a classic substrate for rhodium catalyzed AHF, up to today, there have been a number of chiral ligands[34] reported to be able to offer moderate to excellent enantioselectivity (Figure 1.11). We thus sought to apply our air stable BIBOP ligands into rhodium catalyzed AHF of styrene derivatives.

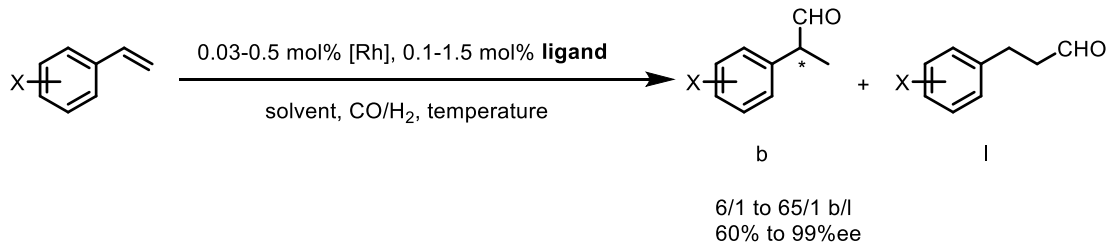

Figure 1.11 AHF of the simple styrene

When 0.5 mol% $Rh(acac)(CO)_2$ and 0.6 mol% (*R*)-BIBOP were applied with 15/5 bar of syngas under 60 ℃ for 20 hours, all the tested styrene substrates were completely hydroformylated (Figure 1.12).

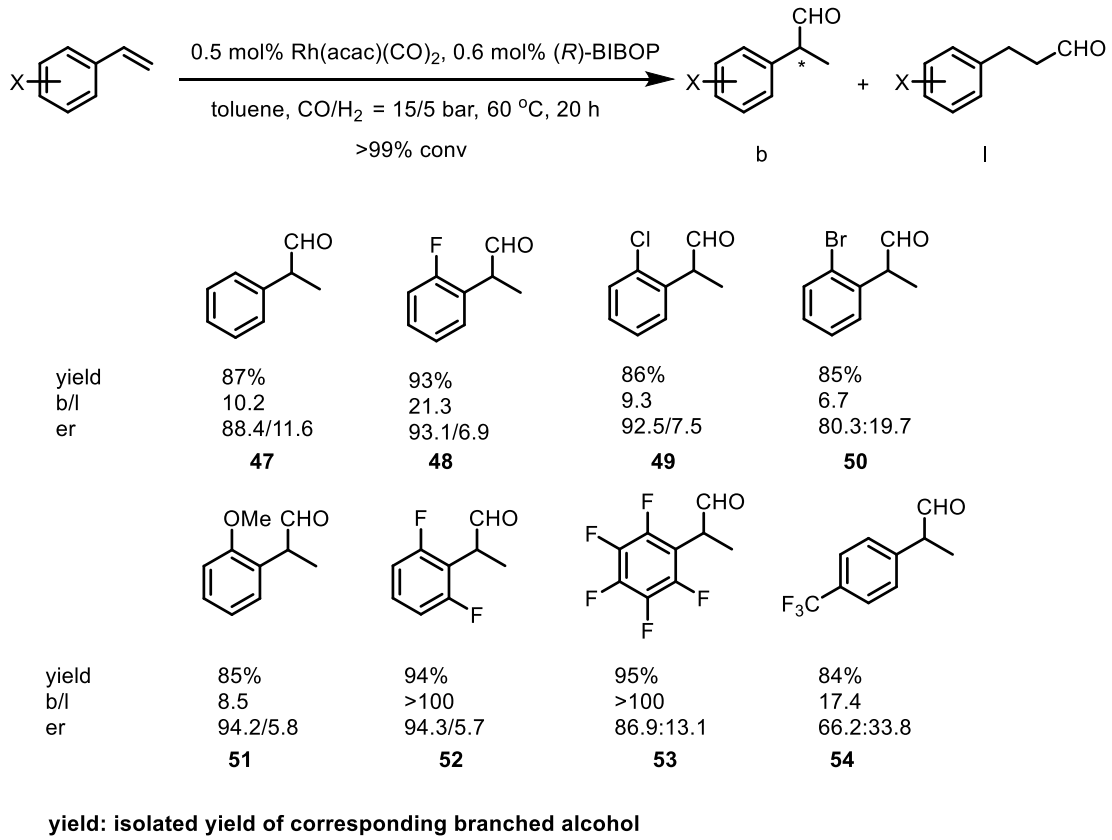

yield: isolated yield of corresponding branched alcohol

Figure 1.12 AHF of the styrene derivatives

Excellent region -(up to >100/1 b/l) and enantioselectivity (up to 94/6 er) were obtained. Comparing to the simple styrene, when 2-position of the phenyl ring is occupied by small to median sized groups (compound **48**, **49**, **50**, **51**), the enantioselectivies were significantly higher. Noticeably, when the substitutions are strong electron-withdrawing fluoro groups, the regioselectivity for AHF was dramatically enhanced, probably because strong electron-withdrawing ability of fluoro groups significantly decreases the electron density of *β*-carbon of the double bond, facilitating the hydride insertion to occur in *β*-carbon, resulting in the branched aldehyde products.

1.3.4 Synthesis of chiral lactone via AHF of styrene derivatives

Chiral lactones are widely distributed in nature, and are important building blocks for many pharmaceutic ingredients.[35] During our exploration of expanding the substrate scope of AHF with BIBOP ligands, we accidentally found new way to synthesize a type of chiral *δ*-lactone (Figure 1.13).

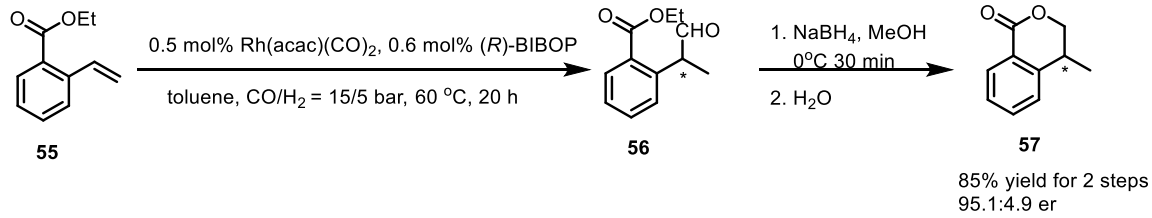

Figure 1.13 Synthesis of chiral *δ*-lactone via AHF

While studying AHF of ethyl 2-vinylbenzoate **55** with BIBOP ligand, we performed a simple reduction to the aldehyde products for HPLC measurement purpose. To our surprise, a chiral *δ*-lactone **57** was formed via spontaneous ring closing process under the workup condition, with 85% yield and over 90% ee.

To further expand this application of AHF and improve the enantioselectivity, we synthesized the amide analogs **58** of ethyl 2-vinylbenzoate following reported C-H activation procedures (Figure 1.14) [36]:

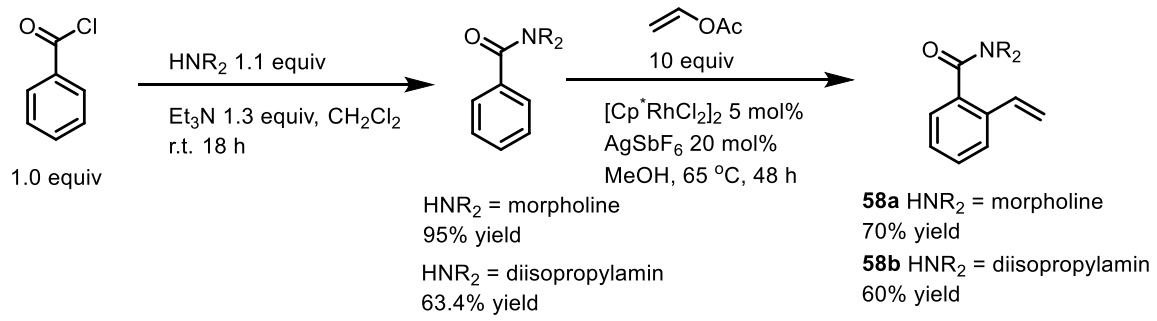

Figure 1.14 Synthesis of amide substrates

Although the resulting amides were successfully hydroformylated with decent yields, the ring closing for the formation of *δ*-lactone failed in the workup step. Thus, we have to focus on the optimization of enantioselectivity in AHF of the original ethyl 2-vinylbenzoate derivatives in the future.

1.4 Conclusion

In summary, bisdihydrobenzooxaphosphole BIBOP ligands were successfully applied in rhodium catalyzed asymmetric hydroformylation reactions. The ease of synthesis and excellent air stability make BIBOP ligands standing out as unique ligand structure in the field of hydroformylation. A wide range of monosubstituted olefins have been converted to chiral aldehydes with excellent conversions and good-to-excellent enantioselectivities. A chiral *δ*-lactone was obtained by AHF and subsequent simple reduction workup. Computational studies provide insights into the reaction mechanism, in particular the Rh-hydride olefin insertion processes in AHF of vinyl acetate.

1.5 Experiment Section

1.5.1 General remarks

Commercially available reagents were used without further purification. The BIBOP ligands were synthesized according to literature procedures. *N*-allylamides were synthesized following previously reported procedures, and all characterization data were consistent with those reported for these compounds. All asymmetric hydroformylation reactions were performed in an inert atmosphere using standard Schlenk techniques. Enantiomeric excesses were determined by Agilent GC 7890A or Agilent HPLC 1200 series.

1.5.2 General procedure for the preparation of amides 58

The indicated benzoyl chloride (1.0 equiv) was added, under nitrogen, to a solution of the amine (1.1 equiv) and triethylamine (1.3 equiv) in CH_2Cl_2 (10 mL, 0.50 M) at ambient temperature. After stirring for 18 h, the reaction mixture was diluted with CH_2Cl_2 (10 mL) and washed successively with HCl (20 mL, 1.0 M) and brine (20 mL). The organic layer was dried over $MgSO_4$, concentrated, and purified as indicated. The formed amides were placed in an oven-dried tube with stir bar, 7 equivalent vinyl acetate, 5 mol% $[Cp^*RhCl_2]_2$ and 20 mol% $AgSbF_6$ were added, the tube was then sealed with a Teflon screw cap. The reaction mixture was placed into a temperature-controlled oil bath at 65 ºC. After 48 hours the reaction mixture was cooled to ambient

temperature. The crude reaction mixture was concentrated and then purified to give the indicated amide product **58**.

1.5.3 General procedure for the asymmetric hydroformylation

In a glovebox under nitrogen, ligand (0.012 mmol) and [Rh(acac)$(CO)_2$] (0.01 mmol in 0.4 mL toluene) were added to a 2 mL vial. After stirring for 10 minutes, the substrate (1.0 mmol) and additional solvent were added to bring the total volume of the reaction mixture to 0.5 mL. The vial was transferred into an autoclave and taken out of the glovebox. Hydrogen and carbon monoxide were added sequentially. The reaction mixture was stirred at 60 ^{o}C for 20 hours. The reaction was cooled and the pressure was carefully released in a well-ventilated fume hood. The conversion and branch to linear ratio of this reaction were determined by ^{1}H NMR spectroscopy from the crude reaction mixture. The enantiomeric excess was determined by GC analysis with a Supelco's Beta Dex 225 column or by Chiral HPLC analysis of the corresponding alcohol resulting from the sodium borohydride reduction of the aldehyde.

2-(2-fluorophenyl)propan-1-ol (**48**):

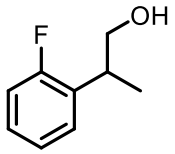

93% yield, 93.1/6.9 er. ^{1}H NMR (400 MHz, $CDCl_3$) δ 7.49 – 6.82 (m, 4H), 3.85 – 3.55 (m, 2H), 3.26 (h, *J* = 6.9 Hz, 1H), 2.04 (d, *J* = 18.7 Hz, 1H), 1.24 (t, *J* = 17.4 Hz, 3H).

2-(2-chlorophenyl)propan-1-ol (**49**):

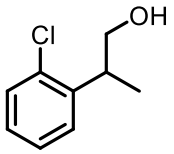

86% yield, 92.5/7.5 er. ^{1}H NMR (400 MHz, $CDCl_3$) δ 7.51 – 6.97 (m, 4H), 3.73 (dddd, *J* = 39.9, 10.8, 6.4, 1.5 Hz, 2H), 3.52 (h, *J* = 6.7 Hz, 1H), 1.71 (s, 1H), 1.28 (d, *J* = 7.0 Hz, 3H).

2-(2-methoxyphenyl)propan-1-ol (**51**):

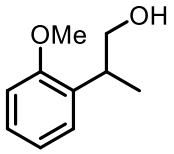

85% yield, 94.2/5.8 er. ^{1}H NMR (400 MHz, $CDCl_3$) δ 7.20 (dd, *J* = 11.5, 4.6 Hz, 2H), 6.99 – 6.90 (m, 1H), 6.87 (d, *J* = 8.4 Hz, 1H), 3.81 (s, 3H), 3.77 – 3.60 (m, 2H), 3.49 – 3.35 (m, 1H), 1.86 – 1.59 (m, 1H), 1.25 (d, *J* = 7.1 Hz, 3H).

2-(2,6-difluorophenyl)propan-1-ol (**52**):

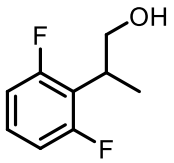

94% yield, 94.3/5.7 er. ^{1}H NMR (500 MHz, $CDCl_3$) δ 7.22 – 7.03 (m, 1H), 6.96 – 6.73 (m, 2H), 3.95 – 3.69 (m, 2H), 3.42 (h, *J* = 7.2 Hz, 1H), 2.04 (d, *J* = 12.4 Hz, 1H), 1.29 (dd, *J* = 31.3, 7.1 Hz, 3H).

2-(perfluorophenyl)propan-1-ol (**53**):

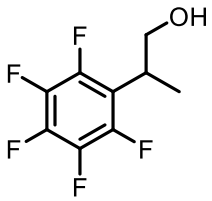

95% yield, 86.9/13.1 er. ^{1}H NMR (500 MHz, $CDCl_3$) δ 3.81 (d, *J* = 7.6 Hz, 2H), 3.55 – 3.31 (m, 1H), 2.35 (s, 1H), 1.34 (d, *J* = 7.2 Hz, 3H).

2-(4-(trifluoromethyl)phenyl)propan-1-ol (**54**):

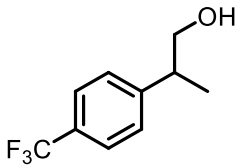

84% yield, 66.2/33.8 er. ^{1}H NMR (500 MHz, $CDCl_3$) δ 7.57 (d, *J* = 8.2 Hz, 2H), 7.34 (d, *J* = 8.1 Hz, 2H), 3.75 – 3.60 (m, 2H), 2.98 (h, *J* = 6.6 Hz, 1H), 1.77 (dd, *J* = 51.8, 42.8 Hz, 1H), 1.27 (d, *J* = 7.0 Hz, 3H).

4-methylisochroman-1-one (**57**):

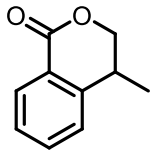

90% yield, 95.1/4.9 er. ^{1}H NMR (500 MHz, $CDCl_3$) δ 8.09 (d, *J* = 7.8 Hz, 1H), 7.58 (t, *J* = 7.6 Hz, 1H), 7.39 (t, *J* = 7.6 Hz, 1H), 7.31 (t, *J* = 5.9 Hz, 1H), 4.51 (dd, *J* = 11.0, 4.1 Hz, 1H), 4.24 (dd, *J* = 10.9, 6.6 Hz, 1H), 3.26 – 3.04 (m, 1H), 1.37 (d, *J* = 7.2 Hz, 3H).

1.5.4 GC and HPLC analysis of the chiral aldehydes

References for chiral separation methods are included. Isolated yields, NMR spectral and HRMS data are provided for chiral aldehydes **21** and **23**, which are unreported as AHF products.

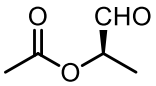

(*R*)-1-oxopropan-2-yl acetate (21)

Enantiomeric excess was determined by GC with a Supelco's Beta Dex 225 column: 100 ^{o}C, stay 5 mins, 4 ^{o}C/min to 160 ^{o}C, stay 5 mins, flow rate = 1.0 mL/min, t_{minor} = 7.6 min, t_{major} = 9.3 min; 95.3:4.7 er.

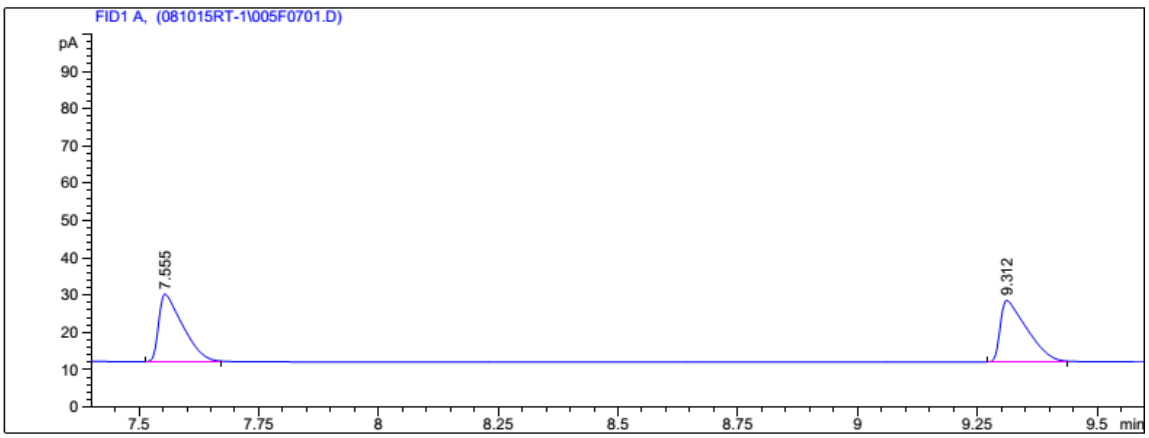

Peak #	RetTime [min]	Type	Width [min]	Area [pA*s]	Height [pA]	Area %
1	7.555	BB	0.0495	62.82764	18.08755	49.83560
2	9.312	BB	0.0529	63.24215	16.43451	50.16440

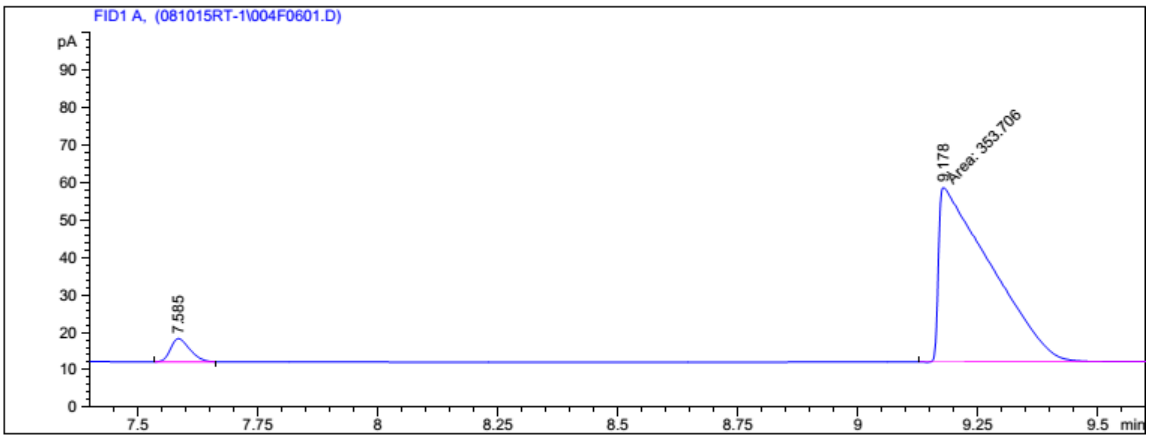

Peak #	RetTime [min]	Type	Width [min]	Area [pA*s]	Height [pA]	Area %
1	7.585	BB	0.0435	17.38674	6.24105	4.68528
2	9.178	MM	0.1259	353.70642	46.83174	95.31472

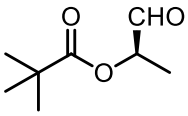

(*R*)-1-oxopropan-2-yl pivalate (23)

Enantiomeric excess was determined by GC with a Supelco's Beta Dex 225 column: 50 ^{o}C, stay 5 mins, 4 ^{o}C/min to 100 ^{o}C, stay 5 mins, flow rate = 1.0 mL/min, t_{minor} = 42.3 min, t_{major} = 43.2 min; 95.2:4.8 er.

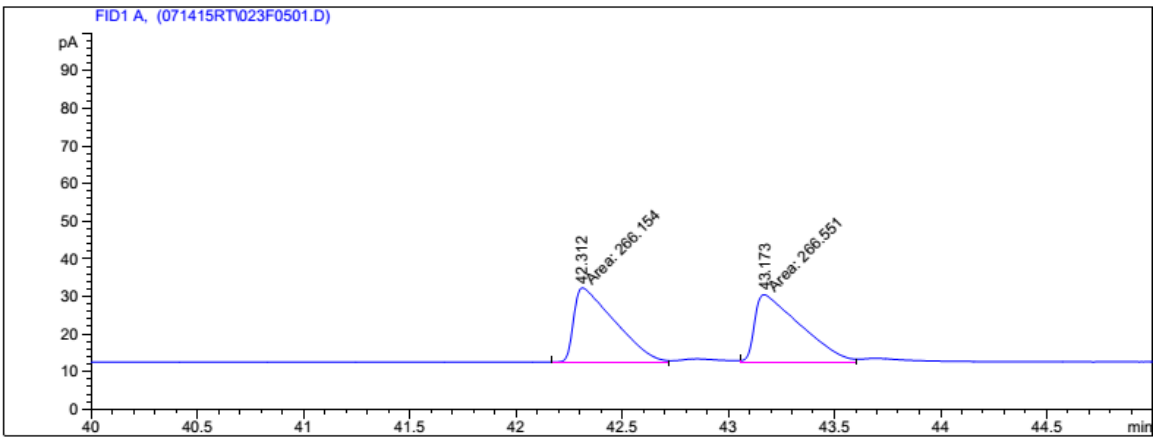

Peak #	RetTime [min]	Type	Width [min]	Area [pA*s]	Height [pA]	Area %
1	42.312	MM	0.2239	266.15427	19.80965	49.96276
2	43.173	MM	0.2488	266.55099	17.85264	50.03724

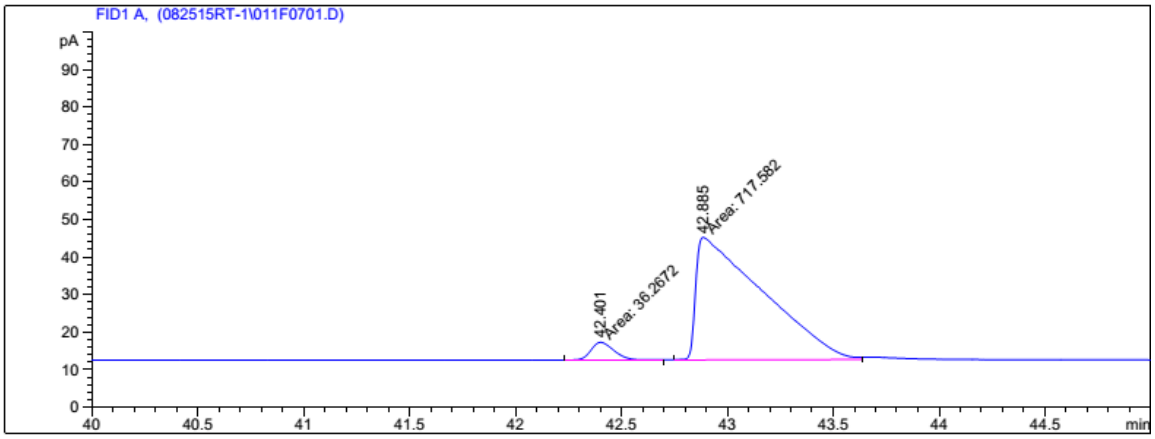

Peak #	RetTime [min]	Type	Width [min]	Area [pA*s]	Height [pA]	Area %
1	42.401	MM	0.1270	36.26717	4.75880	4.81093
2	42.885	MM	0.3662	717.58215	32.65533	95.18907

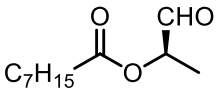

(*R*)-1-oxopropan-2-yl octanoate (25)

Enantiomeric excess was determined by GC with a Supelco's Beta Dex 225 column: 130 ^{o}C, stay 30 mins, flow rate = 1.0 mL/min, t_{minor} = 26.3 min, t_{major} = 27.5 min; 94.5:5.5 er.

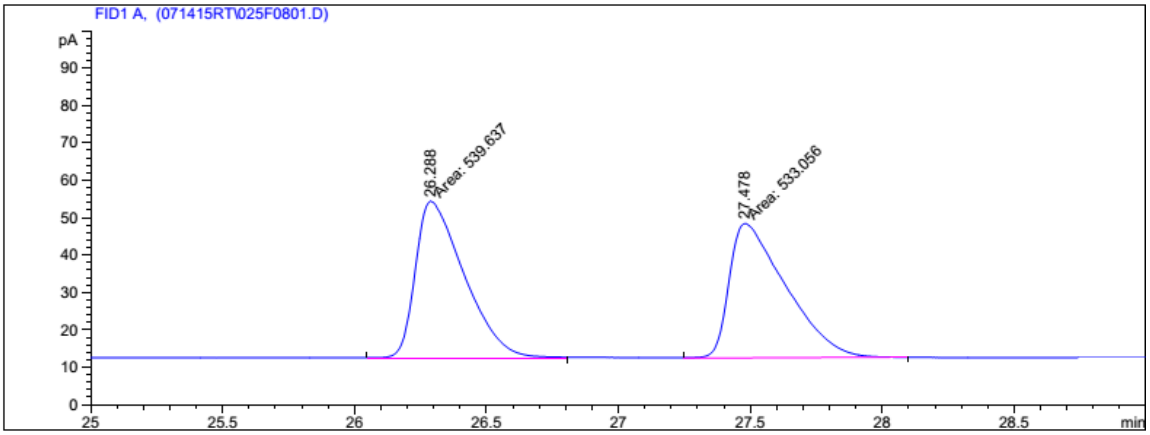

Peak #	RetTime [min]	Type	Width [min]	Area [pA*s]	Height [pA]	Area %
1	26.288	MM	0.2143	539.63702	41.97723	50.30676
2	27.478	MM	0.2477	533.05591	35.87165	49.69324

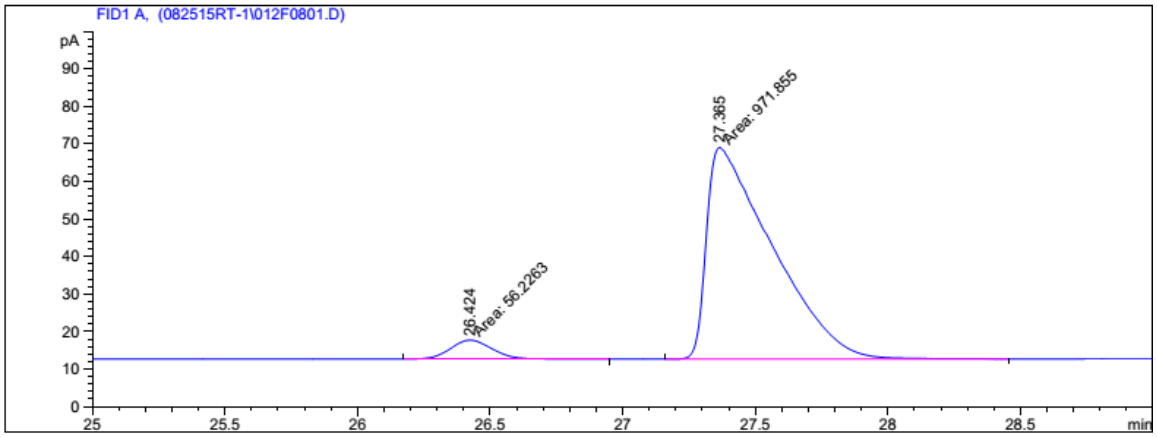

Peak #	RetTime [min]	Type	Width [min]	Area [pA*s]	Height [pA]	Area %
1	26.424	MM	0.1844	56.22626	5.08323	5.46905
2	27.365	MM	0.2876	971.85498	56.32727	94.53095

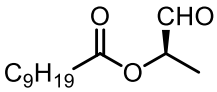

(*R*)-1-oxopropan-2-yl decanoate (27)

Enantiomeric excess was determined by GC with a Supelco's Beta Dex 225 column: 130 ^{o}C, stay 85 mins, flow rate = 1.0 mL/min, t_{minor} = 71.8 min, t_{major} = 75.3 min; 94.4:5.6 er.

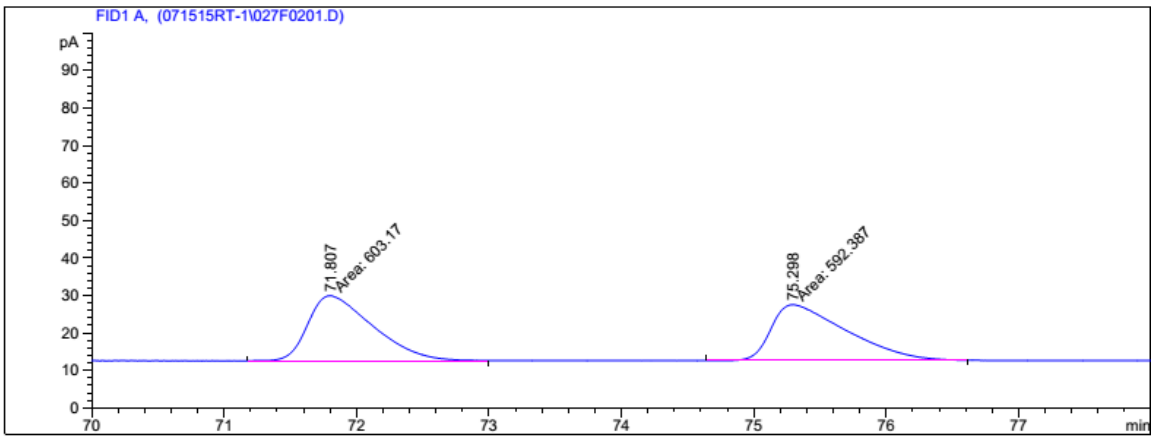

Peak #	RetTime [min]	Type	Width [min]	Area [pA*s]	Height [pA]	Area %
1	71.807	MM	0.5753	603.17004	17.47393	50.45094
2	75.298	MM	0.6601	592.38745	14.95809	49.54906

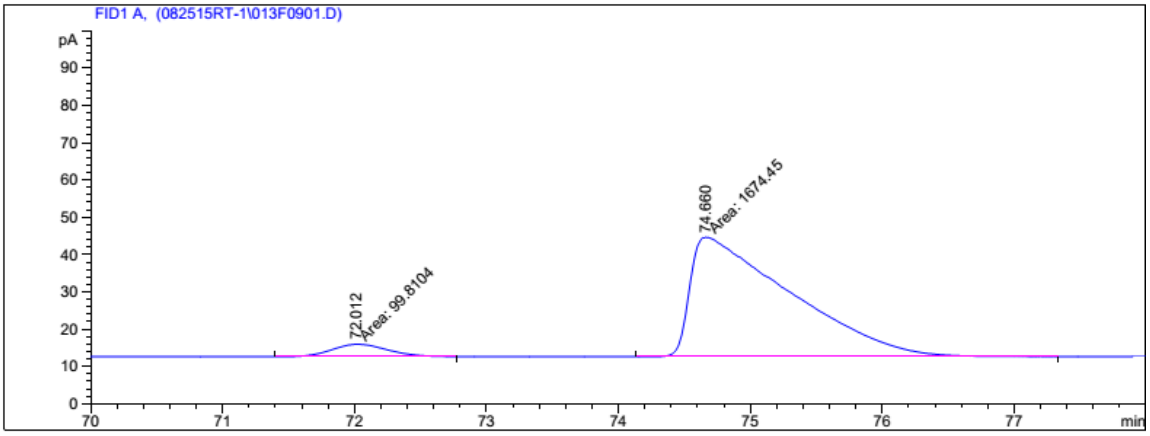

Peak #	RetTime [min]	Type	Width [min]	Area [pA*s]	Height [pA]	Area %
1	72.012	MM	0.4967	99.81042	3.34903	5.62546
2	74.660	MM	0.8757	1674.45300	31.87008	94.37454

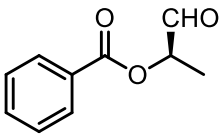

(*R*)-1-oxopropan-2-yl benzoate (29)

Enantiomeric excess was determined by GC with a Supelco's Beta Dex 225 column: 130°C, stay 36 mins, flow rate = 1.0 mL/min, t_{major} = 37.6 min, t_{minor} = 41.3 min; 95.0:5.0 er.

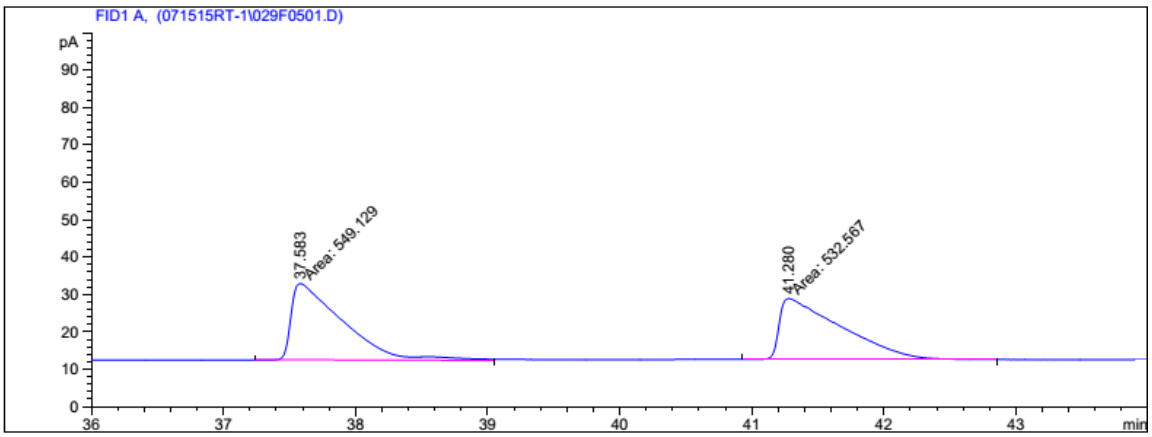

Peak #	RetTime [min]	Type	Width [min]	Area [pA*s]	Height [pA]	Area %
1	37.583	MM	0.4494	549.12946	20.36661	50.76558
2	41.280	MM	0.5423	532.56702	16.36756	49.23442

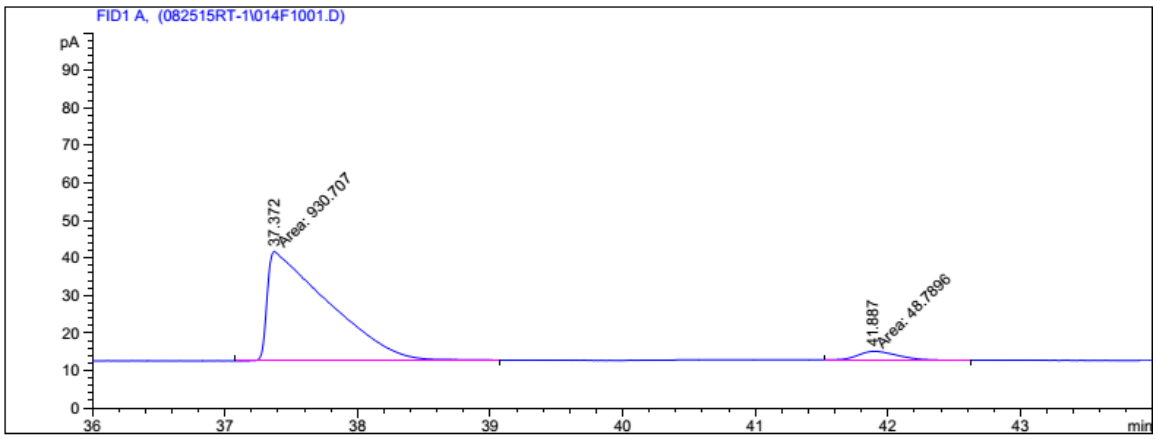

Peak #	RetTime [min]	Type	Width [min]	Area [pA*s]	Height [pA]	Area %
1	37.372	MM	0.5325	930.70734	29.12843	95.01891
2	41.887	MM	0.3472	48.78961	2.34187	4.98109

Peak #	RetTime [min]	Type	Width [min]	Area [pA*s]	Height [pA]	Area %
1	3.918	BB	0.0338	22.19601	10.42944	9.97591
2	4.237	BB	0.0391	200.30005	77.68095	90.02409

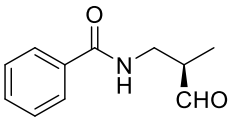

(*R*)-N-(2-methyl-3-oxopropyl)benzamide (31)

Enantiomeric excess was determined by reducing it into alcohol with $NaBH_4$ and analyzing with HPLC: Daicel Chiralcel AD-3, hexane/iPrOH = 95:5, flow rate = 1.0 mL/min, λ= 254 nm, t_{major} = 16.7 min, t_{minor} = 17.6 min, 89.2:10.8 er.

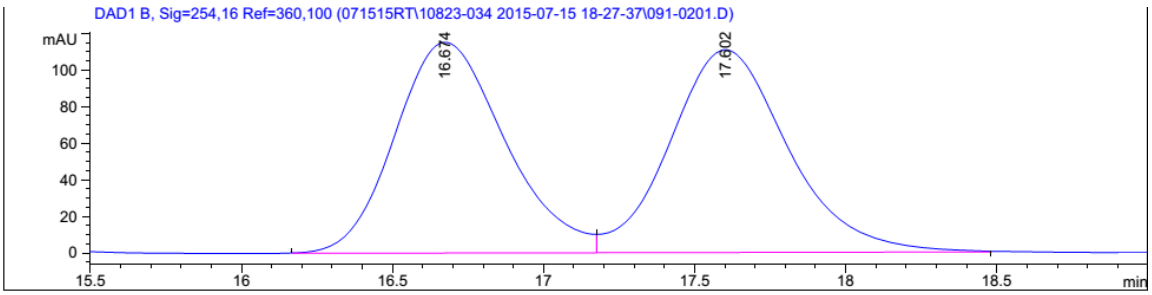

Peak #	RetTime [min]	Type	Width [min]	Area [mAU*s]	Height [mAU]	Area %
1	16.674	BV	0.3913	2915.90967	115.18828	49.2363
2	17.602	VB	0.4148	3006.37036	110.71875	50.7637

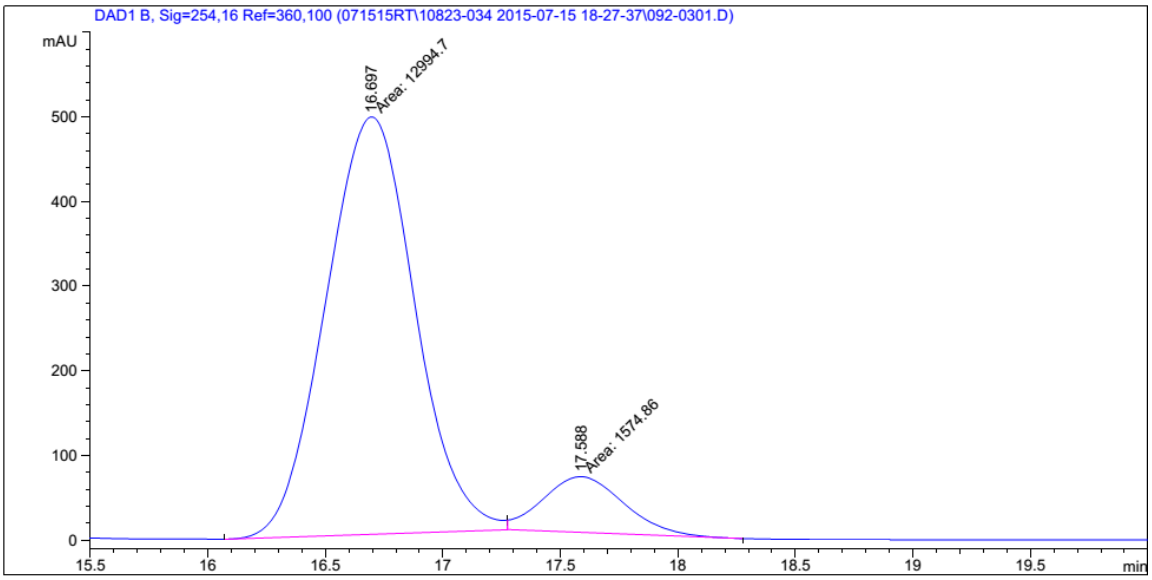

Peak #	RetTime [min]	Type	Width [min]	Area [mAU*s]	Height [mAU]	Area %
1	16.697	MM	0.4390	1.29947e4	493.30255	89.1907
2	17.588	MM	0.3981	1574.86450	65.93553	10.8093

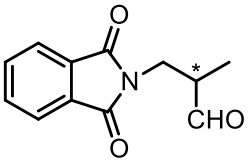

3-(1,3-dioxoisoindolin-2-yl)-2-methylpropanal (33)

Enantiomeric excess was determined by reducing it into alcohol with $NaBH_4$ and analyzing with HPLC: Daicel Chiralcel AD-3, hexane/iPrOH = 95:5, flow rate = 1.0 mL/min, λ= 254 nm, t_{minor} = 16.1 min, t_{major} = 17.6 min, 87.3:12.7 er.

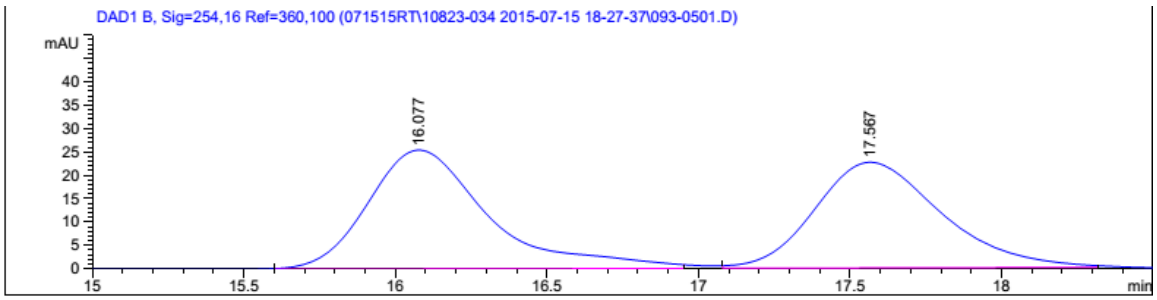

Peak #	RetTime [min]	Type	Width [min]	Area [mAU*s]	Height [mAU]	Area %
1	16.077	BB	0.4155	701.95331	25.46939	51.7474
2	17.567	BB	0.4400	654.54736	22.59428	48.2526

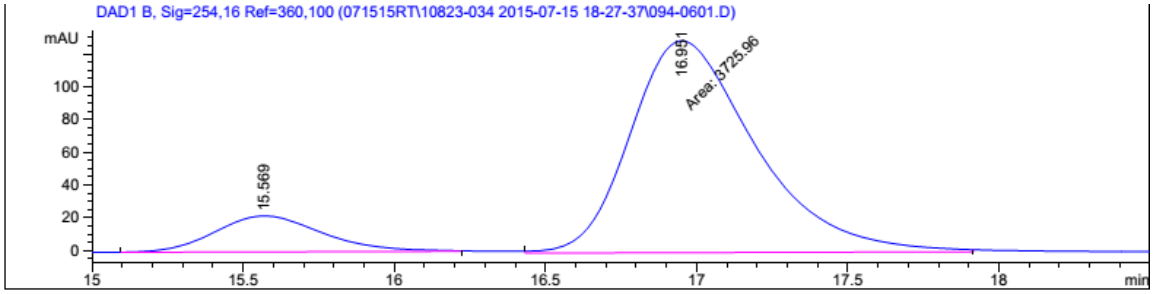

Peak #	RetTime [min]	Type	Width [min]	Area [mAU*s]	Height [mAU]	Area %
1	15.569	BB	0.3815	542.20428	21.99908	12.7035
2	16.951	MM	0.4801	3725.95752	129.34499	87.2965

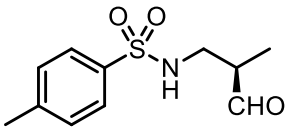

(*R*)-4-methyl-N-(2-methyl-3-oxopropyl)benzenesulfonamide (35)

Enantiomeric excess was determined by reducing it into alcohol with NaBH4 and analyzing with HPLC: Daicel Chiralcel AD-H, hexane/iPrOH = 90:10, flowrate = 1.0 mL/min, λ= 254 nm, t_{minor} = 32.7 min, t_{major} = 45.6 min; 92.2:7.8 er.

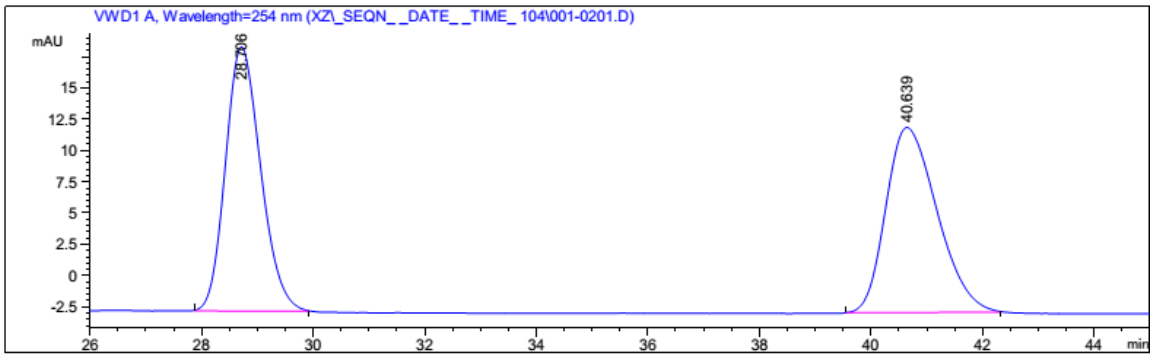

Peak #	RetTime [min]	Type	Width [min]	Area mAU *s	Height [mAU]	Area %
1	28.706	BB	0.6832	929.74310	21.14937	49.5282
2	40.639	BB	0.9771	947.45612	14.82531	50.4718

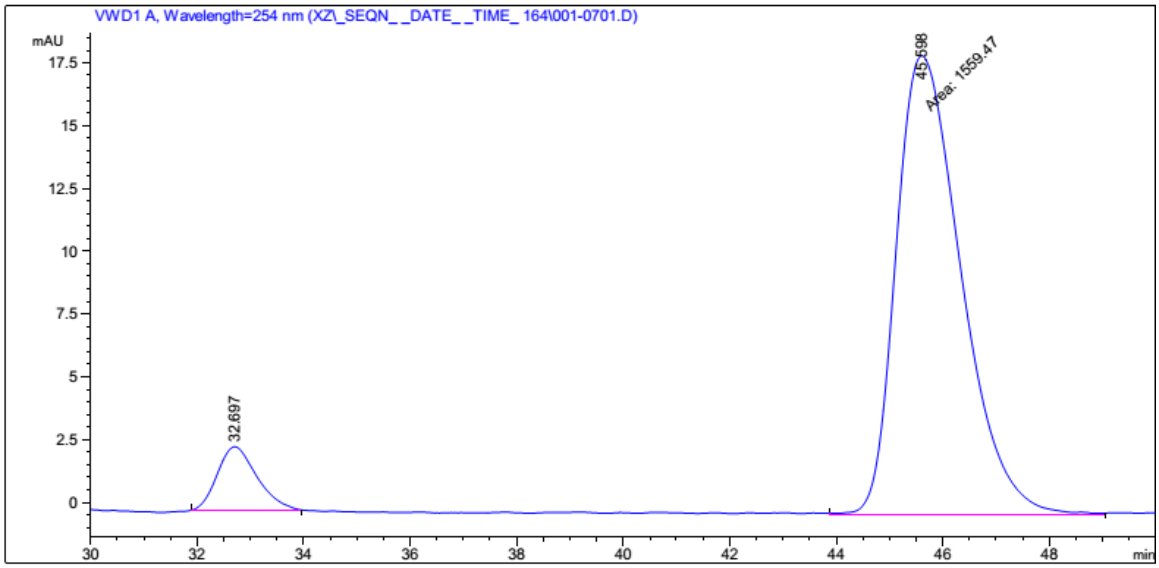

Peak #	RetTime [min]	Type	Width [min]	Area mAU *s	Height [mAU]	Area %
1	32.697	BB	0.6978	132.29135	2.54031	7.8197
2	45.598	MM	1.4191	1559.47168	18.31500	92.1803

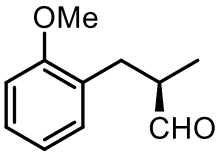

(*R*)-3-(2-methoxyphenyl)-2-methylpropanal (37)

The crude reaction mixture was purified on silica gel (hexane: ethyl acetate = 19:1) to afford a clear colorless oil (87 mg, 49% yield). ^{1}H NMR (400 MHz, $CDCl_3$) δ 9.68 (d, *J* = 1.7 Hz, 1H), 7.20 (td, *J* = 7.9, 1.7 Hz, 1H), 7.10 (dd, *J* = 7.4, 1.6 Hz, 1H), 6.87 (ddd, *J* = 11.0, 8.7, 4.6 Hz, 2H), 3.80 (s, 3H), 3.07 (dd, *J* = 13.1, 6.4 Hz, 1H), 2.75 – 2.59 (m, 2H), 1.05 (d, *J* = 6.9 Hz, 3H). ^{13}C NMR (400 MHz, $CDCl_3$) δ 205.0, 157.4, 131.0, 127.8, 127.1, 120.3, 110.3, 55.1, 46.5, 31.8, 13.3. All spectral data are in accordance with

literature.[6] HRMS (ESI) m/z: calc. for $C_{11}H_{15}O_2$ $[M + H]^+$ 179.10666; found 179.10672.

Enantiomeric excess was determined by reducing it into alcohol with $NaBH_4$ and analyzing with HPLC: Daicel Chiralcel OD-H, hexane/iPrOH = 95:5, flowrate = 1.0 mL/min, λ= 220 nm, t_{minor} = 10.6 min, t_{major} = 16.5 min; 93.0:7.0 er.

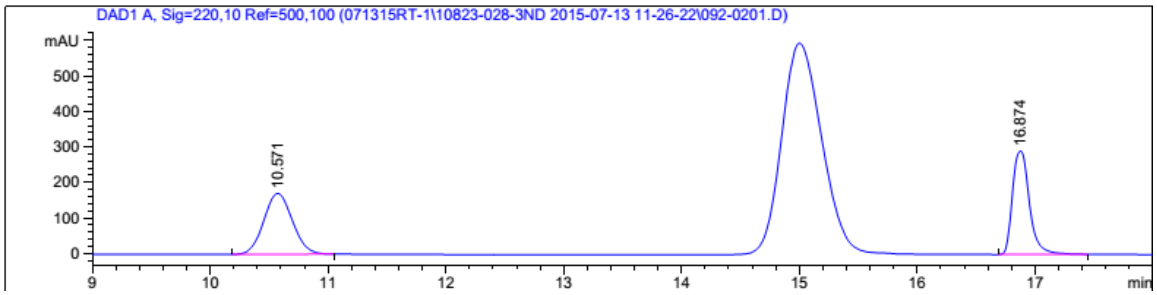

Peak #	RetTime [min]	Type	Width [min]	Area [mAU*s]	Height [mAU]	Area %
1	10.571	BB	0.2622	2887.74023	171.69167	49.8070
2	16.874	BB	0.1566	2910.12549	291.29602	50.1930

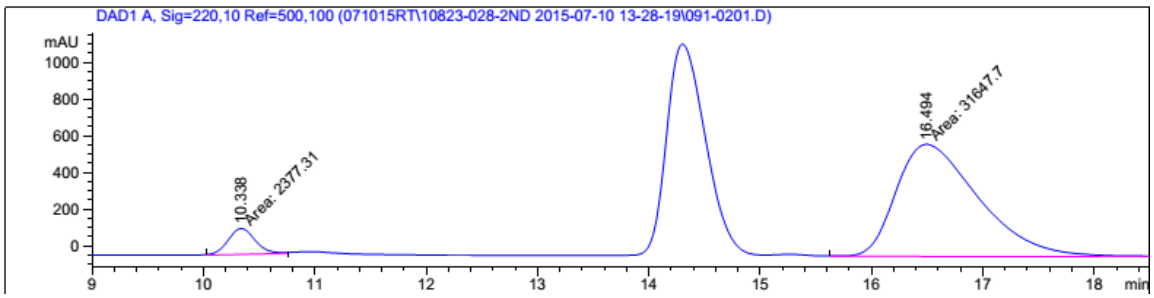

Peak #	RetTime [min]	Type	Width [min]	Area [mAU*s]	Height [mAU]	Area %
1	10.338	MM	0.2803	2377.30640	141.35471	6.9869
2	16.494	MM	0.8644	3.16477e4	610.22107	93.0131

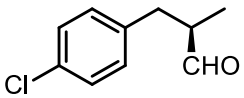

(*R*)-3-(4-chlorophenyl)-2-methylpropanal (39)

The crude reaction mixture was purified on silica gel

(hexane: ethyl acetate = 19:1) to afford a clear pale oil (73 mg, 40% yield). ^{1}H NMR (400 MHz, $CDCl_3$) δ 9.70 (d, *J* = 1.4 Hz, 1H), 7.28 – 7.24 (m, 2H), 7.13 – 7.08 (m, 2H), 3.05 (dd, *J* = 13.4, 5.7 Hz, 1H), 2.63 (dddd, *J* = 26.6, 21.5, 10.2, 6.9 Hz, 2H), 1.09 (d, *J* = 6.9 Hz, 3H). ^{13}C NMR (400 MHz, $CDCl_3$) δ 203.9, 137.3, 132.2, 130.4, 128.6, 47.9, 35.9, 13.2. HRMS (ESI) m/z: calc. for $C_{10}H_{15}NOCl$ $[M + NH_4]^+$ 200.08367; found 200.08376.

Enantiomeric excess was determined by reducing it into alcohol with $NaBH_4$ and analyzing with HPLC: Daicel Chiralcel OD-H, hexane/iPrOH = 95:5, flowrate = 1.0 mL/min, λ= 220 nm, t_{major} = 7.4 min, t_{minor} = 7.9 min; 88.1:11.9 er.

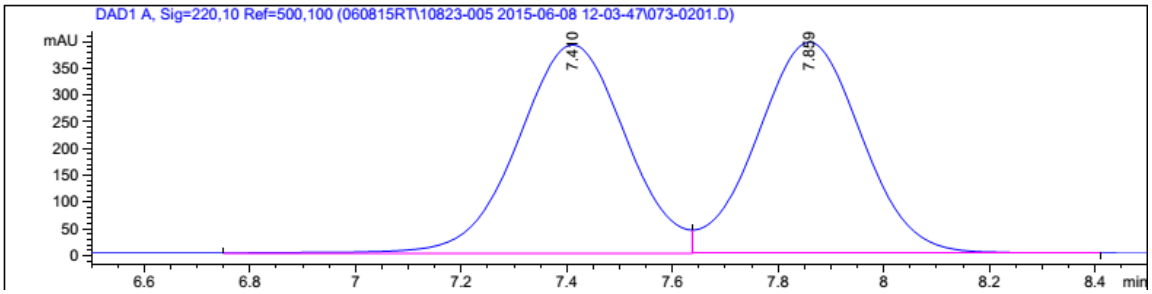

Peak #	RetTime [min]	Type	Width [min]	Area [mAU*s]	Height [mAU]	Area %
1	7.410	BV	0.2210	5589.13135	390.35101	50.4939
2	7.859	VB	0.2158	5479.78320	395.15179	49.5061

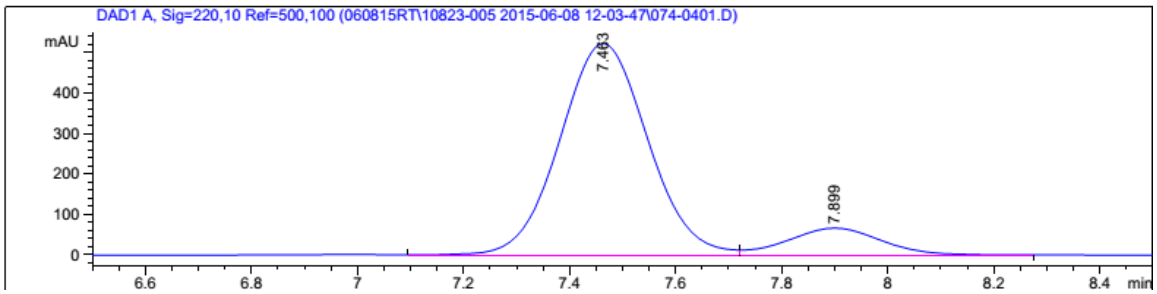

Peak #	RetTime [min]	Type	Width [min]	Area [mAU*s]	Height [mAU]	Area %
1	7.463	VV	0.1781	6011.87646	522.96301	88.0832
2	7.899	VB	0.1886	813.34637	66.52518	11.9168

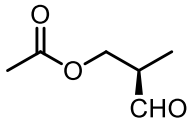

(*R*)-2-methyl-3-oxopropyl acetate (41)

Enantiomeric excess was determined by GC with a Supelco's Beta Dex 225 column: 90 ^{o}C, stay 10 mins, 0.8 ^{o}C/min to 100 ^{o}C, stay 2 mins, 0.8 ^{o}C/min to 110 ^{o}C, stay 10 mins, flow rate = 1.0 mL/min, t_{minor} = 28.0 min, t_{major} = 28.5 min; 93.3:6.7 er.

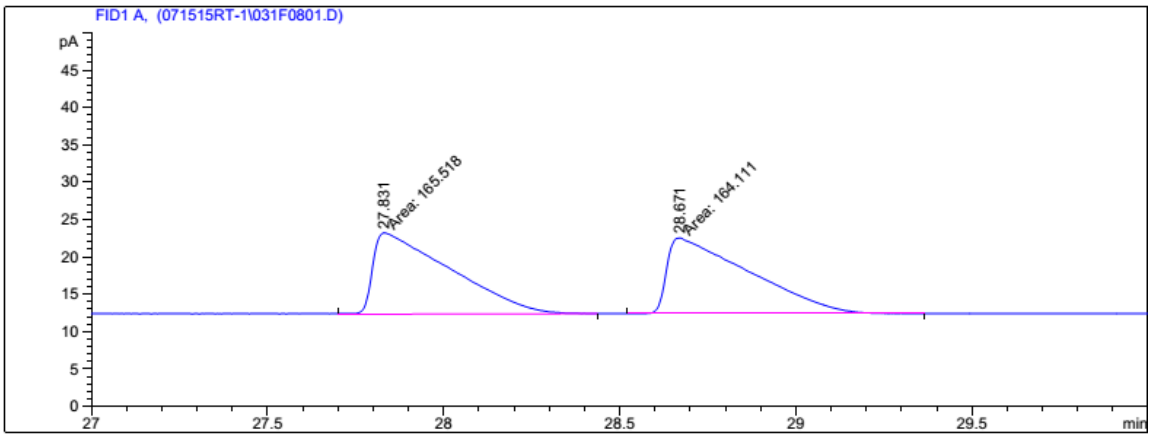

Peak #	RetTime [min]	Type	Width [min]	Area [pA*s]	Height [pA]	Area %
1	27.831	MM	0.2538	165.51833	10.87058	50.21350
2	28.671	MM	0.2707	164.11084	10.10436	49.78650

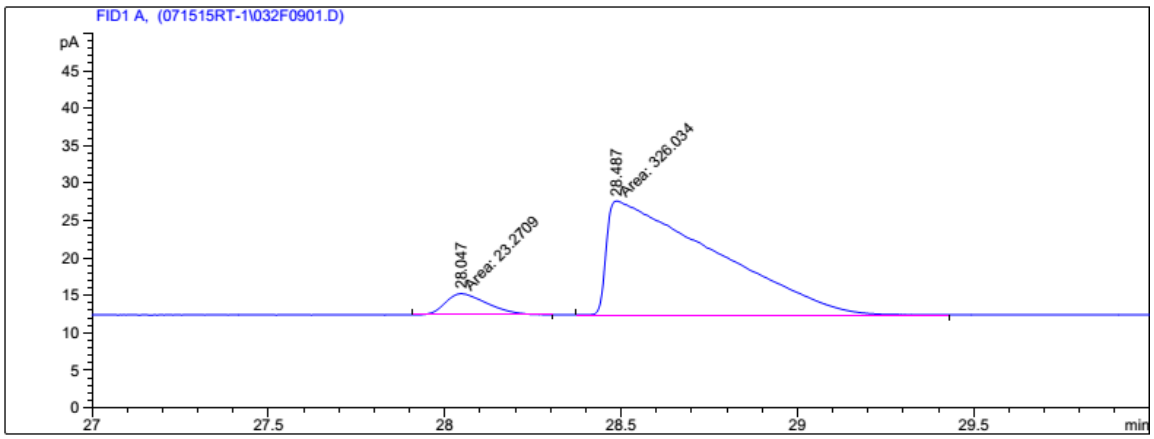

Peak #	RetTime [min]	Type	Width [min]	Area [pA*s]	Height [pA]	Area %
1	28.047	MM	0.1371	23.27093	2.82842	6.66207
2	28.487	MM	0.3569	326.03357	15.22648	93.33793

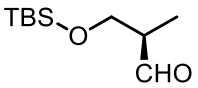

(*R*)-3-((tert-butyldimethylsilyl)oxy)-2-methylpropanal (43)

Enantiomeric excess was determined by GC with a Supelco's Beta Dex 225 column: 65 °C, stay 30 mins, 0.7 °C/min to 80 °C, stay 10 mins, 0.7 °C/min to 90 °C, stay 15 mins, flow rate = 1.0 mL/min, t_{major}= 70.1 min, t_{minor}= 70.9 min; 88.8:11.2 er.

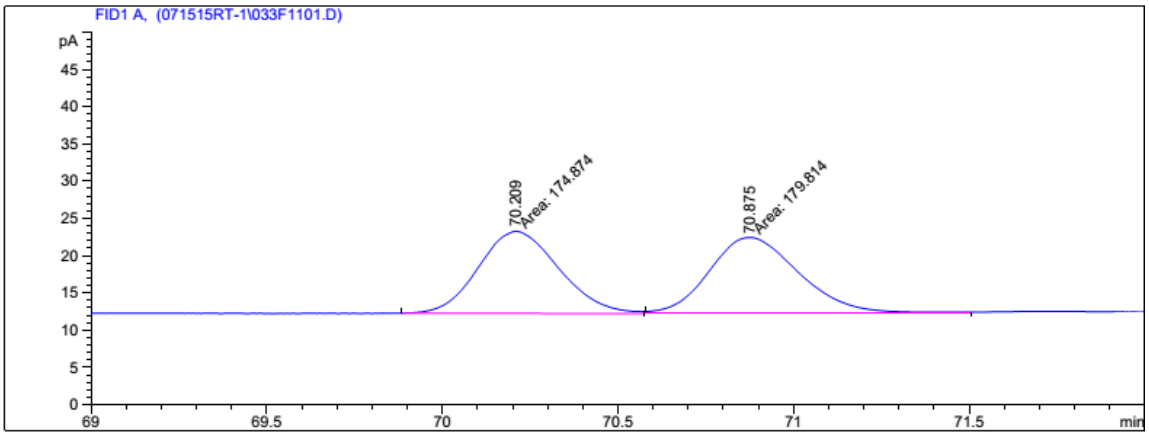

Peak #	RetTime [min]	Type	Width [min]	Area [pA*s]	Height [pA]	Area %
1	70.209	MM	0.2646	174.87355	11.01422	49.30359
2	70.875	MM	0.2953	179.81372	10.14775	50.69641

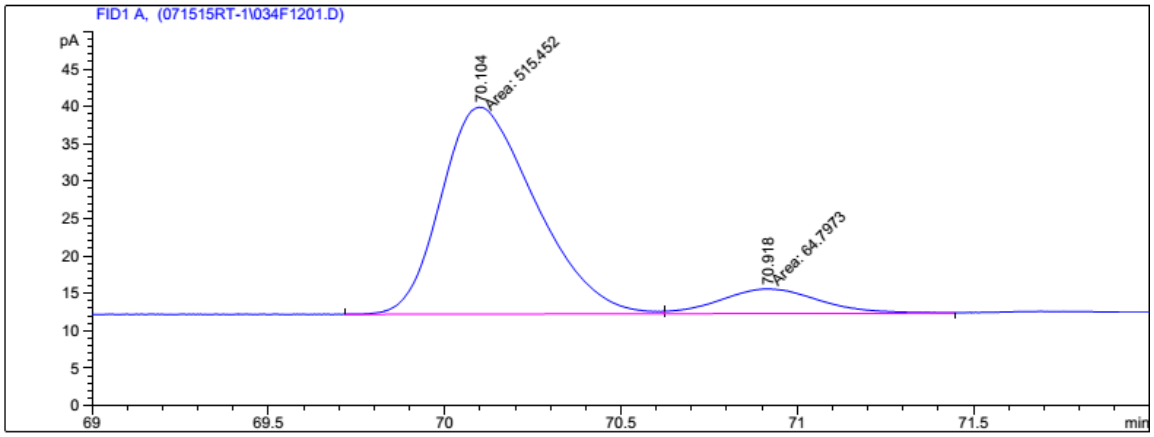

Peak #	RetTime [min]	Type	Width [min]	Area [pA*s]	Height [pA]	Area %
1	70.104	MF	0.3105	515.45172	27.66763	88.83285
2	70.918	FM	0.3284	64.79728	3.28817	11.16715

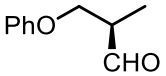

(*R*)-2-methyl-3-phenoxypropanal (45)

Enantiomeric excess was determined by GC with a Supelco's Beta Dex 225 column: 90 ^{o}C, stay 0 min, 1 ^{o}C/min to 160 ^{o}C, flow rate = 1.0 mL/min, t_{major}= 49.3 min, t_{minor}= 49.7 min; 86.8:13.2 er.

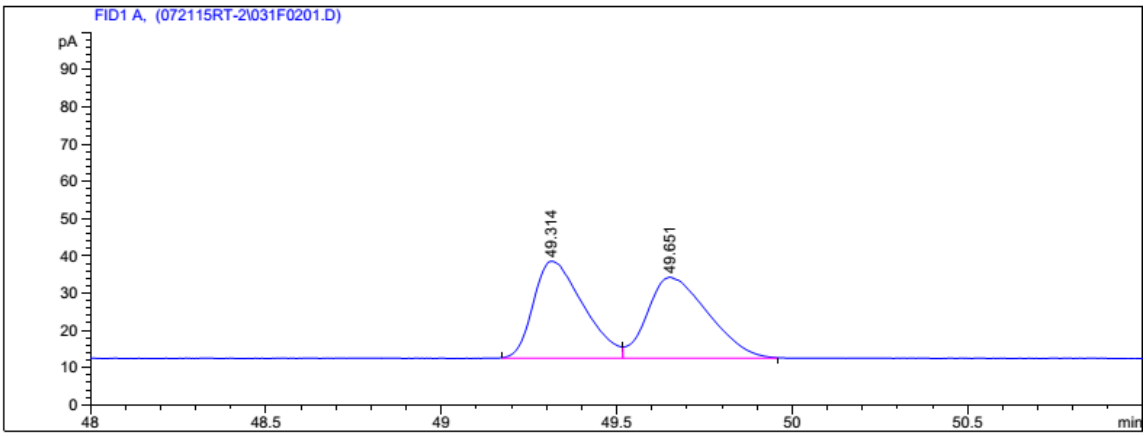

Peak #	RetTime [min]	Type	Width [min]	Area [pA*s]	Height [pA]	Area %
1	49.314	BV	0.1332	256.14853	25.94542	49.64802
2	49.651	VB	0.1547	259.78049	21.70042	50.35198

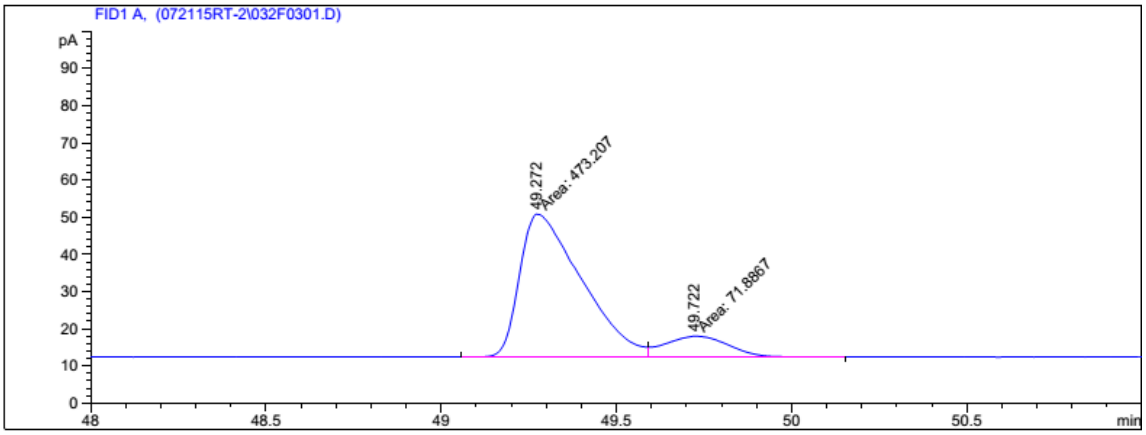

Peak #	RetTime [min]	Type	Width [min]	Area [pA*s]	Height [pA]	Area %
1	49.272	MF	0.2047	473.20676	38.52391	86.81204
2	49.722	FM	0.2114	71.88669	5.66666	13.18796

1.5.5 ^{1}H NMR Spectra of Crude AHF Reaction Mixtures (toluene as solvent)

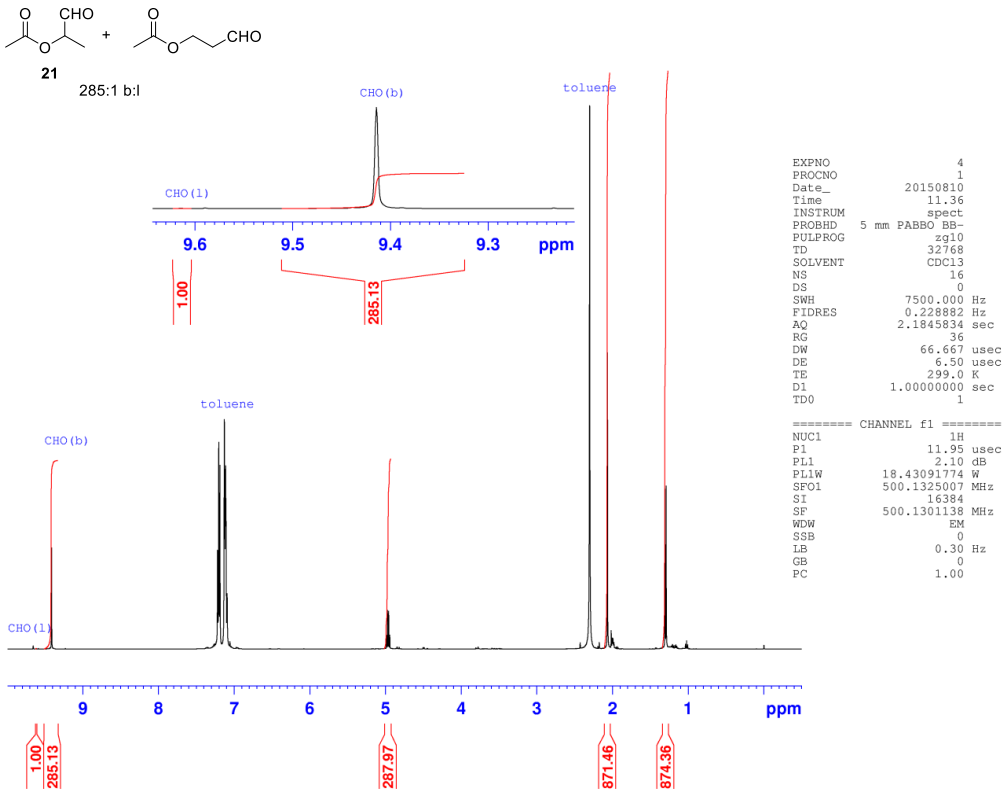

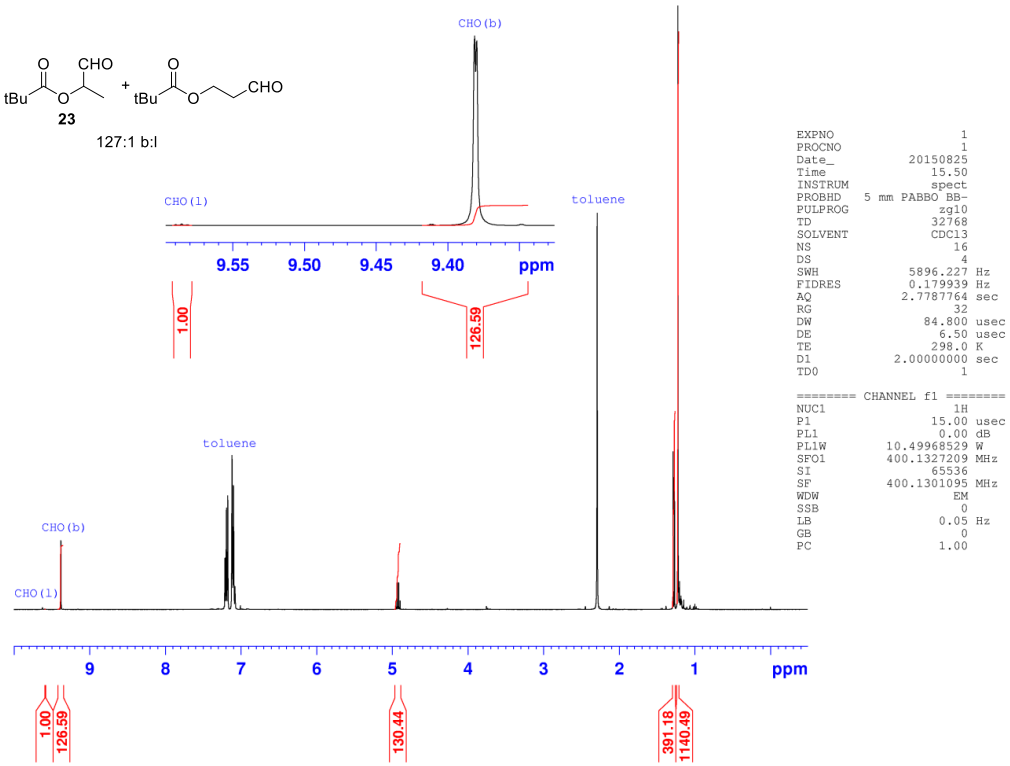
tBu
O
CHO
O
+
tBu
O
O
CHO
23
127:1 b:l
CHO (b)
CHO (1)
toluene
9.55
9.50
9.45
9.40
ppm
1.00
126.59
toluene
CHO (b)
CHO (1)
9
8
7
6
5
4
3
2
1
ppm
1.00
126.59
130.44
391.18
1140.49
EXPNO 1
PROCNO 1
Date_ 20150825
Time 15.50
INSTRUM spect
PROBHD 5 mm PABBO BB-
PULPROG zg10
TD 32768
SOLVENT CDCl3
NS 16
DS 4
SWH 5896.227 Hz
FIDRES 0.179939 Hz
AQ 2.7787764 sec
RG 32
DW 84.800 usec
DE 6.50 usec
TE 298.0 K
D1 2.00000000 sec
TD0 1
======== CHANNEL f1 ========
NUC1 1H
P1 15.00 usec
PL1 0.00 dB
PL1W 10.49968529 W
SFO1 400.1327209 MHz
SI 65536
SF 400.1301095 MHz
WDW EM
SSB 0
LB 0.05 Hz
GB 0
PC 1.00

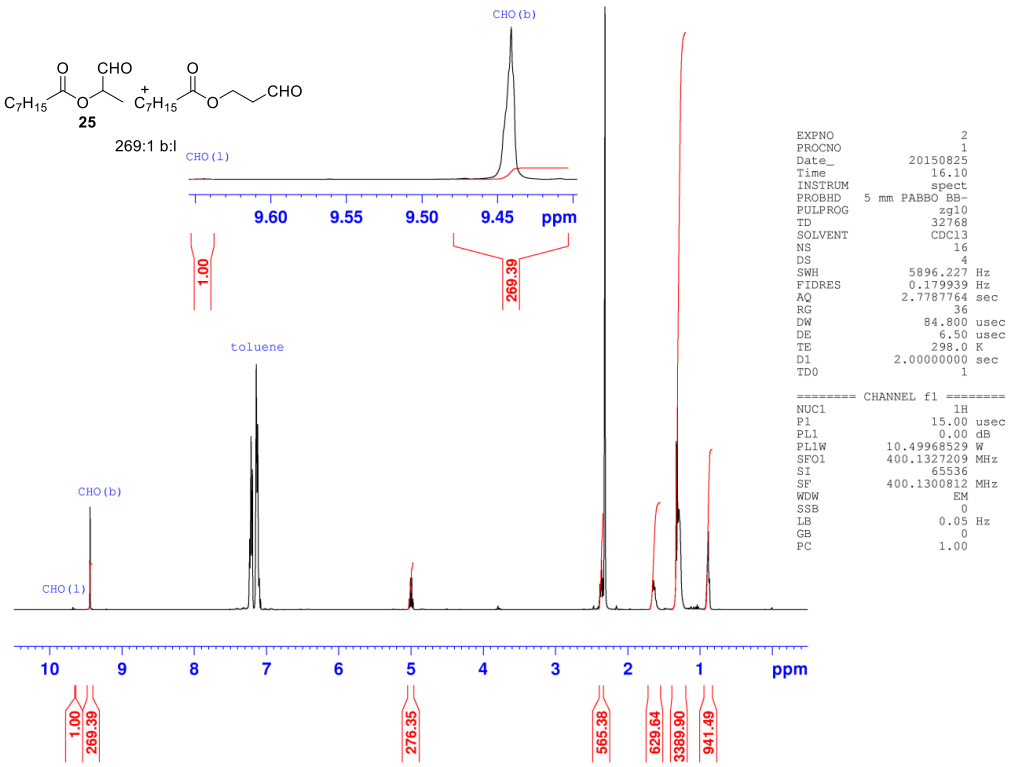
C7H15
O
CHO
O
+
C7H15
O
O
CHO
25
269:1 b:l
CHO (b)
CHO (1)
9.60
9.55
9.50
9.45
ppm
1.00
269.39
toluene
CHO (b)
CHO (1)
10
9
8
7
6
5
4
3
2
1
ppm
1.00
269.39
276.35
565.38
629.64
3389.90
941.49
EXPNO 2
PROCNO 1
Date_ 20150825
Time 16.10
INSTRUM spect
PROBHD 5 mm PABBO BB-
PULPROG zg10
TD 32768
SOLVENT CDCl3
NS 16
DS 4
SWH 5896.227 Hz
FIDRES 0.179939 Hz
AQ 2.7787764 sec
RG 36
DW 84.800 usec
DE 6.50 usec
TE 298.0 K
D1 2.00000000 sec
TD0 1
======== CHANNEL f1 ========
NUC1 1H
P1 15.00 usec
PL1 0.00 dB
PL1W 10.49968529 W
SFO1 400.1327209 MHz
SI 65536
SF 400.1300812 MHz
WDW EM
SSB 0
LB 0.05 Hz
GB 0
PC 1.00

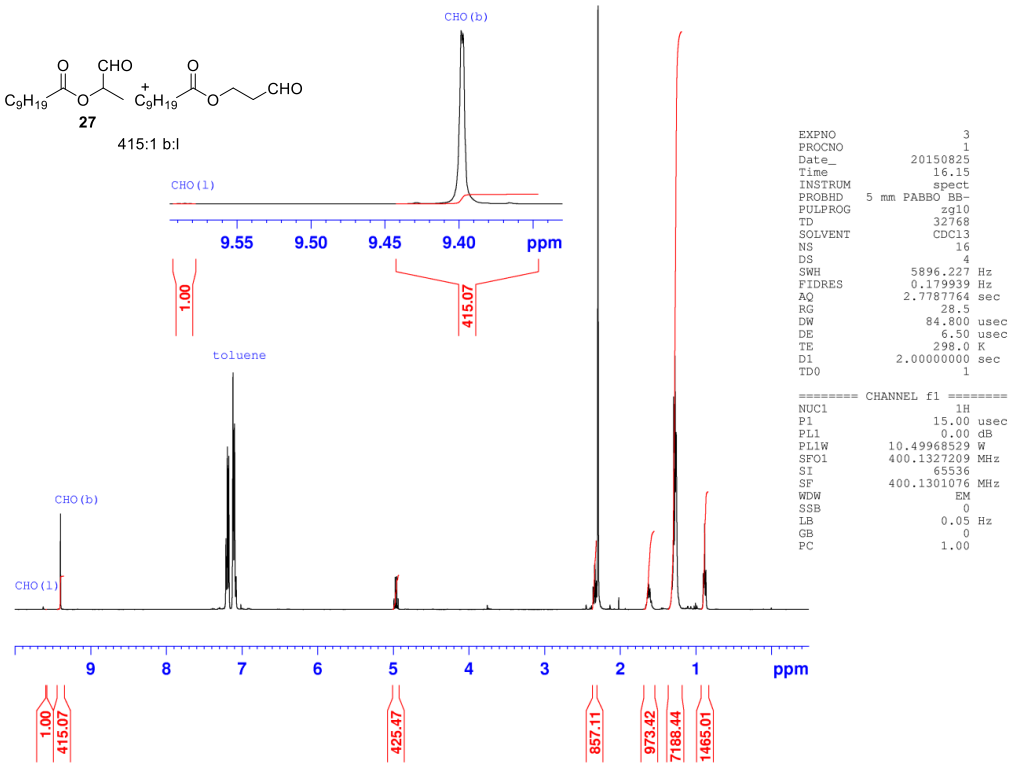
27
415:1 b:l
CHO (b)
CHO (l)
toluene
9.55 9.50 9.45 9.40 ppm
1.00
415.07
9 8 7 6 5 4 3 2 1 ppm
425.47
857.11
973.42
7188.44
1465.01
EXPNO 3
PROCNO 1
Date_ 20150825
Time 16.15
INSTRUM spect
PROBHD 5 mm PABBO BB-
PULPROG zg10
TD 32768
SOLVENT CDCl3
NS 16
DS 4
SWH 5896.227 Hz
FIDRES 0.179939 Hz
AQ 2.7787764 sec
RG 28.5
DW 84.800 usec
DE 6.50 usec
TE 298.0 K
D1 2.00000000 sec
TD0 1
======== CHANNEL f1 ========
NUC1 1H
P1 15.00 usec
PL1 0.00 dB
PL1W 10.49968529 W
SFO1 400.1327209 MHz
SI 65536
SF 400.1301076 MHz
WDW EM
SSB 0
LB 0.05 Hz
GB 0
PC 1.00

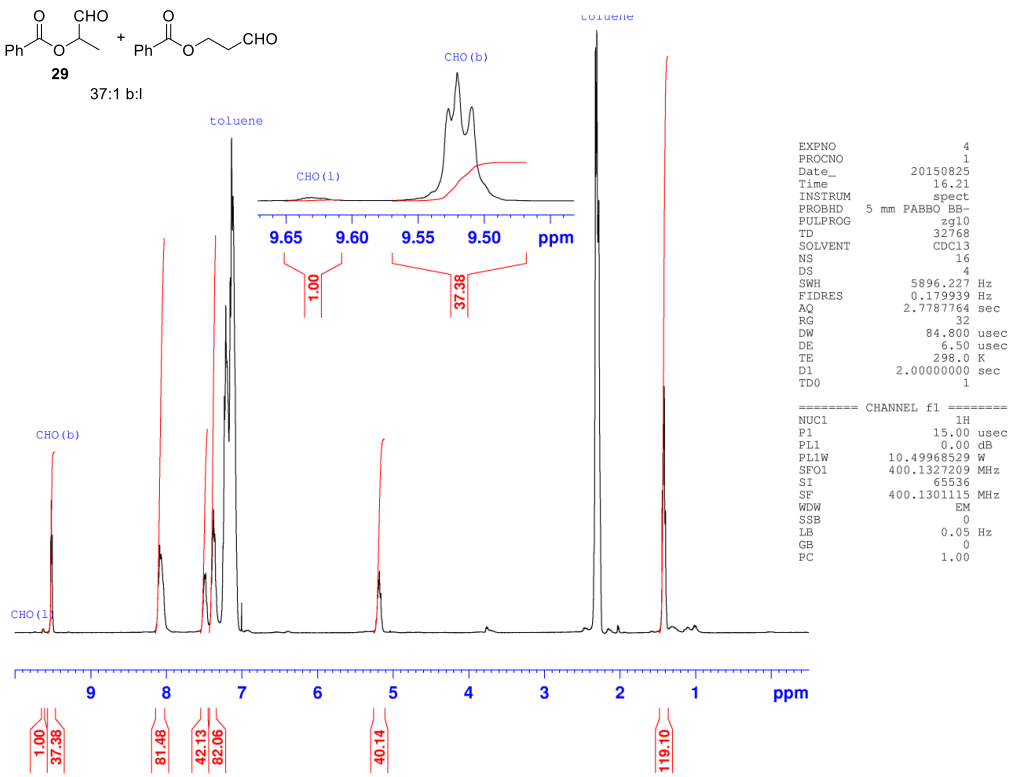
29
37:1 b:l
toluene
CHO (b)
CHO (l)
9.65 9.60 9.55 9.50 ppm
1.00
37.38
9 8 7 6 5 4 3 2 1 ppm
81.48
42.13
82.06
40.14
119.10
EXPNO 4
PROCNO 1
Date_ 20150825
Time 16.21
INSTRUM spect
PROBHD 5 mm PABBO BB-
PULPROG zg10
TD 32768
SOLVENT CDCl3
NS 16
DS 4
SWH 5896.227 Hz
FIDRES 0.179939 Hz
AQ 2.7787764 sec
RG 32
DW 84.800 usec
DE 6.50 usec
TE 298.0 K
D1 2.00000000 sec
TD0 1
======== CHANNEL f1 ========
NUC1 1H
P1 15.00 usec
PL1 0.00 dB
PL1W 10.49968529 W
SFO1 400.1327209 MHz
SI 65536
SF 400.1301115 MHz
WDW EM
SSB 0
LB 0.05 Hz
GB 0
PC 1.00

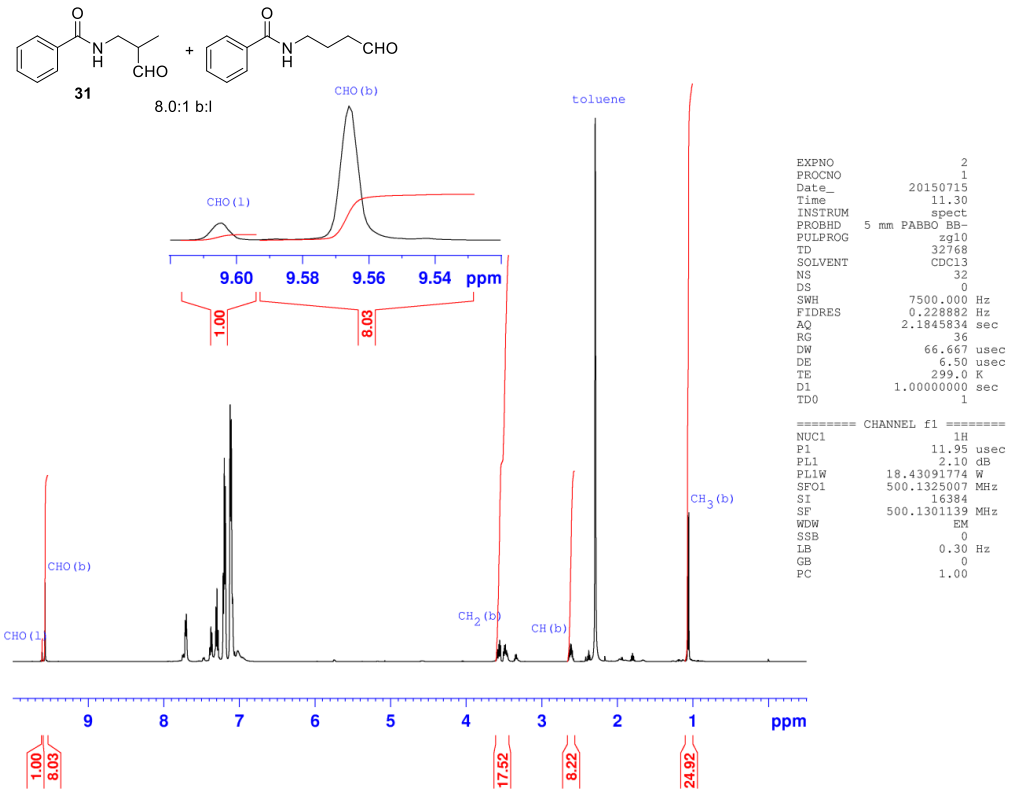
31
8.0:1 b:l
CHO(b)
CHO(l)
toluene
9.60
9.58
9.56
9.54
ppm
1.00
8.03
CHO(b)
CHO(l)
CH2(b)
CH(b)
CH3(b)
9
8
7
6
5
4
3
2
1
ppm
1.00
8.03
17.52
8.22
24.92
EXPNO 2
PROCNO 1
Date_ 20150715
Time 11.30
INSTRUM spect
PROBHD 5 mm PABBO BB-
PULPROG zg10
TD 32768
SOLVENT CDCl3
NS 32
DS 0
SWH 7500.000 Hz
FIDRES 0.228882 Hz
AQ 2.1845834 sec
RG 36
DW 66.667 usec
DE 6.50 usec
TE 299.0 K
D1 1.00000000 sec
TD0 1
======== CHANNEL f1 ========
NUC1 1H
P1 11.95 usec
PL1 2.10 dB
PL1W 18.43091774 W
SFO1 500.1325007 MHz
SI 16384
SF 500.1301139 MHz
WDW EM
SSB 0
LB 0.30 Hz
GB 0
PC 1.00

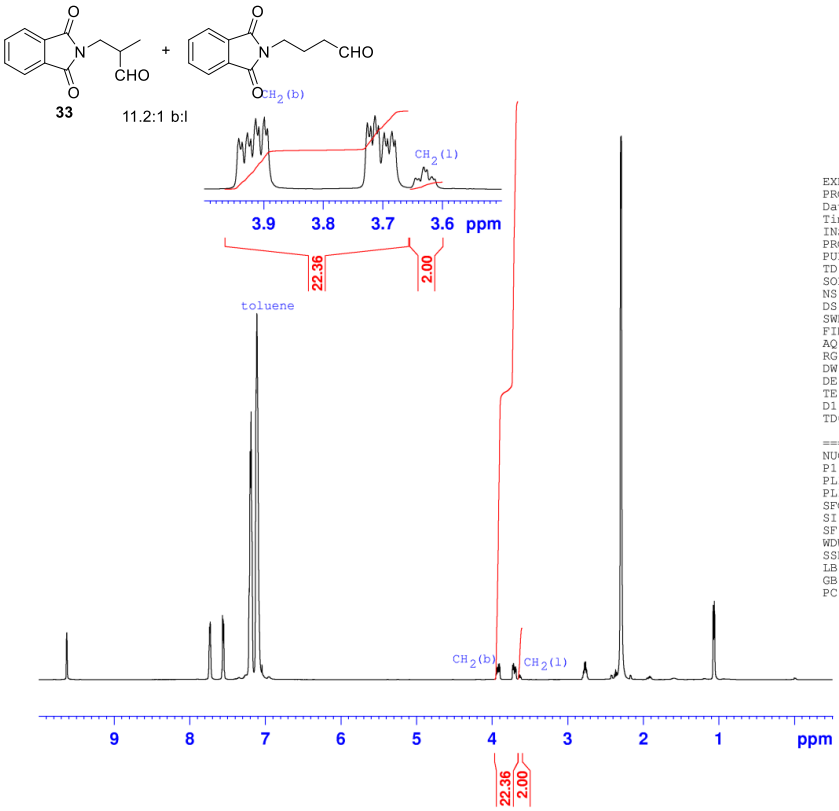


```
EXPNO                  8
PROCNO                 1
Date_           20150715
Time               12.03
INSTRUM            spect
PROBHD   5 mm PABBO BB-
PULPROG            zg10
TD                32768
SOLVENT           CDCl3
NS                   32
DS                    0
SWH            7500.000 Hz
FIDRES         0.228882 Hz
AQ           2.1845834 sec
RG                 40.3
DW               66.667 usec
DE                6.50 usec
TE                299.0 K
D1           1.00000000 sec
TD0                    1

======== CHANNEL f1 =======
NUC1                  1H
P1                11.95 usec
PL1                2.10 dB
PL1W        18.43091774 W
SFO1        500.1325007 MHz
SI                16384
SF          500.1301220 MHz
WDW                  EM
SSB                   0
LB                 0.30 Hz
GB                    0
PC                 1.00
```

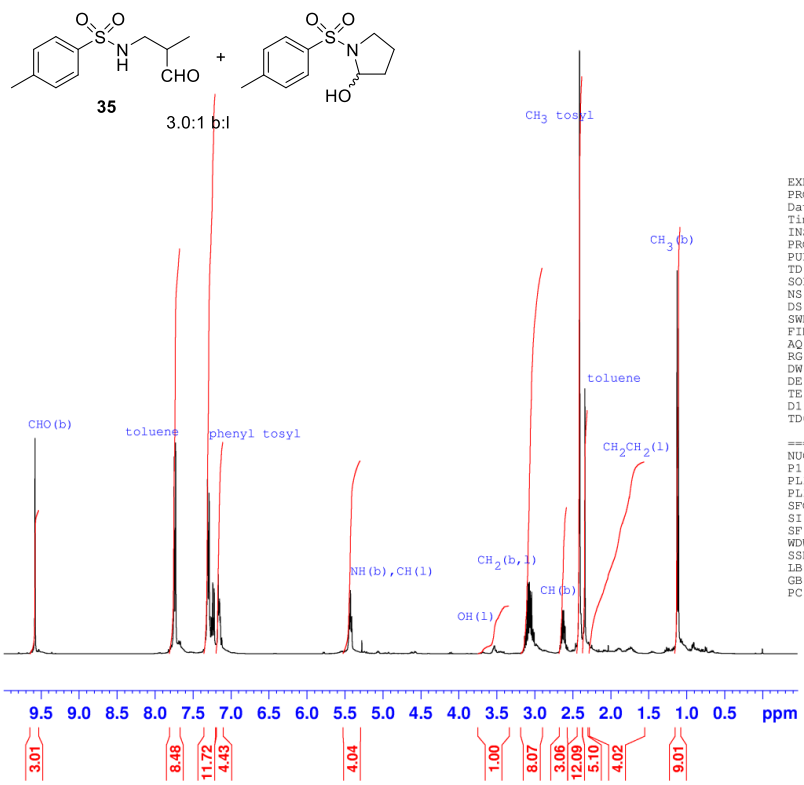


```
EXPNO                  1
PROCNO                 1
Date_           20160218
Time               17.32
INSTRUM            spect
PROBHD   5 mm PABBO BB-
PULPROG            zg30
TD                65536
SOLVENT           CDCl3
NS                   16
DS                    2
SWH            8223.685 Hz
FIDRES         0.125483 Hz
AQ           3.9846387 sec
RG                   32
DW               60.800 usec
DE                6.50 usec
TE                295.6 K
D1           1.00000000 sec
TD0                    1

======== CHANNEL f1 =======
NUC1                  1H
P1                 8.76 usec
PL1               -2.00 dB
PL1W        31.17179108 W
SFO1        400.1324710 MHz
SI                32768
SF          400.1300045 MHz
WDW                  EM
SSB                   0
LB                 0.30 Hz
GB                    0
PC                 1.00
```

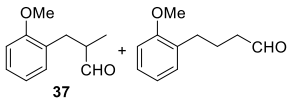

37

1.2:1 b:l

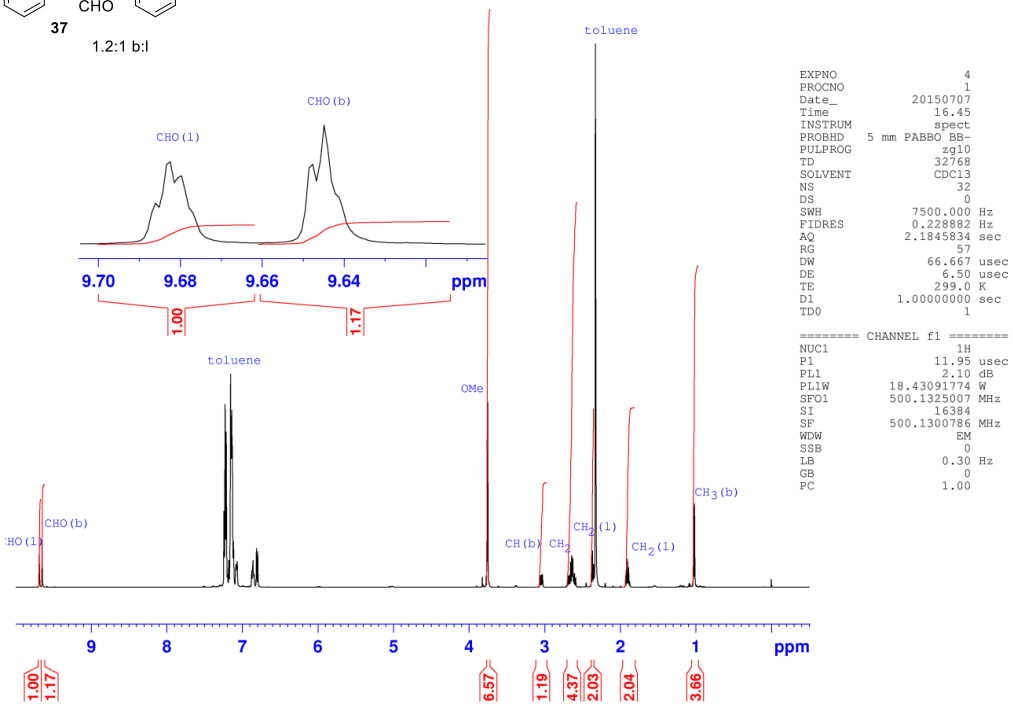


```
EXPNO                  4
PROCNO                 1
Date_           20150707
Time               16.45
INSTRUM            spect
PROBHD   5 mm PABBO BB-
PULPROG             zg10
TD                 32768
SOLVENT            CDCl3
NS                    32
DS                     0
SWH            7500.000 Hz
FIDRES         0.228882 Hz
AQ           2.1845834 sec
RG                    57
DW               66.667 usec
DE                 6.50 usec
TE                299.0 K
D1          1.00000000 sec
TD0                    1

======== CHANNEL f1 =======
NUC1                  1H
P1                11.95 usec
PL1                2.10 dB
PL1W         18.43091774 W
SFO1        500.1325007 MHz
SI                16384
SF          500.1300786 MHz
WDW                   EM
SSB                    0
LB                  0.30 Hz
GB                     0
PC                  1.00
```

39

1.1:1 b:l

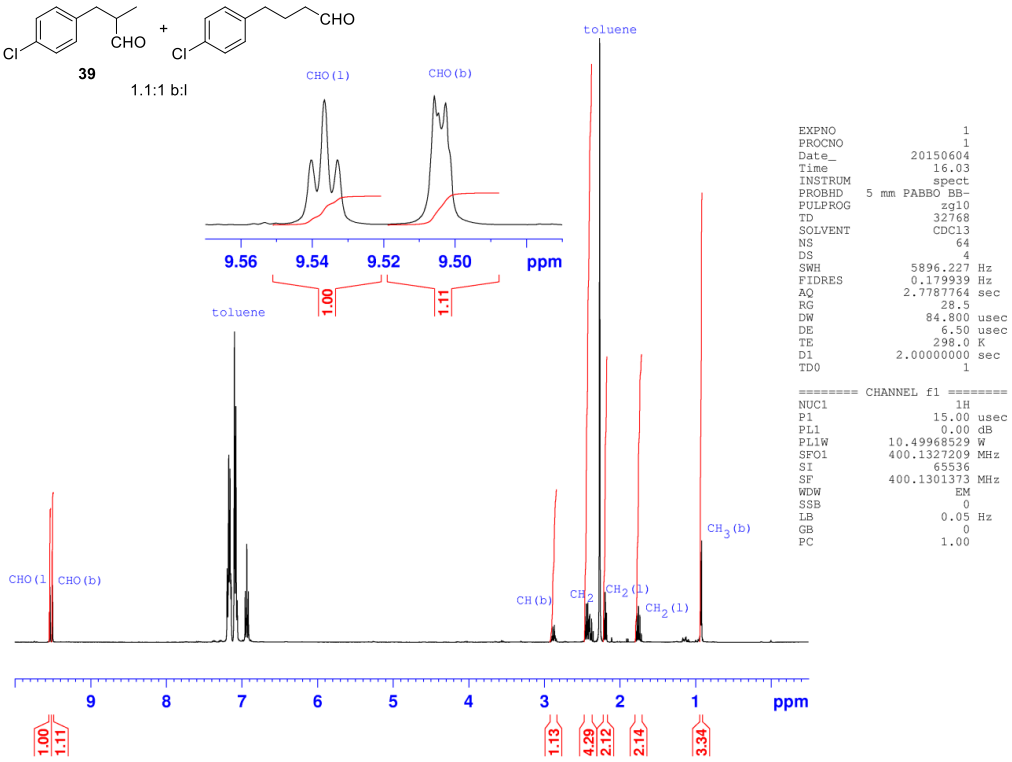

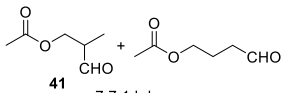

41

7.7:1 b:l

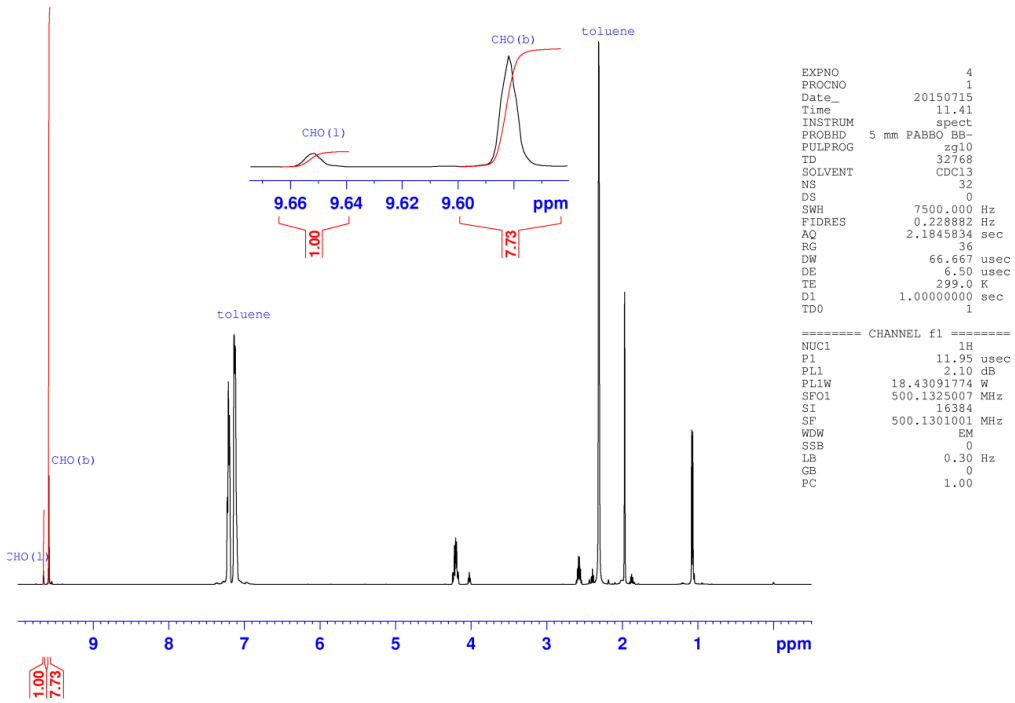

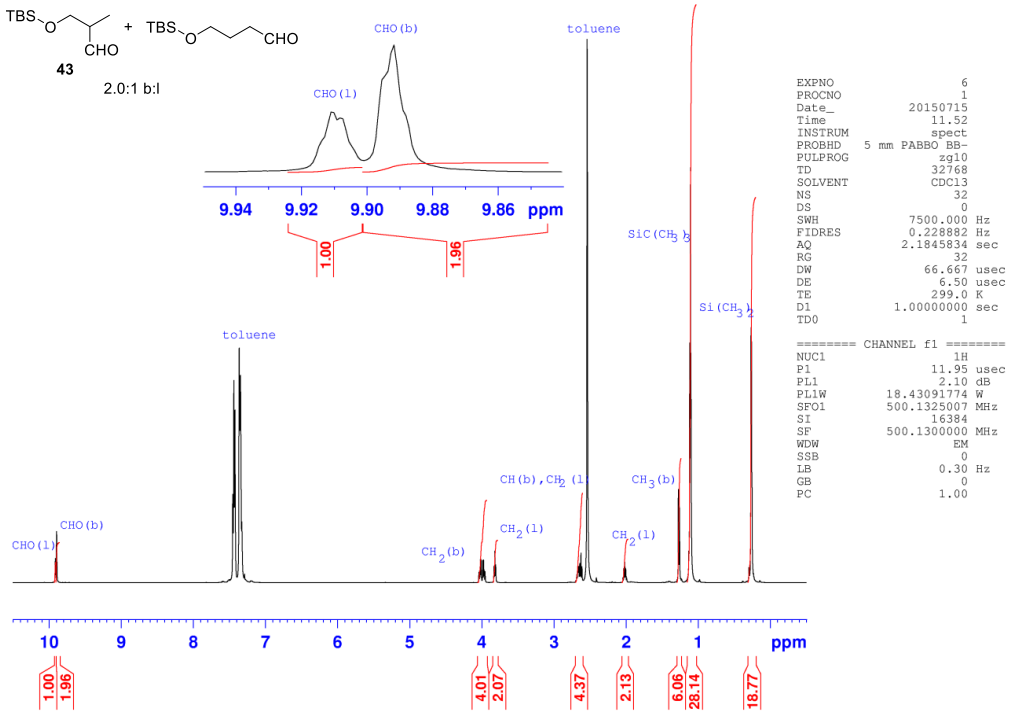
TBS
O
CHO
43
+
TBS
O
CHO
2.0:1 b:l
CHO(b)
CHO(l)
toluene
9.94
9.92
9.90
9.88
9.86
ppm
1.00
1.96
SiC(CH3)3
Si(CH3)2
toluene
CH(b),CH2 (l
CH3(b)
CHO(b)
CHO(l)
CH2(b)
CH2(l)
CH2(l)
10
9
8
7
6
5
4
3
2
1
ppm
1.00
1.96
4.01
2.07
4.37
2.13
6.06
28.14
18.77
EXPNO 6
PROCNO 1
Date_ 20150715
Time 11.52
INSTRUM spect
PROBHD 5 mm PABBO BB-
PULPROG zg10
TD 32768
SOLVENT CDCl3
NS 32
DS 0
SWH 7500.000 Hz
FIDRES 0.228882 Hz
AQ 2.1845834 sec
RG 32
DW 66.667 usec
DE 6.50 usec
TE 299.0 K
D1 1.00000000 sec
TD0 1
======== CHANNEL f1 ========
NUC1 1H
P1 11.95 usec
PL1 2.10 dB
PL1W 18.43091774 W
SFO1 500.1325007 MHz
SI 16384
SF 500.1300000 MHz
WDW EM
SSB 0
LB 0.30 Hz
GB 0
PC 1.00

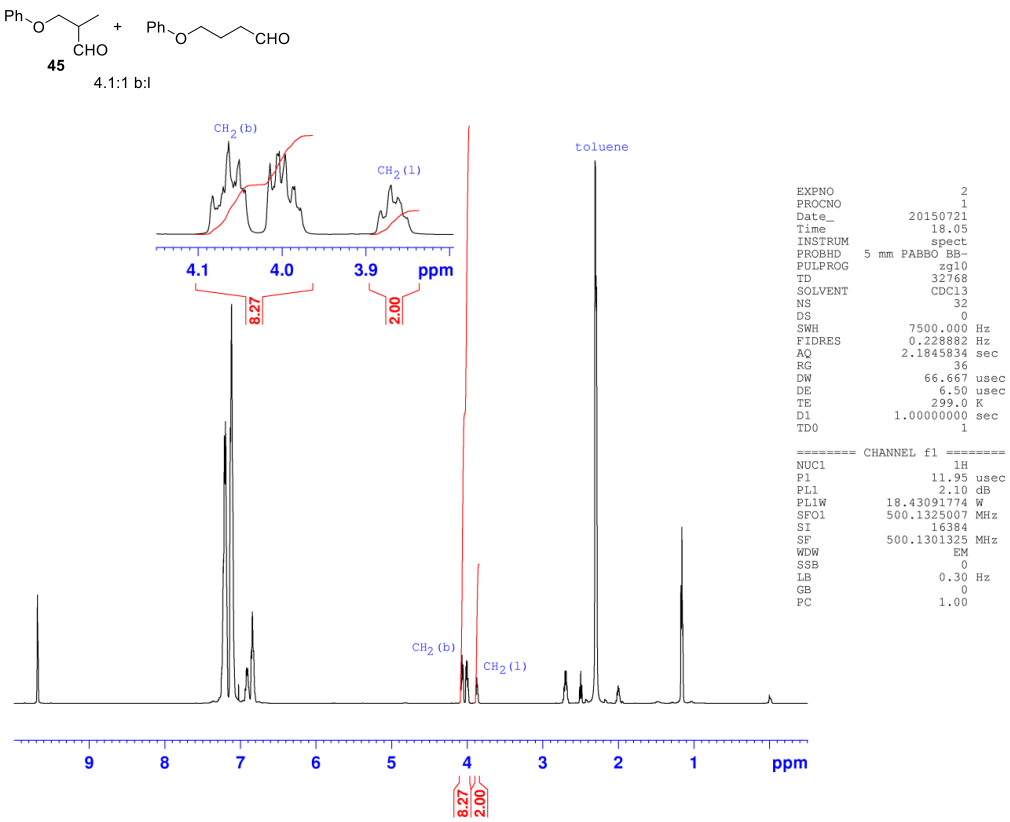
Ph
O
CHO
45
+
Ph
O
CHO
4.1:1 b:l
CH2(b)
CH2(l)
toluene
4.1
4.0
3.9
ppm
8.27
2.00
CH2(b)
CH2(l)
9
8
7
6
5
4
3
2
1
ppm
8.27
2.00
EXPNO 2
PROCNO 1
Date_ 20150721
Time 18.05
INSTRUM spect
PROBHD 5 mm PABBO BB-
PULPROG zg10
TD 32768
SOLVENT CDCl3
NS 32
DS 0
SWH 7500.000 Hz
FIDRES 0.228882 Hz
AQ 2.1845834 sec
RG 36
DW 66.667 usec
DE 6.50 usec
TE 299.0 K
D1 1.00000000 sec
TD0 1
======== CHANNEL f1 ========
NUC1 1H
P1 11.95 usec
PL1 2.10 dB
PL1W 18.43091774 W
SFO1 500.1325007 MHz
SI 16384
SF 500.1301325 MHz
WDW EM
SSB 0
LB 0.30 Hz
GB 0
PC 1.00

1.6 References

1. Roelen, O. (Chemische Verwertungsgesellschaft, mbH Oberhausen) German Patent DE 849 548 (1938/1952) Roelen, O. (Chemische Verwertungsgesellschaft, mbH Oberhausen) U.S. Patent 2 327 066 (1943); *Chem. Abstr.***1944**, *38*, 5501.
2. Evans, D. A.; Osborn, J. A.; Wilkinson, G. *J. Chem. Soc. A.* **1968**, 3133.
3. Pruchnik, F. P. Organometallic Chemistry of Transition Elements; Plenum Press: New York, 1990; p 691.
4. Beller, M.; Cornils, B.; Frohning, C. D.; Kohlpaintner, C. W. *J. Mol. Catal. A: Chem.* **1995**, *104*, 17.
5. Heck, R. F.; Breslow, D. S. *J. Am. Chem. Soc.* **1961**, *83*, 4023.
6. Jardine, F. H. *Polyhedron* **1982**, *1*, 569.
7. Csontos, G.; Heil, B.; Marko, L. *Ann. N. Y. Acad. Sci.* **1974**, *239*, 47.
8. Versluis, L.; Ziegler, T.; Fau, L. *Inorg. Chem.* **1990**, *29*, 4530.
9. (a) Musaev, D. G.; Matsubara, T.; Mebel, A. M.; Koga, N.; Morokuma, K. *Pure & Appl. Chem.* **1995**, *67*, 257. (b) Matsubara, T.; Koga, N.; Ding, Y.; Musaev, D. G.; Morokuma, K. *Organometallics* **1997**, *16*, 1065.
10. (a) Claver, C.; van Leeuwen, P. W. N. M. *Rhodium Catalyzed Hydroformylation*, Kluwer Academic Publishers, Dordrecht, **2002**. (b) Franke, R.; Selent, D.; Börner, A. *Chem. Rev.* **2012**, *112*, 5675. (c) Agbossou, F.; Carpentier, J. F.; Mortreaux, A. *Chem. Rev.* **1995**, *95*, 2485. (d) Gual, A.; Godard, C.; Castillón, S.; Claver, C. *Tetrahedron: Asymmetry* **2010**, *21*, 1135.
11. Sakai, N.; Mano, S.; Nozaki, K.; Takaya, H. *J. Am. Chem. Soc.* **1993**, *115*, 7033.
12. (a) Babin, J. E.; Whiteker, G. T. (Union Carbide Corporation), WO 9303839, **1993**. (b) Whiteker, G. T.; Briggs, J. R.; Babin, J. E.; Barner, B. A. *Chemical Industries*, Vol. 89, Marcel Dekker, New York, **2003**, 359.
13. Breeden, S.; Cole-Hamilton, D. J.; Foster, D. F.; Schwarz, G. J.; Wills, M. *Angew. Chem., Int. Ed.* **2000**, *39*, 4106.
14. Cobley, C. C.; Klosin, J.; Qin, C.; Whiteker, G. T. *Org. Lett.* **2004**, *6*, 3277.
15. (a) Clark, T. P.; Landis, C. R.; Freed, S. L.; Klosin, J.; Abboud, K. A. *J. Am. Chem. Soc*. **2005**, *127*, 5040. (b) Axtell, A. T.; Cobley, C. J.; Klosin, J.; Whiteker, G. T.; Zanotti-Gerosa, A.; Abboud, K. A*. Angew. Chem., Int. Ed.* **2005**, *44*, 5834. (c) Klosin, J.; Landis, C. R. *Acc. Chem. Res.* **2007**, *40*, 1251.
16. Axtell, A. T.; Cobley, C. J.; Klosin, J.; Whiteker, G. T.; Zanotti-Gerosa, A.; Abboud, K. A. *Angew. Chem., Int. Ed.* **2005**, *44*, 5834.
17. Huang, J.; Bunel, E.; Allgeier, A.; Tedrow, J. Storz, T.; Preston, J.; Correll, T.; Manley, D.; Soukup, T.; Jensen, R.; Syed, R.; Moniz, G.; Larsen, R.; Martinelli, M.; Reider, P. J. *Tetrahedron Letters* **2005**, *46*, 7831.
18. Axtell, A. T.; Klosin, J. *Organometallics* **2006**, *25*, 5003.
19. Wang, X.; Buchwald, S. L. *J. Org. Chem.* **2013**, *78*, 3429.
20. (a) *Angew. Chem. Int. Ed.,* **2002**, *41*, 1612. (b) *Org. Lett.*, **2003**, *5*, 205. (c) *Org. Lett.*, **2002**, *4*, 4159. (d) *Angew. Chem. Int. Ed.*, **2006**, *45*, 3832.
21. 1. *Angew. Chem. Int. Ed.*, **2005**, *44*, 1687.

22. Tang, W.; Qu, B.; Capacci, A. G.; Rodriguez, S.; Wei, X.; Haddad, N.; Narayanan, B.; Ma, S.; Grinberg, N.; Yee, N. K.; Krishnamurthy, D.; Senanayake, C. H. *Org. Lett*. **2010**, *12*, 176.
23. Franke, R.; Selent, D.; Börner, A. *Chem. Rev.* **2012**, *112*, 5675.
24. Gaussian 09, Revision C.01, Frisch, M. J.; Trucks, G. W.; Schlegel, H. B.; Scuseria, G. E.; Robb, M. A.; Cheeseman, J. R.; Scalmani, G.; Barone, V.; Mennucci, B.; Petersson, G. A. et al. Gaussian, Inc., Wallingford CT, **2010**.
25. (a) Becke, A. D. *J. Chem. Phys.* **1993**, *98*, 5648. (b) Lee, C.; Yang, W.; Parr, R. G. *Phys. Rev. B* **1988**, *37,* 785.
26. (a) Hay, P. J.; Wadt, W. R. *J. Chem. Phys.* **1985**, *82*, 270. (b) Wadt, W. R.; Hay, P. J. *J. Chem. Phys.* **1985**, *82*, 299. (c) Dunning, T. H. Jr.; Hay, P. J. in *Modern Theoretical Chemistry*, Ed. H. F. Schaefer III, Vol. 3 (Plenum, New York, 1977) 1-28.
27. Kruse, H.; Grimme, S. *J. Chem. Phys.* **2012**, *136*, 154101.
28. (a) Grimme, S.; Ehrlich, S.; Goerigk, L. *J. Comput. Chem.* **2011**, *32*, 1456. (b) Kruse, H.; Goerigk, L.; Grimme, S. *J. Org. Chem.* **2012**, *77*, 10824.
29. (a) Tonks, I. A.; Froese, R. D.; Landis, C. R. *ACS Catal.* **2013**, *3*, 2905. (b) For DFT computed rhodium catalyzed asymmetric hydroformylation pathway, see: Luo, X.; Tang, D.; Li, M. *Int. J. Quantum Chem.* **2005**, *105*, 108.
30. Breit, B.; Seiche, W.; *Synthesis*. **2001**, *1*, 1.
31. (a) Garst, M. E.; Lukton, D. *J. Org. Chem.* **1981**, *46*, 4433. (b) Amer, I.; Alper, H. *J. Am. Chem. Soc.* **1990**, *112*, 3674. (c) Axet, M. R.; Castillon, S.; Claver, C. *Inorg. Chim. Acta.* **2006**, *359*, 2973. (d) Dübon, P.; Farwick, A.; Helmchen, G. *Synlett* **2009**, *9*, 1413.
32. Zhang, X.; Cao, B.; Yu, S.; Zhang, X. *Angew. Chem. Int. Ed.* **2010**, *49*, 4047.
33. Barrow, R. A.; Hemscheidt, T.; Liang, J.; Paik, S.; Moore, R. E.; Tius, M. A. *J. Am. Chem. Soc.* **1995**, *117*, 2479. (b) Nazaré, M.; Waldmann, H. *Chem. Eur. J.* **2001**, *7*, 3363.
34. (a) Nozaki, K. *et al. J. Am. Chem. Soc.* **1997,** *119,* 4413. (b) Zhang, X. *et al*. *J. Am. Chem. Soc*. **2006**, *128*, 7198. (c) Landis, C. *et al. Org. Lett.* **2008***, 10*, 4553. (c) Zhang, X. *et al. Chem. Eur. J.* **2014**, *20*, 4357. (d) Breit, B. *et al. Adv. Synth. Catal.* **2015**, *357*, 41.
35. (a) Cabaj, J. E.; Kairys, D.; Benson, T. R. *Org. Process Res. Dev.*, **2007**, *11*, 378. (b) Gil, S.; Parra, M.; Rodriguez, P.; Segura, J. *Mini-Reviews in Organic Chemistry***, 2009**, *6*, 345.
36. Otley, K. D.; Ellman, J. A. *Org. Lett.*, **2015**, *17*, 1332.

Chapter 2

Asymmetric Hydroformylation of 1,1-Disubstituted Alkenes

2.1 Introduction

Although various substrates have been reported for successful asymmetric hydroformylstion (AHF)[1] and several important complex compounds[2] have been synthesized with methods based on AHF, these substrates are mostly monosubstituted or 1,2-disubstituted alkenes. 1,1-disubstituted alkenes remain unsolved and very challenging substrates. Actually, 1,1-disubstitued alkenes are challenging in many asymmetric reactions[3] (ex. asymmetric hydrogenation, epoxidation and hydroboration) aiming to generate chiral products. It is because (1) the disubstituted feature makes them more bulky around the carbon-carbon double bonds, comparing to monosubstituted alkenes, resulting in generally lower association rate of alkenes to catalytic metal centers, thus lower reaction rates; (2) comparing to mono substituted alkenes, the two substitutions on disubstituted alkenes are normally much more difficult to be differentiated by chiral catalysts, since their similar sized enantiotopic faces are difficult for differentiating, thus high enantioselectivity is more difficult to achieve. Despite they are challenging, there is a great advantage for AHF of 1,1-disubstituted alkenes: both branched and linear aldehyde products are chiral (Figure 2.1).

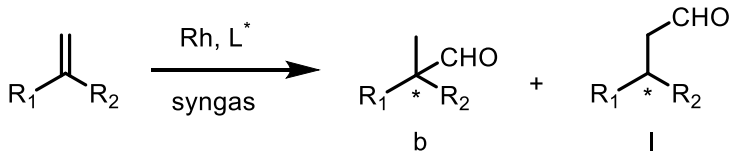

Figure 2.1 Asymmetric hydroformylation of 1,1-disubstituted alkenes

The first AHF 1,1-disbstituted alkenes were reported by Consiglio and Morandini in 1985[4], in which the authors applied various $PtCl_2/SnCl_2$ and Rh based catalysts with (*S*,*S*)-ChiraPhos or (*R*,*R*)-DIOP to the AHF of *α*-methyl styrene, with low enantioselectivity (up to 21% ee) favoring linear aldehyde products, even under harsh reaction conditions. Ever since that, a few examples[5] on AHF of α-methyl styrene, methyl methacrylate and α-alkyl acrylates catalyzing by $PtCl_2/SnCl_2$ and Rh based catalysts have been reported, however all suffered from poor reactivity and/or stereoselectivity.

The first remarkable Rh based AHF of 1,1-disbstituted alkenes was reported by Landis and coworkers in 2010 (Figure 2.2)[6], they applied their powerful chiral diazaphospholane ligands for Rh catalyzed AHF of *N*-(1-alkyl)vinyl phthalimide, obtaining a chiral β^3-aminoaldehyde with 74% ee, along with 24% starting material and a significant amount of isomerization product.

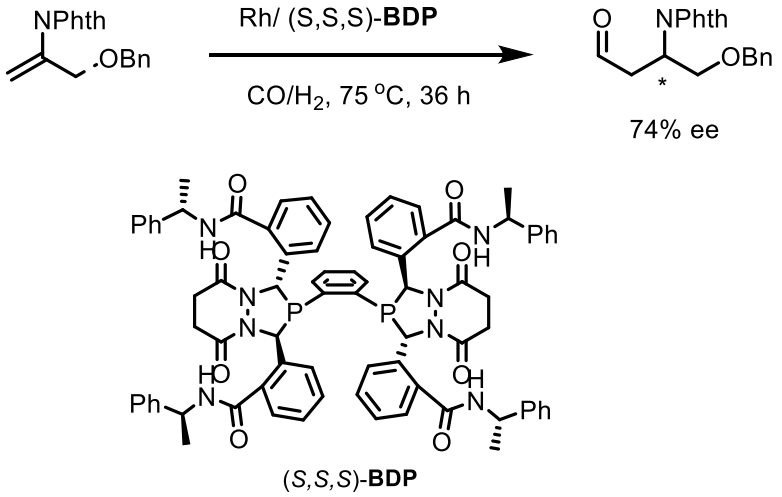

Figure 2.2 Asymmetric hydroformylation of *N*-(1-alkyl)vinyl phthalimide

In 2011, Buchwald[7] and coworkers reported a successful highly enantioselective process for the Rh catalyzed hydroformylation of *α*-alkylacrylates (Fighre 2.3) , in which (*R,R*)-BenzP* was demonstrated to be capable of hydroformylating various of *α*-alkylacrylates into linear aldehyde products with moderate to good yields and up to 94% ee values, along with branched aldehyde and hydrogenation side products. The resulting linear aldehydes can be easily further transformed into 2-isopropyl- and 2-cyclohexyl-1,4-dicarbonyl structures (which were previously synthesized via multi-steep asymmetric hydrogenation based methods), which have potential applications many biologically active compounds(Figure 2.3).[8]

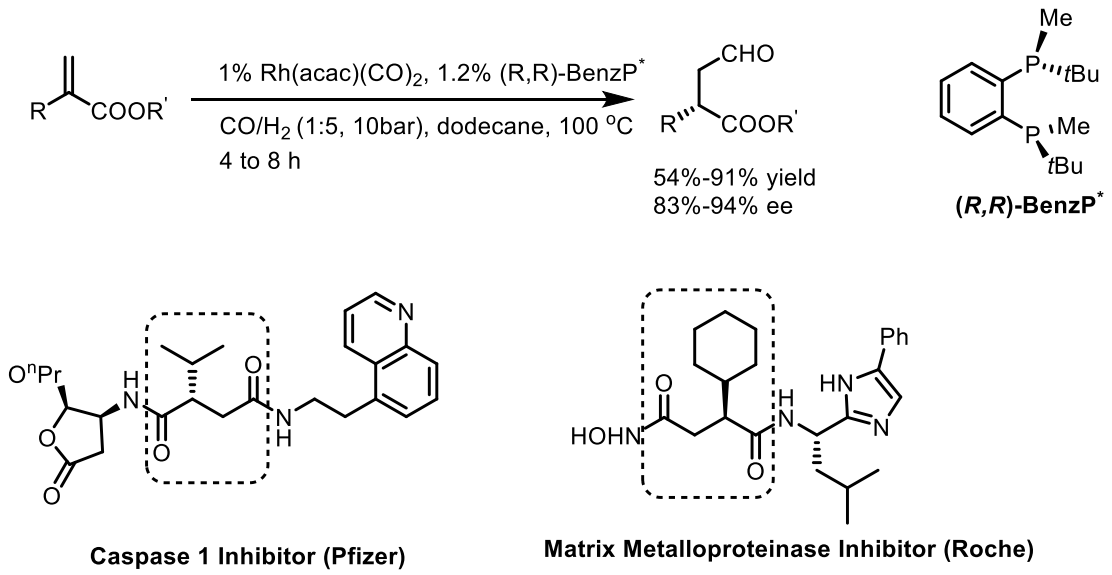

Figure 2.3 Asymmetric hydroformylation of *α*-alkylacrylates and potential applications

In 2013, the same group[9] reported the Rh catalyzed AHF of 1-(trifluoromethyl)-ethenyl acetate (Figure 2.4), in which, branched aldehyde was favored. When (*R,R,S,S*)-DuanPhos was used, the branched aldehyde was generated in high yield and excellent enantioselectivity (92% ee), which was then oxidized into enantiomerically pure 2-trifluoromethyllactic acid (TFMLA, >99% ee after recrystallization), an important building block for many active pharmaceutical ingredients.[10]

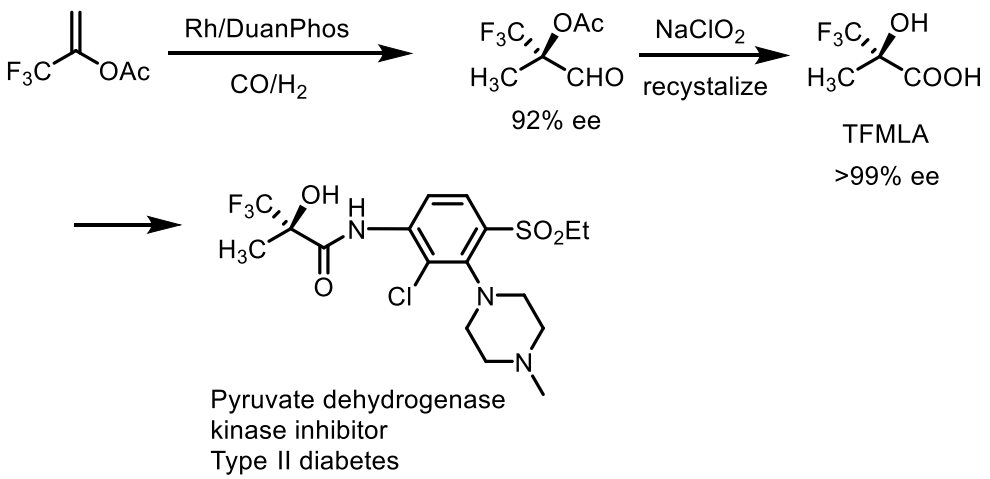

Figure 2.4 Asymmetric hydroformylation of 1-(trifluoromethyl)-ethenyl acetate and example application

Recently, our group[11] reported the Rh catalyzed AHF of 1,1-disubstituted allylphthalimides (Figure 2.5), as a catalytic route β^3-amino acids, among the screened 10 different chiral phosphorus ligands, (S,S)-Ph-BPE was found to be most efficient, giving the corresponding linear aldehydes in moderate to excellent yields and up to 95% ee. The resulting chiral aldehydes can be easily oxidized or reduced into important synthetic building blocks in drug synthesis (Figure 2.5).[12]

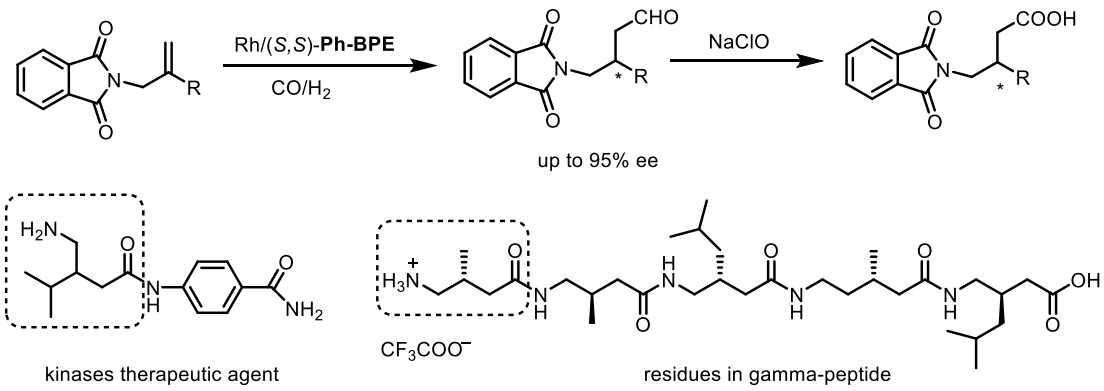

Figure 2.5 Asymmetric hydroformylation of 1,1-disubstituted allylphthalimides and potential applications

Despite these a few successful examples of AHF of 1,1-disubstituted alkenes, this class of substrates are still very challenging for simultaneously controlling chemo-, regioo- and stereoselectivities, and meanwhile achieving high reactivity.

2.2 Asymmetric hydroformylation of 1-(trifluoromethyl)-ethenyl acetate

Encouraged by the successful AHF of monosubstituted alkenes with BIBOP ligands, we started our exploration of applying BIBOP ligands to AHF of 1-(trifluoromethyl)-ethenyl acetate **1** (Table 2.1). Considering it is a challenging 1,1-disubstituted alkene, we set the reaction temperature to be 100 ℃ for the initial trial. Among the four tested BIBOP ligands with different substitution on 4-position of the benzene ring, Me-BIBOP and Ph-BIBOP performed very badly (Table 2.1, entries 3 and 4), giving very low conversion or no reaction at all, in the presence of 15/5 bar syngas.

Table 2.1 Ligand screening for AHF of 1-(trifluoromethyl)-ethenyl acetate 1[a]

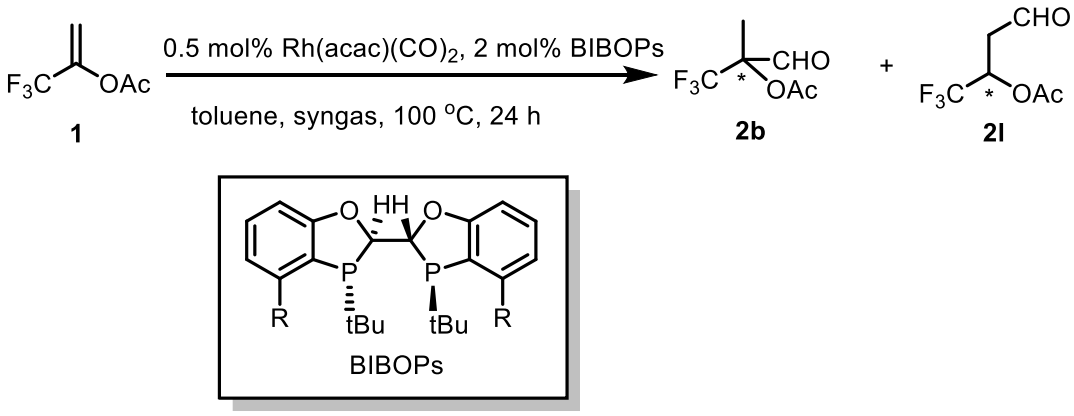

Entry	ligand	CO/H_2	Conv. (%)	b/l [b]	er [c]
1	MeO-BIBOP	15/5	40	1.6	64.5/35.5
2	BIBOP	15/5	41	9.0	91.6/8.4
3	Me-BIBOP	15/5	13	NA	NA
4	Ph-BIBOP	15/5	NR	NA	NA
5	BIBOP	5/5	>99	10.0	90.0/10.0

[a] Reaction conditions: **1** (1.0 mmol) catalyzed by Rh-ligand in toluene (0.5 mL) at 100 ℃ for 24 h under syngas pressure of 20 bar. [b] Conversions and branch to linear ratio (b:l) of the products were determined by ^{1}H NMR spectroscopy. [c] Determined by Chiral GC.

Such poor performances for Me-BIBOP and Ph-BIBOP are probably due to the stereo hinders in the chiral catalytic pocket generated by the ligand and rhodium center, making it very difficult for the bulky itself substrate to bind to

the rhodium center. And for those two ligands succeeding the hydroformylation, they both favor the branched aldehyde as the product. BIBOP provides much better region- and enantioselectivity than MeO-BIBOP does, although they give very similar conversions (both about 40%, Table 2.1 entries 1 and 2). Thus, we focused on BIBOP for further condition screening.

Since it is a normal phenomenon[13] in AHF that lower CO partial pressure will increase the conversion and decrease the enantioselectivity. We lowered the CO partial pressure to 5 bar and remaining the H_2 pressure unchanged (Table 2.1 entry 5), the conversion was dramatically increased to >99%, the enantioselectivity only slightly decreased to 90/10 er.

Then, the ligand to rhodium ratio was screened (Table 2.2), it turns out that only 1 equivalent ligand was needed to maintain the high enantioselectivity, comparing to amount of rhodium. Also, since these screening were conducted under a lower reaction temperature 80 ℃, slightly high er's and lower conversions were obtained.

Thus, 100 ℃ and 5/5 bar CO/H_2 were used as the optimized reaction condition, in which 1-(trifluoromethyl)-ethenyl acetate **1** was fully hydroformylated with 10/1 b/l ratio and 90/10 er.

Table 2.2 Ligand/Rh ratio screening for AHF of 1-(trifluoromethyl)-ethenyl acetate 1[a]

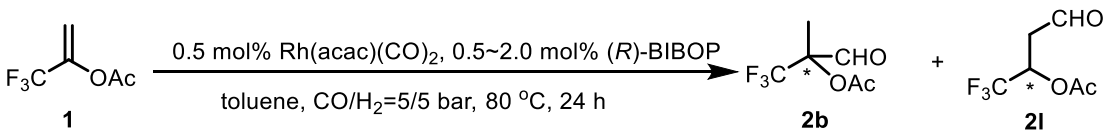

Entry	Rh/L	Conv (%)	b/l[b]	er[c]
1	1/1	77.8	7.7	92.1/7.9
2	1/2	78.8	7.6	92.1/7.9
3	1/3	80.4	7.4	92.1/7.9
4	1/4	76.5	7.6	92.1/7.9

[a] Reaction conditions: **1** (1.0 mmol) catalyzed by Rh-ligand in toluene (0.5 mL) at 80 ℃ for 24 h under syngas. [b] Conversions and branch to linear ratio (b:l) of the products were determined by ^{1}H NMR spectroscopy. [c] Determined by Chiral GC.

2.3 Asymmetric hydroformylation of *α*-(trifluoromethyl)styrene

We next examined another 1,1-disubstituted alkene, *α*-(trifluoromethyl)styrene **3**. It is an analog compound to 1-(trifluoromethyl)-ethenyl acetate **1**, by replacing the acetyl group with phenyl ring. The first rhodium catalyzed AHF of this substrate derivative was reported by Breit[14] and coworkers in 2014 (Figure 2.6), in which 1,3-dichloro-5-(3,3,3-trifluoroprop-1-en-2-yl)benzene was hydroformylated. (*R,R*)-Ph-BPE was proved to be the best ligand which exclusively favors the

branched aldehyde product, although giving only 59% ee. Noticeably, ligand properties play a vital role in regioselectivity for this substrate.

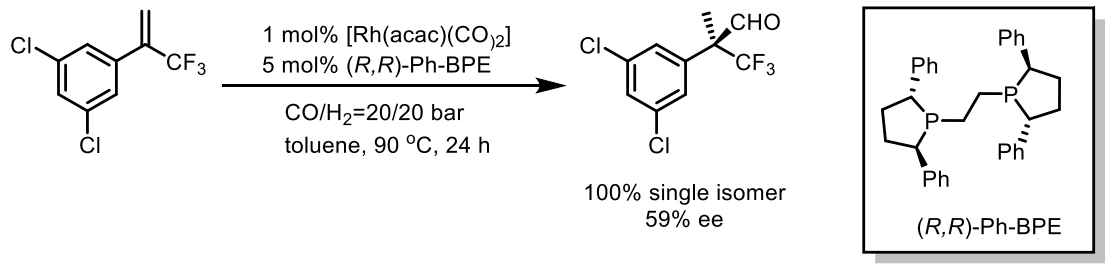

Figure 2.6 Asymmetric hydroformylation of 1,3-dichloro-5-(3,3,3-trifluoroprop-1-en-2-yl)benzene

Cooperating with Boehringer Ingelheim, we extensively screened the chiral ligand library for AHF of *α*-(trifluoromethyl)styrene **3** (Figure 2.7). Similar to Breit's work, we found that the chiral ligands basically can be separated into two sub groups favoring linear and branched aldehyde product respectively.

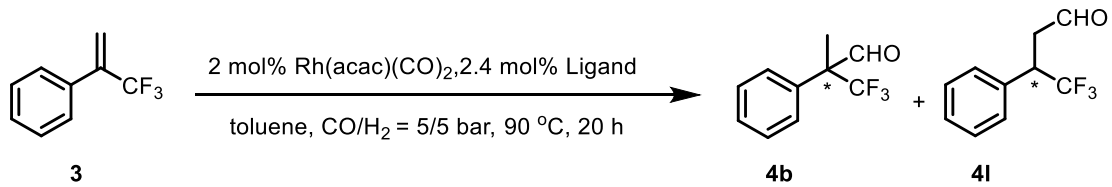

Figure 2.7 Ligand screening for asymmetric hydroformylation of *α*-(trifluoromethyl)styrene

Among the screened chiral ligands, lots of them suffered from reactivity of chemoselectivity giving no reaction or large amount of hydrogenation product. For those succeeding the AHF, seven of them favored the linear aldehyde product **4l** (Figure 2.8). The first 5 ligands all give very high linear product ratio, althou the first 4 give low conversions. Our BIBOP and BI-PN ligand give

almost full conversion. Since we are more interested in applying this AHF strategy for generating quaternary carbon centers, only ee of the branched product was measured, the enantioselectivity for branched product turned out to be very low (up to 22% ee)

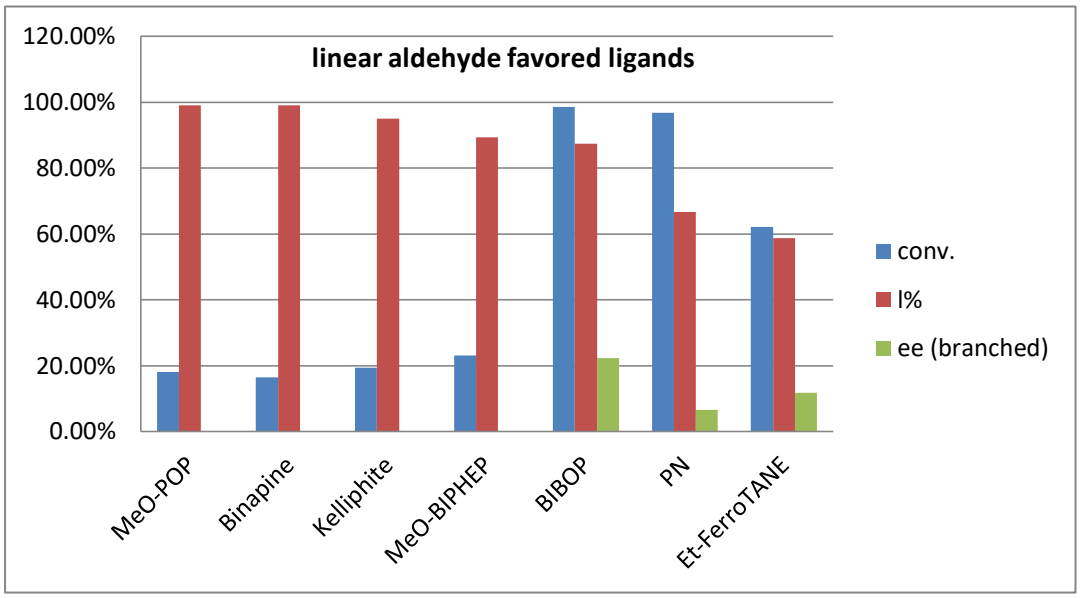

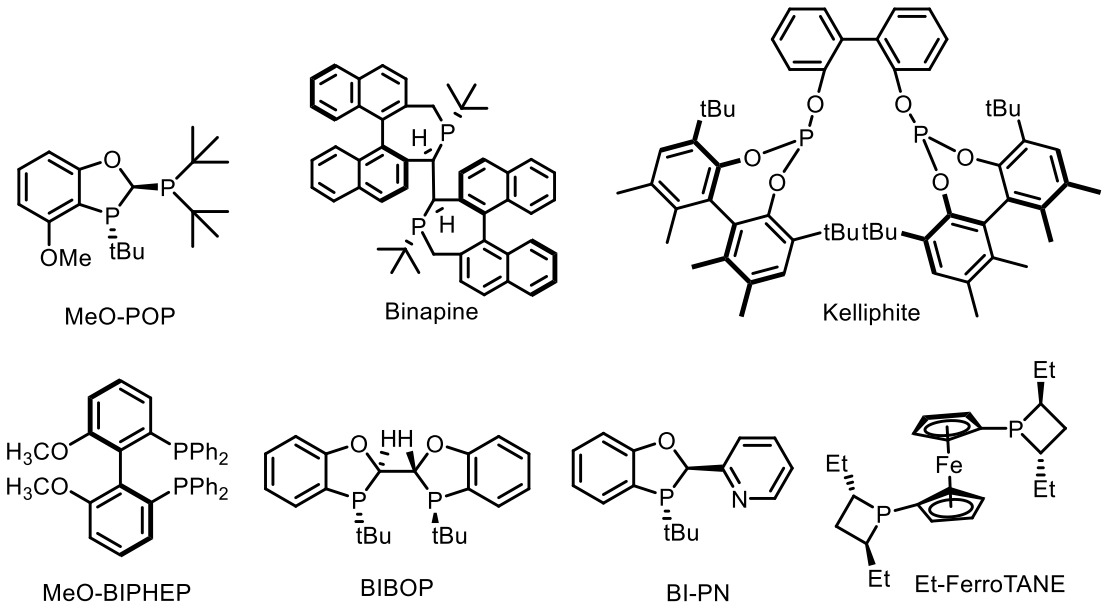

Figure 2.8 Linear aldehyde favored ligands for AHF of *α*-(trifluoromethyl)styrene

Five of the screened ligands favored the branched aldehyde product (Figure 2.9), under CO/H2 = 5/5 bar, 90 ℃ for 20 h, Ph-BPE, Me-DuPhos, DuanPhos and QuinoxP* all offered full conversions, among them, the first two ligands give about 70% branched aldehyde product. Regarding the enantioselectivity, Me-DuPhos, DuanPhos and BenzP* have the best performances, giving more than 60% ee for the branched aldehyde product. Interestingly, Ph-BPE offered 60% ee for the linear aldehyde product, although it is not the major product.

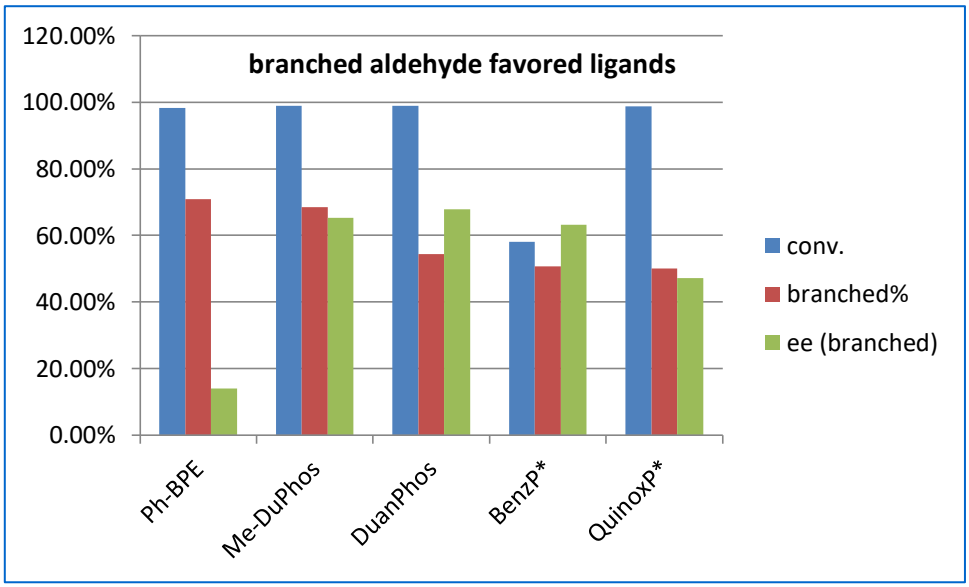

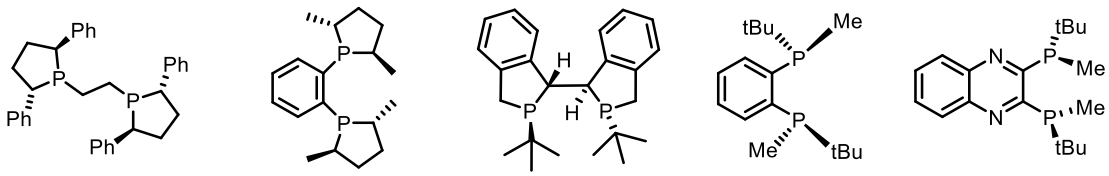

b/l = 2.5/1
er (linear) = 80:20

Figure 2.9 Branched aldehyde favored ligands for AHF of *α*-(trifluoromethyl)styrene

2.4 Conclusion

Although some progresses have been demonstrated for AHF of 1-(trifluoromethyl)-ethenyl acetate and *α*-(trifluoromethyl)styrene substrates, the 1,1-disubstituted alkenes remain very challenging, regrading reactivity and stereoselectivity, chiral ligands with unique structure and suitable electronic properties may be the key for overcoming these difficulties.

2.5 Experiment Section

2.5.1 General remarks

Commercially available reagents were used without further purification. The BIBOP ligands were synthesized according to literature procedures. All asymmetric hydroformylation reactions were performed in an inert atmosphere using standard Schlenk techniques unless otherwise noted. Column chromatography was performed using Sorbent silica gel 60 (230 – 450 mesh). ^{1}H NMR, and ^{13}C NMR spectral data were obtained from Bruker 400 MHz or 500 MHz spectrometers. Enantiomeric excesses were determined by Agilent GC 7890A or Agilent HPLC 1200 series.

2.5.2 General Procedure for the Asymmetric Hydroformylation

In a glovebox under nitrogen, ligand (0.006 to 0.024 mmol) and [Rh(acac)$(CO)_2$] (0.005 to 0.02 mmol in 0.4 mL toluene) were added to a 2 mL vial. After stirring for 10 minutes, the substrate (1.0 mmol) and additional solvent were added to bring the total volume of the reaction mixture to 0.5 mL. The vial was transferred into an autoclave and taken out of the glovebox. Hydrogen and carbon monoxide were added sequentially. The reaction mixture was stirred at set temperature for 20 or 24 hours. The reaction was cooled and the pressure was carefully released in a well-ventilated fume hood. The conversion and branch to linear ratio of this reaction were determined by ^{1}H NMR spectroscopy from the crude reaction mixture. The enantiomeric excess was determined by GC analysis with a Supelco's Beta Dex 225 column or by Chiral HPLC analysis of the corresponding alcohol resulting from the sodium borohydride reduction of the aldehyde.

2.5.3 GC and HPLC analysis of the chiral aldehydes

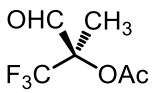

(*R*)-1,1,1-trifluoro-2-methyl-3-oxopropan-2-yl acetate (2b)

Enantiomeric excess was determined by GC with a Supelco's Beta Dex 225 column: 100 ^{o}C, stay 5 mins, 4 ^{o}C/min to 160 ^{o}C, stay 5 mins, flow rate = 1.0 mL/min, t_{minor} = 3.9 min, t_{major} = 4.2 min; 90.0:10.0 er.

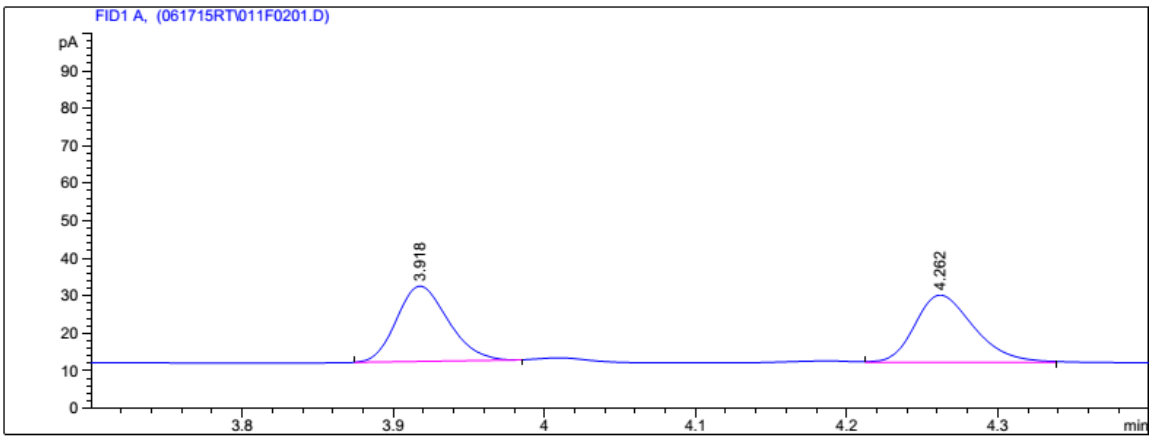

Peak #	RetTime [min]	Type	Width [min]	Area [pA*s]	Height [pA]	Area %
1	3.918	BB	0.0366	47.40533	20.02883	49.46972
2	4.262	BB	0.0425	48.42164	17.92649	50.53028

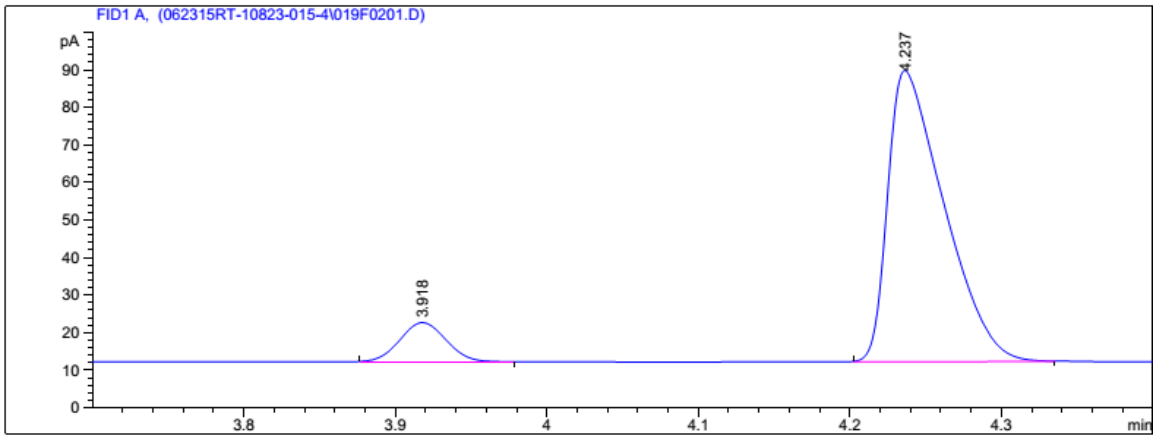

Peak #	RetTime [min]	Type	Width [min]	Area [pA*s]	Height [pA]	Area %
1	3.918	BB	0.0338	22.19601	10.42944	9.97591
2	4.237	BB	0.0391	200.30005	77.68095	90.02409

2.5.4 ^{1}H NMR Spectra of Crude AHF Reaction Mixtures (toluene as solvent)

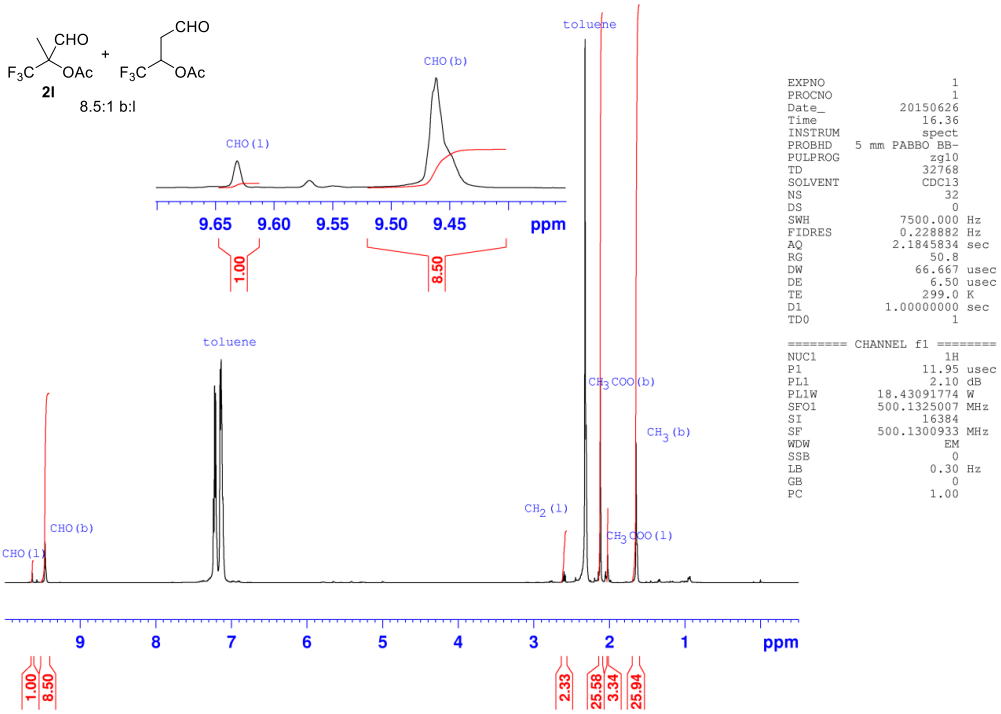
CHO
F3C
OAc
+
CHO
F3C
OAc
2l
8.5:1 b:l
CHO (l)
CHO (b)
toluene
9.65
9.60
9.55
9.50
9.45
ppm
1.00
8.50
toluene
CH3COO (b)
CH3 (b)
CH2 (l)
CH3COO (l)
CHO (b)
CHO (l)
9
8
7
6
5
4
3
2
1
ppm
1.00
8.50
2.33
25.58
3.34
25.94
EXPNO 1
PROCNO 1
Date_ 20150626
Time 16.36
INSTRUM spect
PROBHD 5 mm PABBO BB-
PULPROG zg10
TD 32768
SOLVENT CDCl3
NS 32
DS 0
SWH 7500.000 Hz
FIDRES 0.228882 Hz
AQ 2.1845834 sec
RG 50.8
DW 66.667 usec
DE 6.50 usec
TE 299.0 K
D1 1.00000000 sec
TD0 1
======== CHANNEL f1 ========
NUC1 1H
P1 11.95 usec
PL1 2.10 dB
PL1W 18.43091774 W
SFO1 500.1325007 MHz
SI 16384
SF 500.1300933 MHz
WDW EM
SSB 0
LB 0.30 Hz
GB 0
PC 1.00

2.6 References

1. (a) Sakai, N.; Mano, S.; Nozaki, K.; Takaya, H. *J. Am. Chem. Soc.* **1993**, *115*, 7033. (b) Cobley, C. J.; Gardner, K.; Klosin, J.; Praquin, C.; Hill, C.; Whiteker, G. T.; Zanotti-Gerosa, A.; Petersen, J. L.; Abboud, K. A. *J. Org. Chem*. **2004**, *69*, 4031. (c) Yan, Y.; Zhang, X. *J. Am. Chem. Soc.* **2006**, *128*, 7198. (c) Axtell, A. T.; Klosin, J.; Abboud, K. A. *Organometallics* **2006**, *25*, 5003. (d) Clark, T. P.; Landis, C. R.; Freed, S. L.; Klosin, J.; Abboud, K. A. *J. Am.Chem. Soc*. **2005**, *127*, 5040. (e) Watkins, A. L.; Hashiguchi, B. G.; Landis, C. R. *Org. Lett*. **2008**, *10*, 4553.
2. (a) Zhang, X.; Cao, B.; Yu, S.; Zhang, X. *Angew. Chem. Int. Ed.* **2010**, *49*, 4047. (b) Yu, Z.; Eno, M. S.; Annis, A. H.; Morken, J. P. *Org. Lett.* **2015**, *17*, 3264.
3. (a) McIntyre, S.; H€ ormann, E.; Menges, F.; Smidt, S. P.; Pfaltz, A. *Adv. Synth. Catal.* **2005**, *347*, 282. (b) Roseblade, S. J.; Pfaltz, A. *Acc. Chem. Res*. **2007**, *40*, 1402. (c) Xia, Q.-H.; Ge, H.-Q.; Ye, C.-P.; Liu, Z.-M.; Su, K.-X. *Chem. Rev.* **2005**, *105*, 1603. (d) Wang, B.; Wong, O. A.;
Zhao, M.-X.; Shi, Y. *J. Org. Chem.* **2008**, *73*, 9539. (e) Gonzalez, A. Z.; Rom an, J. G.; Gonzalez, E.; Martinez, J.; Medina, J. R.; Matos, K.; Soderquist, J. A. *J. Am. Chem. Soc.* **2008**, *130*, 9218. (f) Corber an, R.; Mszar, N. W.; Hoveyda, A. H. *Angew. Chem., Int. Ed.* **2011**, *50*, 7079.
4. (a) Consiglio, G.; Morandini, F.; Scalone, M.; Pino, P. *J. Organomet. Chem.* **1985**, *279*, 193.
5. (a) Ojima, I.; Takai, M.; Takahashi, T.; Mitsubishi Chemical Corporation, Iwao Ojima, Takayoshi Takahashi, Masaki Takai, Research Foundation for the State University of New York WO2004078766, 2004. (b) Parrinello, G.; Stille, J. K. *J. Am. Chem. Soc.* **1987**, *109*, 7122. (c) Kollár, L.; Consiglio, G.; Pino, P. *J. Organomet. Chem.* **1987**, *330*, 305. (d) Kollár, L.; Bakos, J.; Tóth, I.; Heil, B. *J. Organomet. Chem.* **1988**, *350*, 277. (e) Consiglio, G.; Kollár, L.; Kölliker, R. *J. Organomet. Chem.* **1990**, *396*, 375. (f) Uhlemann, M.; Börner, A. *ChemCatChem* **2012**, *4*, 753. (g) Breit, B. *Angew. Chem. Int. Ed.* **1996**, *35*, 2835-2837. (h) Alper, H.; Zhou, J.-Q. *J. Org. Chem.* **1992**, *57*, 3729. (i) Lee, C. W.; Alper, H. *J. Org. Chem.* **1995**, *60*, 499.
6. McDonald, R.I.; Wong, G. W.; Neupane, R. P.; Stahl, S. S.; Landis, C. R. *J. Am. Chem. Soc.*, **2010**, *132*, 14027.
7. Wang, X.; Buchwald, S. L. *J. Am. Chem. Soc.* **2011**, *133*, 19080.
8. (a) Galatsis, P.; Caprathe, B.; Gilmore, J.; Thomas, A.; Linn, K.; Sheehan, S.; Harter, W.; Kostlan, C.; Lunney, E.; Stankovic, C.; Rubin, J.; Brady, K.; Allen, H.; Talanian, R. *Bioorg. Med. Chem. Lett.* **2010**, *20*, 5184. (b) Chen, J. J.; Zhang, Y.; Hammond, S.; Dewdney, N.; Ho, T.; Lin, X.; Browner, M. F.; Castelhano, A. L. *Bioorg. Med. Chem. Lett.* **1996**, *6*, 1601.
9. Wang, X.; Buchwald, S. L. *J. Org. Chem.* **2013**, *78*, 3429.
10. (a) Parker, J. S.; Bower, J. F.; Murray, P. M.; Patel, B.; Talavera, P. *Org. Process Res. Dev*. **2008**, *12*, 1060. (b) Menzel, K.; Machrouhi, F.; Bodenstein, M.; Alorati, A.; Cowden, C.; Gibson, A. W.; Bishop, B.; Ikemoto, N.; Nelson, T. D.; Kress, M. H.; Frantz, D. E. *Org. Process Res. Dev.* **2009**, *13*, 519. (c) Sculptoreanu, A.; Yoshimura, N.; de Groat, W. C. *J. Pharmacol. Exp. Ther.* **2004**, *310*, 159. (d) Banner, D.; Guba, W.; Hilpert, H.; Mauser, H.; Mayweg, A. V.; Narquizian, R.; Pinard, E.; Power, E.; Rogers-Evans, M.; Woltering, T.;

Wostl, W. WO Patent
069934 A1, **2011**.
11. Zheng, X.; Cao, B.; Liu, T.-l.; Zhang, X. *Adv. Synth. Catal.* **2013**, *355*, 679.
12. Blumberg, L. C.; Brown, M. F.; Munchhof, M. J.; Reiter, L. A. Patent WO 004038, **2007**.
13. Franke, R.; Selent, D.; Börner, A. *Chem. Rev.* **2012**, *112*, 5675.
14. Fanfonia, L.; Diaba, L.; Smejkal, T.; Breit, B. *CHIMIA* **2014**, *68*, 371.

Chapter 3

Rhodium-Catalyzed Asymmetric Hydrogenation of Indoles via Anion Binding

3.1 Introduction

The strategy of cooperative catalysis has emerged in recent years, aiming to combine two or more catalytic centers for achieving a single reaction.[1-4] Recently, several important breakthroughs have been made with the application of this strategy in various kinds of reactions, such as Pararov reaction,[5] hydrogenation,[6] hydroformylation[7-9] and Diels-Alder reaction.[10] Combining thiourea/urea derivatives and simple Brønsted acids offers a similar effect to that of chiral phosphoric acids in catalysis, while rendering a broader acidity range. Moreover, tunable substituents on bifunctional thiourea/urea catalysts can introduce many kinds of secondary interactions.[11-15] Anion binding makes the chiral catalyst associate with a protonated substrate via establishing a bridge between the thiourea and the conjugate base anion of the Brønsted acid. This strategy combines the essences of both approaches. Transition metal catalysis, with high turnover numbers and potent reactivity, plays a crucial role in modern synthetic chemistry. It shows a very broad application in pharmaceutical and fine chemical industries. The integration of transition metal catalysis and organocatalysis has

demonstrated its potential in the synthetic chemistry communities.[16-17] We envision that certain kinds of reactions could be catalyzed by the cooperative catalysis of transition metal, Brønsted acid and thiourea anion binding.

As quoted by R. Knowles and E. Jacobsen,[18] in order to achieve high enantioselectivity, “small molecule catalysts are designed to introduce steric hindrance to increase the transition state energy of one diastereomer of the two catalyst-substrate complexes; while macromolecule catalysis is to lowering the energy of transition state for one enantiomer.” Non-covalent interactions, such as hydrogen bonding, cation-π or anion-π interaction, π-π stacking are easily found in enzyme catalysis. With remarkably high enantioselectivity and efficiency, the latter strategy deserves more attention in catalytic organic reactions.

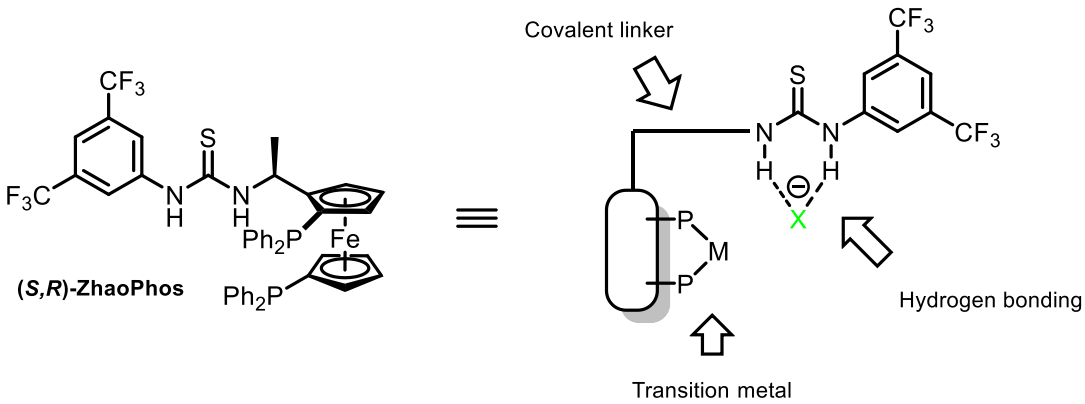

Figure 3.1 A novel thiourea-bisphosphine ligand: strategy of hydrogen bonding and cooperative catalysis.

Guided by such strategies as cooperative catalysis and H-bonding effect, we recently designed and synthesized a ferrocene-based chiral bisphosphine-thiourea ligand, ZhaoPhos.[19] Previous successful examples involved non-covalent interactions between catalytically reactive units, such as ion pair and hydrogen bond. Within ZhaoPhos (Figure 3.1), a covalent linker connects the transition metal catalyst unit and the thiourea moiety. The length of the linker is believed to be crucial for high efficiency and selectivity.

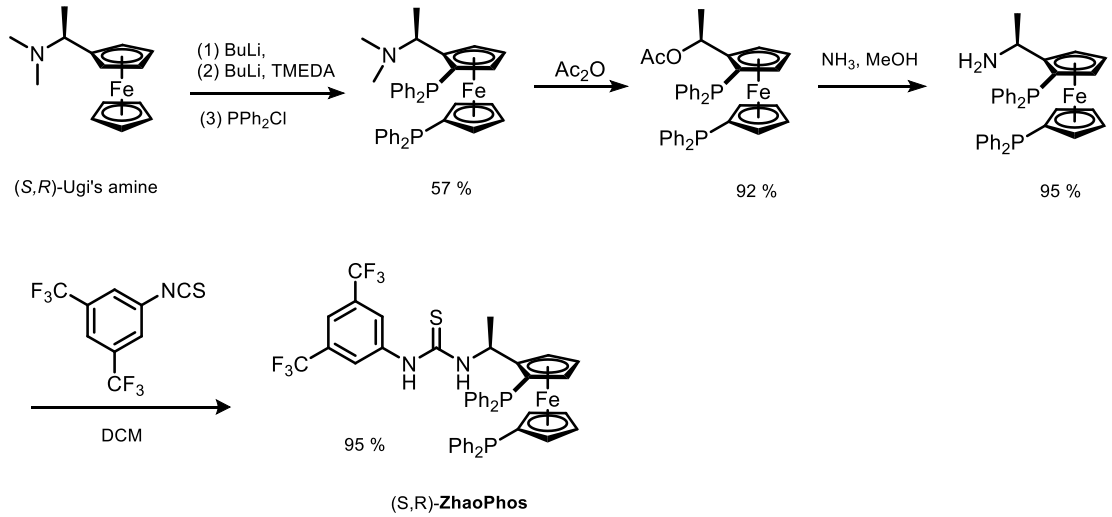

Figure 3.2 Synthetic route for ZhaoPhos.

Preparation of ZhaoPhos is readily reported in the preliminary works of our group by Dr. Qingyang Zhao. From the cheap commercially available enantiopure Ugi's amine, this ligand can be easily obtained with a four-step synthesis (Figure 3.2). This synthesis is highly scalable: a 10-gram scale preparation can easily proceed with good repeatability.

ZhaoPhos has been successfully applied in asymmetric hydrogenation of nitroalkenes (Figure 3.3) with remarkable yields and enantioselectivity. Control experiments were conducted to confirm the cooperation of thiourea motif and the ferrocene-based bisphosphine unit. Based on studies in organocatalysis, a thiourea-nitro interaction was proposed to explain the high selectivity. This secondary interaction was believed to bring two benefits: (1) activate the conjugate C=C bond by hydrogen bonding; (2) create a suitable chiral catalytic environment and therefore generate very good enantioselectivity.

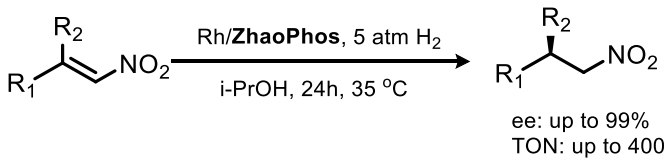

Figure 3.3 Asymmetric hydrogenation of nitroalkenes with ZhaoPhos

Using synthetic routes similar to that of ZhaoPhos, a series of ferrocene-based bisphosphine-thiourea ligands have been successfully prepared. Conjugated nitroalkenes with various substituents on *β*-position have been successfully reduced. Control experiments support the assumption that thiourea motif and bisphosphine unit cooperate to achieve high reactivity and selectivity. Both components in ZhaoPhos are essential and the covalent linker is crucial for effective catalysis.

Proton can be regarded as the simplest efficient catalyst. There has been prosperous development of chiral Brønsted acid catalysis during the past 20 years.[20-21] Chiral Brønsted acid catalysis has been demonstrated to be a powerful tool in organic synthesis.[22-24] Anion binding, on the other hand, commonly exists in various biologic systems and enzyme catalysis. As a non-covalent interaction, hydrogen bonding has some unique characteristics, such as moderate bonding energy and specific directionality.[25-30] However, each of these catalytic systems has some limitations: the pKa's of phosphoric acids are in a the range of 1~3, the acidity is weak to catalyze reactions that require stronger activating reagents; chiral thiourea catalysts with anion binding usually require a high catalyst loading (5%~20%). These drawbacks severely limit their applications in large-scale organic synthesis.

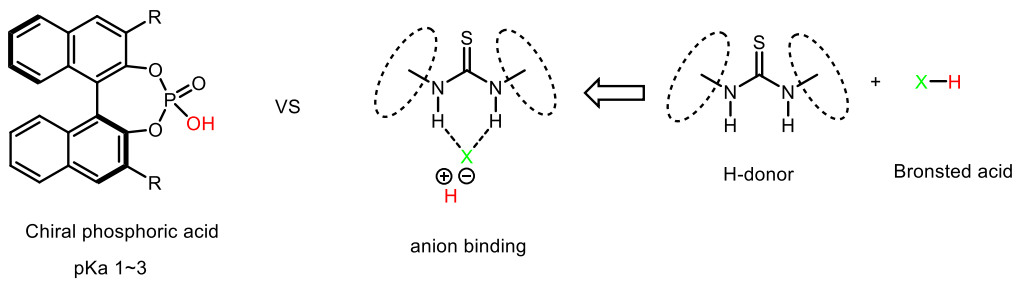

Figure 3.4 Chiral Brønsted acid catalysis versus thiourea anion binding with simple Brønsted acid.

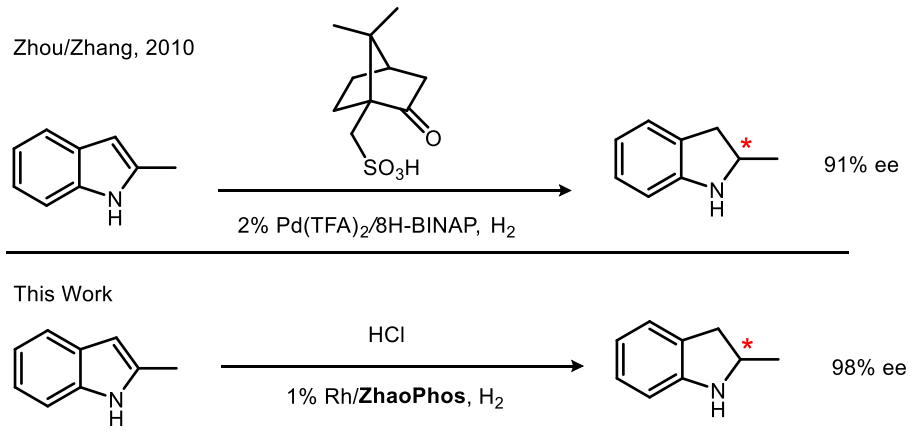

Figure 3.5 Asymmetric hydrogenation of unprotected indole

Chiral indolines are a series of ubiquitous *N*-heterocycles. This structural motif could be found in many natural alkaloids and drugs.[31-33] Comparing with other synthetic approaches, asymmetric hydrogenation is the most straight forward and efficient method to obtain chiral indolines because of its high atom efficiency. *N*-protected indoles have been successfully reduced with Ru, Ir or Rh complexes.[34-35] The protecting groups on nitrogen weaken the aromaticity of indoles, therefore facilitate the asymmetric reduction on enamide C=C bonds. However, the removal of protecting groups requires extra steps and leads to loss of yields, thus increasing the cost of synthetic routes. The only successful example of asymmetric hydrogenation of unprotected indoles was reported by Zhang and Zhou group with a palladium/H8-BINAP complex (Figure 3.5).[36-37] In this case, good enantioselectivity (91% ee) was achieved in hydrogenation of 2-methylindole, but it requires the addition of a chiral auxiliary, camphorsulfonic acid. Moreover, the use of expensive trifluoroethanol increases the cost for its potential industrial application. Thus, we looked

forward to developing a new methodology to generate chiral indoles with excellent selectivity and low cost.

To achieve this goal, we envisioned to utilize the strategy of cooperative catalysis (Figure 3.6). Strong Brønsted acid such as HCl was introduced to activate the aromatic indoles, while the thiourea (linked to the bisphosphine ligand) formed a secondary interaction with the protonated indoles. Rhodium/bisphosphine complex delivers a hydride to reduce the C=N bond which is formed via a tautomerization process. Based on these theoretical thinkings, we initiated our research with asymmetric hydrogenation of 2-methylindole.

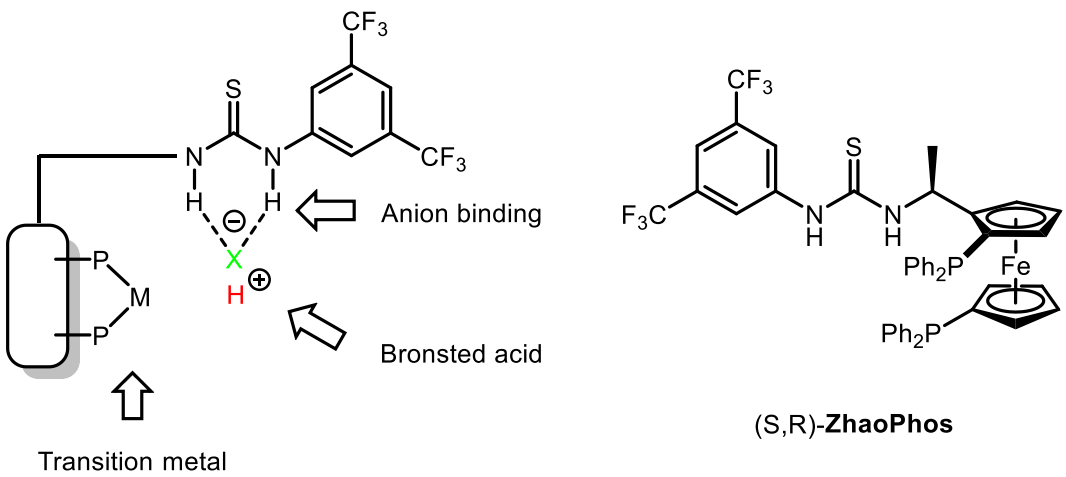

Figure 3.6 ZhaoPhos and cooperative catalysis of transition metal, Brønsted acid and thiourea anion binding.

3.2 Asymmetric hydrogenation of indoles with ZhaoPhos

We conducted asymmetric hydrogenation with (*S,R*)-ZhaoPhos and used $[Rh(COD)Cl]_2$ as the metal precursor since this rhodium(I) dimer gave excellent results in the previous examples. We introduced strong Brønsted acid HCl by adding its diethyl ether solution. After screening solvents from alcohols, alkyl chlorides, ethers and toluene, we found that dichloromethane and 1,2-dichloroethane gave the highest conversion and enantiomeric excess (Table 3.1, entry 7 and 8). ^{1}H NMR study showed no dimer or other byproducts which could usually be found in acidic conditions. Application of HCl ether solution leads to mixed solvents. Diethyl ether is extraordinarily volatile and therefore its HCl solution is difficult to handle and measure accurately, especially in a sealed container like a nitrogen gas protected glovebox. The concentration of HCl in reaction mixture can hardly maintain since it is a gas-liquid equilibrium system. Isopropanol, with much higher boiling point and better solubility towards HCl, might be a desirable alternative to ether. Another reason for using isopropanol is that it was reported to give excellent results in asymmetric hydrogenation of nitroalkenes and iminium with Rh/ZhaoPhos.[38-39] When HCl (5M) in isopropanol was applied, the conversion was driven to nearly 100% with the retention of high enantioselectivity (Table 3.1, entry 9).

Table 3.1 Condition optimization for 2-methylindole. [a]

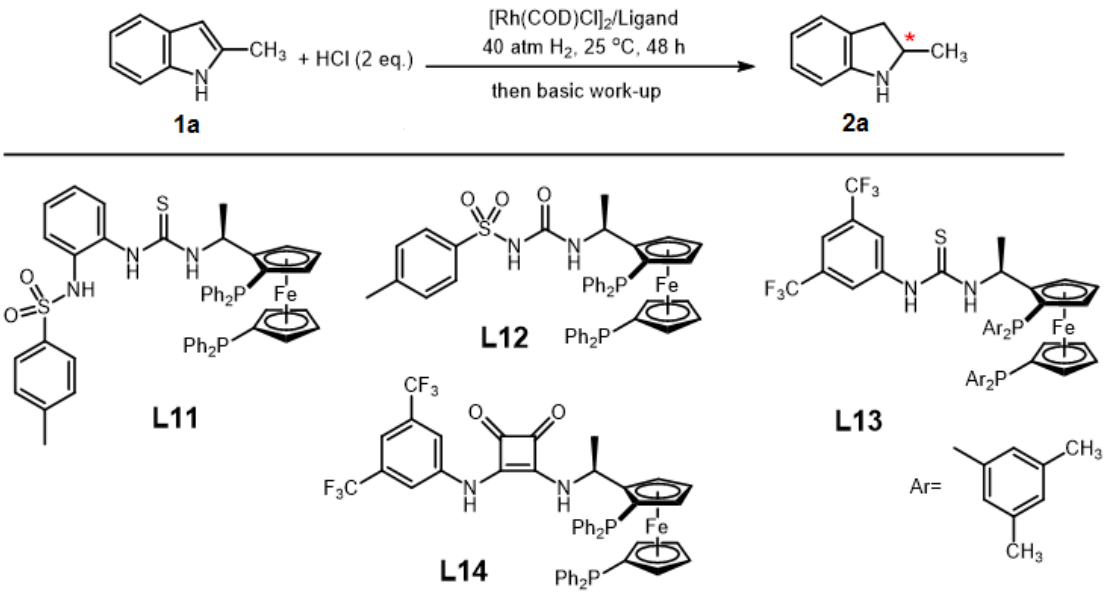

entry	Ligand	solvent	conv[b]	ee[c]
1	(*S*,*R*)-ZhaoPhos	MeOH	56%	27%
2	(*S*,*R*)-ZhaoPhos	i-PrOH	>99%	60%
3	(*S*,*R*)-ZhaoPhos	CF3CH2OH	21%	84%
4	(*S*,*R*)-ZhaoPhos	Toluene	26%	91%
5	(*S*,*R*)-ZhaoPhos	THF	14%	84%
6	(*S*,*R*)-ZhaoPhos	1,4-dioxane	trace	N.D.
7	(*S*,*R*)-ZhaoPhos	DCM	76%	94%
8	(*S*,*R*)-ZhaoPhos	1,2-DCE	71%	95%
9[d]	(*S*,*R*)-ZhaoPhos	DCM	>99%	95%
10[d]	(*S*,*R*)-L11	DCM	6%	80%
11[d]	(*S*,*R*)-L12	DCM	0	N.D.
12[d]	(*S*,*R*)-L13	DCM	68%	89%
13[d]	(*S*,*R*)-L14	DCM	0	N.D.
14[e]	(*S*,*R*)-ZhaoPhos	DCM	99%	98%

[a] reaction condition: 1a (0.1 mmol) in 1.0 ml solvent, 1/[Rh(COD)Cl]$_2$/ligand ratio=100/0.50/1.0, 0.1 ml of HCl (2 M) in Et2O solution was added; [b] conversion was determined by 1H NMR analysis, no side product was observed; [c] ee was determined by GC with a chiral stationary phase; [d] 0.04

ml of HCl (5 M) in i-PrOH solution was added; [e] 0.1 ml of HCl (1 M) in AcOH solution was applied.

To expand the ligand scope, various ligand analogues of ZhaoPhos were prepared and tested. Multi-hydrogen-donor ligand **L11** could not catalyze this hydrogenation efficiently under the optimized condition (Table 3.1, entry 10). Sulfonyl urea catalyst **L12** does not give any hydrogenation product (entry 11). More bulky substituents on the phosphorus centers failed to improve either reactivity or enantioselectivity (entry 12). Comparing with thiourea, the analogue ligand with squaramide **L14** failed catalyzing this reaction (entry 13).

Table 3.2 Brønsted acid screening for 2,3-disustituted indole. [a]

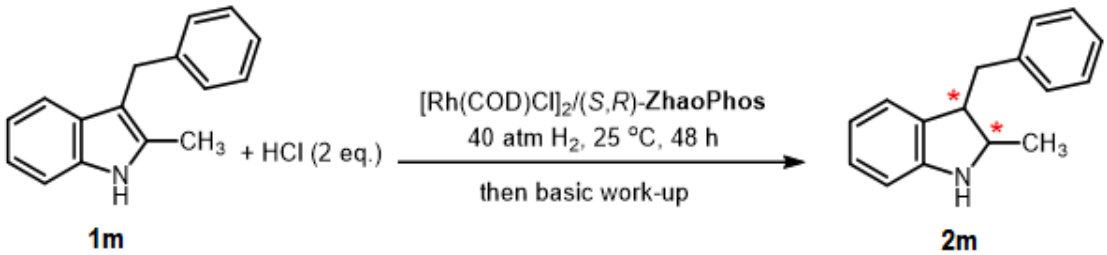

entry	Brønsted acid	actual solvent	conv[b]	ee[c]
1	HCl (2 eq.)	DCM/i-PrOH = 10:1	41%	94%
2	TfOH (1 eq.)	DCM	trace	N.D.
3	*p*-TsOH•H2O (1 eq.)	DCM	80%	90%
4	CF_3COOH (1 eq.)	DCM	7%	92%
5	2 HCl + 1 TfOH	DCM/i-PrOH = 10:1	70%	90%

6	2 HCl + 1 *p*-TsOH•H2O	DCM/i-PrOH = 10:1	67%	90%
7	2 HCl + 1 CF_3COOH	DCM/i-PrOH = 10:1	49%	94%
8	HCl (2 eq.)	DCM/AcOH = 10:1	60%	98%
9	HCl (2 eq.)	DCM/AcOH = 5:1	74%	97%
10	HCl (2 eq.)	DCM/AcOH = 2:1	88%	96%
11	HCl (2 eq.)	DCM/AcOH = 1:1	90%	95%
12	HCl (2 eq.)	DCM/AcOH = 1:2	93%	93%
13	HCl (2 eq.)	DCM/AcOH = 1:5	94%	92%

[a] reaction condition: 1m (0.1 mmol) in 1.0 ml solvent, 1/$[Rh(COD)Cl]_2$/ligand ratio=100/0.50/1.0; [b] conversion was determined by 1H NMR analysis, no side product was observed; [c] ee was determined by HPLC with a chiral stationary phase.

When the optimized condition was applied to asymmetric hydrogenation of 2,3-disubstituted indole (2-methyl-3-benzyl indole), only moderate conversion was observed with high enantioselectivity (Table 3.2, entry 1). Only one of diastereomers was observed. Lower conversion was probably caused by the difficulty in protonation and thus the activation. In order to achieve higher yield, altering the acidity of the protonation reagent would be a plausible solution. A

series of strong Brønsted acids were applied in this reaction since the anion binding between the thiourea/urea and sulfonate anions was well studied.[40] Triflic acid gave no hydrogenation product and lead to full recovery of starting material. This might be due to its extraordinarily strong acidity (pKa = -12),[41] which would probably protonate the catalyst, fail the catalyst and therefore inhibits the reaction.[42] *p*-Toluenesulfonic acid also works for this reaction, giving higher conversion and moderate enantioselectivity. Trifluoroacetic acid, on the other hand, gives higher ee but low conversion. When combined with HCl in isopropanol, these strong Brønsted acids improved the performance of HCl (entry 5, 6, 7).

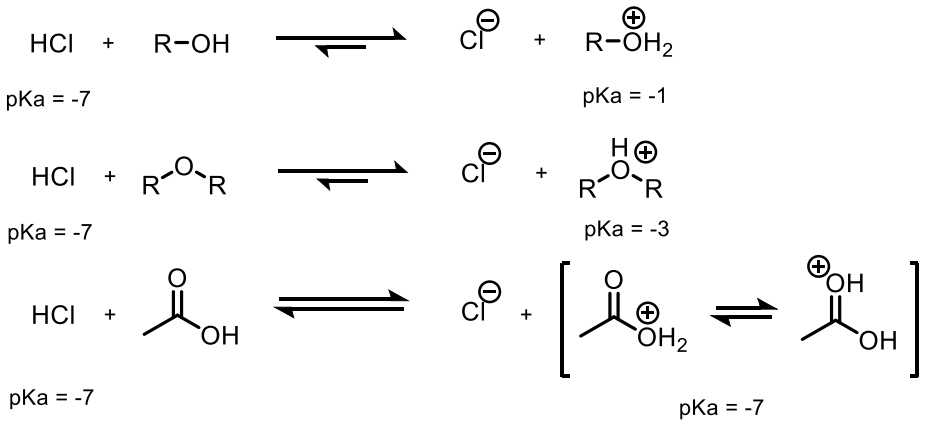

Figure 3.7 Leveling effect of HCl in solutions.

Solvation effect was analyzed as well, since it is another factor that influences the acidity of Brønsted acid. In water or alcohols, the strongest species of acidity is protonated hydroxyl group, whose pKa's are around -1. Protonated ethers offer similar pKa's (~ -3). Due to leveling effect, HCl in

solutions such as alcohols and ethers cannot provide stronger acidity. When the solvent is switched to acetic acid, the strength of acidity of HCl can be maintained, the protonation of indole substrates thus would be much more efficient. Encouraged by this qualitative reasoning, we use HCl in acetic acid solution. It turned out that both conversion and ee were increased. The ratio of acetic acid and dichloromethane is tricky though: higher proportion of acetic acid leads to higher conversion but lower ee (Table 3.2, entry 8~13). We then apply this Brønsted acid source back to the hydrogenation of the standard substrate 2-methylindole, the ee was increased to 98% with full conversion (Table 3.1, entry 14). Again, no significant sign of by-products was observed by ^{1}H NMR study on the crude products. These results suggest that Rh/ZhaoPhos complex can tolerate this highly acidic reaction condition.

The high stereoselectivity in hydrogenation of 2,3-disubstituted indoles could be explained as a result of a dynamic kinetic resolution process (Figure 3.8). After protonating the substrates, two enantiomers both exist in the solution. But due to the chiral environment generated by the catalyst, only one isomer could be reduced efficiently ($k_1 >> k_3 >> k_2$) in the hydride transfer step. Due to the steric effect, addition of hydride could only happen on one side of iminium intermediates, resulting in trans- addition and thus a cis- product.

The ligand/metal ratio was then examined for a wide range of values. Good performance (>95% conv. and 97% ee for chiral 2-methylindoline) was

retained with a ligand/Rh ratio from 0.5 to 2.0. In addition, the equivalent of hydrogen chloride to indole substrate can also be wide-ranged.[43] These advantages make the ZhaoPhos/Rh catalytic system an ease in organic synthesis communities. However, without Brønsted acid HCl, no product was observed, leading to almost full recovery of starting material, which implies the significance of a proton source.

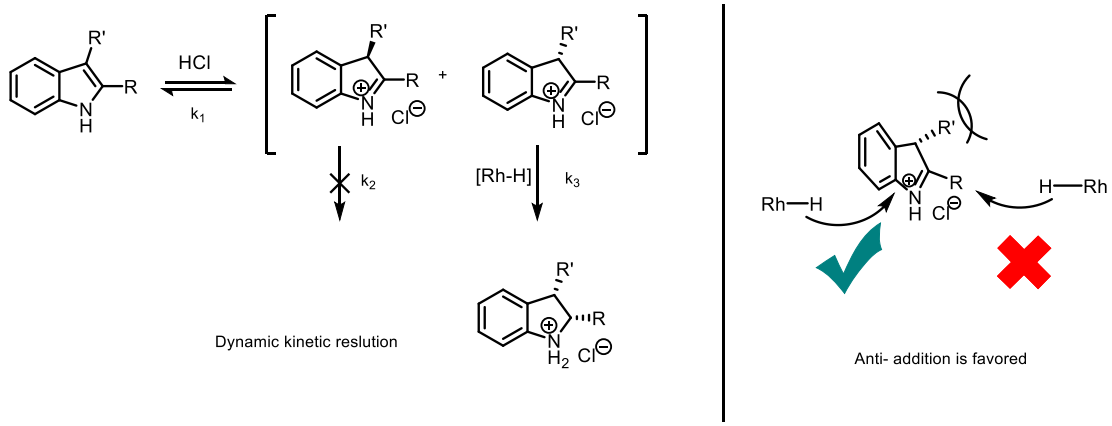

Figure 3.8 Origin of stereoselectivity in the hydrogenation of disubstituted indoles.

We then expanded the substrate scope with optimized reaction conditions (Table 3.3). By adding hydrogen chloride in acetic acid solution as the Brønsted acid source, 2-substituted indoles and 2,3-disubstituted indoles were hydrogenated with excellent enantioselectivities (94%~99% ee). Various substituents on 2- position or on the benzene ring did not show significant influences on the enantioselectivity, while the yields vary from case to case. Phenyl substituent on the 2-position remains a challenge, probably because of the fact of a more stable conjugated enamine C=C bond, which is more difficult

for protonation. 2,3-Disubstituted indoles were also successfully hydrogenated with both good diastereoselectivities (>25:1) and excellent enantioselectivities.

Table 3.3 Substrate scope for asymmetric hydrogenation of indoles. [a]

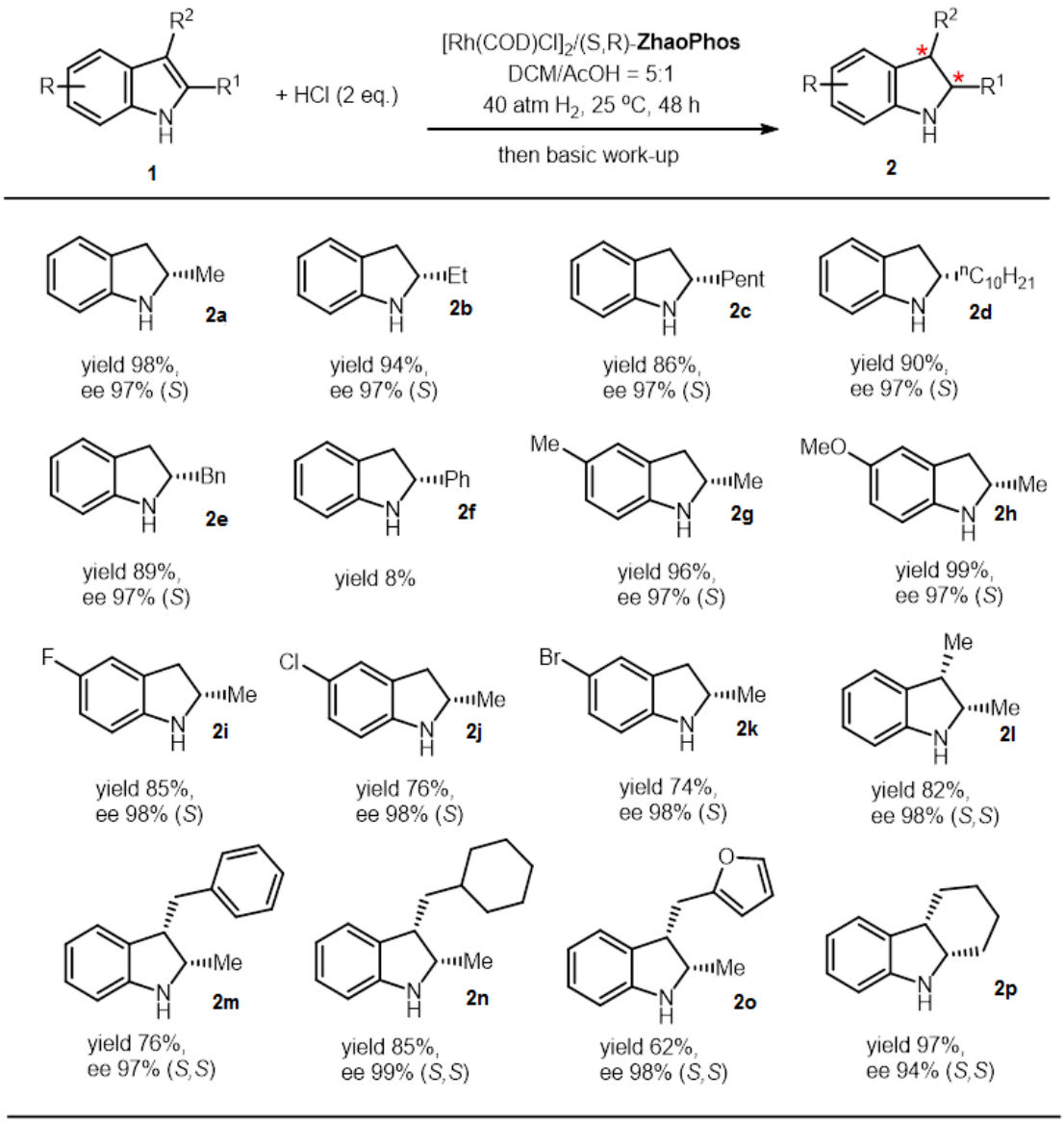

[a] reaction condition: 1 (0.2 mmol) in 2.0 ml solvent, 1/[Rh(COD)Cl]$_2$/ligand ratio=100/0.50/1.0, 0.4 ml of HCl (1.0 M) in AcOH solution was added; isolation yield, no significant sign of side product was observed; ee was determined by HPLC or GC with a chiral stationary phase

3.3 Mechanistic study

The anion binding effect of ZhaoPhos with chloride ion was observed in previous studies.[39, 44] Control experiments were conducted to prove the importance of cooperation between thiourea moiety and the bisphosphine unit (Table 3.4). Each part within ZhaoPhos was demonstrated to be necessary for an efficient asymmetric hydrogenation of 2-methylindole. We synthesized a series of analogues of ZhaoPhos and conducted control experiments to evaluate the collaborating manner of each unit in ZhaoPhos. Urea bisphosphine ligand **L1**fails catalyzing the reaction, this sharp contrast suggests a crucial role of thiourea moiety. Comparing with the H on (**L2**) and methyl group on (**L3**), the more electron-withdrawing trifluoromethyl group at 3- and 5- position on the phenyl ring of ZhaoPhos increases both reactivity and enantioselectivity, which is probably due to the stronger acidity of N-H proton on the thiourea. After methylation of the less acidic thiourea N-H proton, enantioselectivity results in a negligible decrease. This observation reveals that the more acidic thiourea N-H proton contributes the most in anion binding with chloride. Furthermore, the mixture of monophosphine ligand **L6** and ferrocene-thiourea compound **L7** with triphenylphosphine can hardly catalyzed the hydrogenation reaction. On the other hand, the mixture of thiourea and bisphosphine-Ugi's amine **L8** failed to show catalytic activity. These results (ZhaoPhos vs **L6** or **L7** with PPh_3 and **L8**/thiourea) demonstrate the importance of a covalent incorporation of bisphosphine moiety and thiourea.

The idea of secondary interaction offers a powerful alternative strategy to traditional asymmetric hydrogenation.

Table 3.4 Control experiments and ligand evaluation. [a]

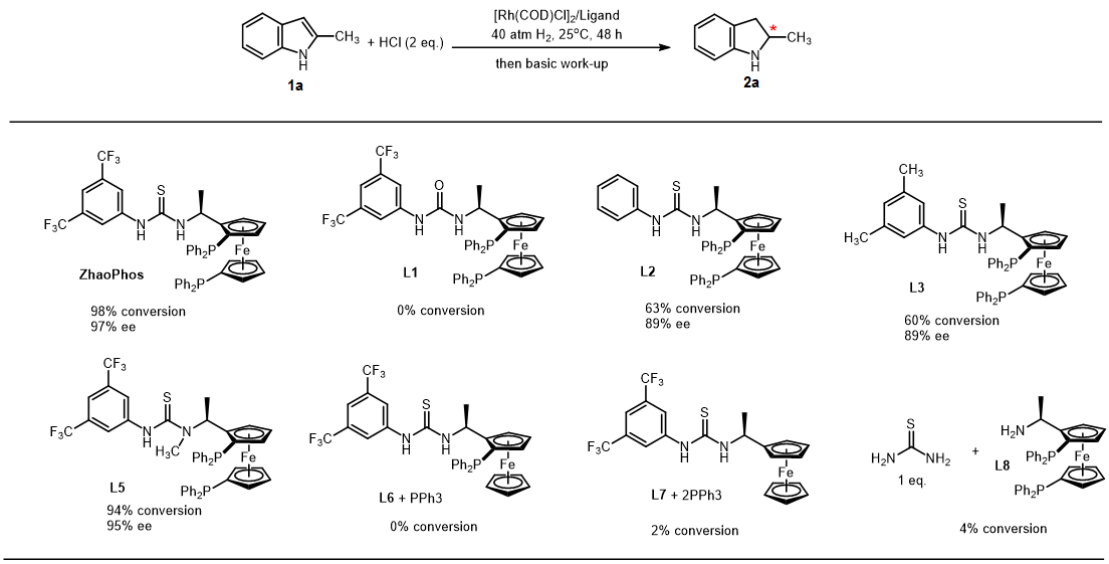

[a] reaction condition: 1a (0.2 mmol) in 2.0 ml solvent,1/$[Rh(COD)Cl]_2$/ligand ratio=100/0.50/1.0, 0.4 ml of HCl (1.0 M) in AcOH solution was added; conversion was determined by ^{1}H NMR analysis, no side product was observed; ee was determined by HPLC or GC with a chiral stationary phase.

Counterion effect was also examined. When tetrabutylammonium chloride (TBAC) was added, no significant changes in conversion and enantioselectivity were observed (Table 3.5, entry 2 vs 1). This suggests the spectator role of tetrabutylammonium cation. The introduction of fluoride anion from TBAF does not influence this catalytic reaction (entry 3 vs 2). The presence of bromide anion decreases the conversion, but it shows trace influence on the enantioselectivity (entry 4 vs 2). Iodide, however, lowers both conversion and enantioselectivity dramatically (entry 5 vs 2). These results

imply that a suitable size of halide anion is vital for the catalytic system to work efficiently.

Table 3.5 Counterion effect. [a]

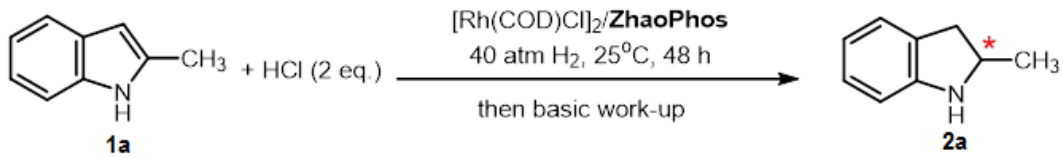

Entry	Additive	conversion[b]	ee[c]
1	None	98%	97%
2	TBAC (1.0 eq.)	92%	94%
3	TBAF (1.0 eq.)	93%	93%
4	TBAB (1.0 eq.)	61%	92%
5	TBAI (1.0 eq.)	13%	76%

[a] reaction condition: 1a (0.2 mmol) in 2.0 ml solvent, 1/$[Rh(COD)Cl]_2$/ligand ratio=100/0.50/1.0, 0.4 ml of HCl (1.0 M) in AcOH solution was added; [b] conversion was determined by ^{1}H NMR analysis, no side product was observed; [c] ee was determined by HPLC or GC with a chiral stationary phase.

In order to get a deeper insight of this reaction progress, we conducted isotope labeling experiments (Figure 3.9). When the reaction was performed in deuterated solvent (CD_3OD/CD_2Cl_2) with hydrogen gas, D atoms were added only at 3-position while H atom was added at 2-position. When regular solvent and deuterium gas were applied, D atom was added exclusively at 2-position, no significant sign of D atom was observed at 3-position. This result suggests that it is the C=N bond, rather than the C=C, to be hydrogenated. A protonation

and the following enamine-imine tautomerization probably occur prior to the hydrogenation. The low abundance (32%) of deuterium at 2-position in experiment 2 seems to suggest an H-D exchange before the hydrogenation step. In order to gain a plausible explanation, systematic kinetic studies will be conducted in the future.

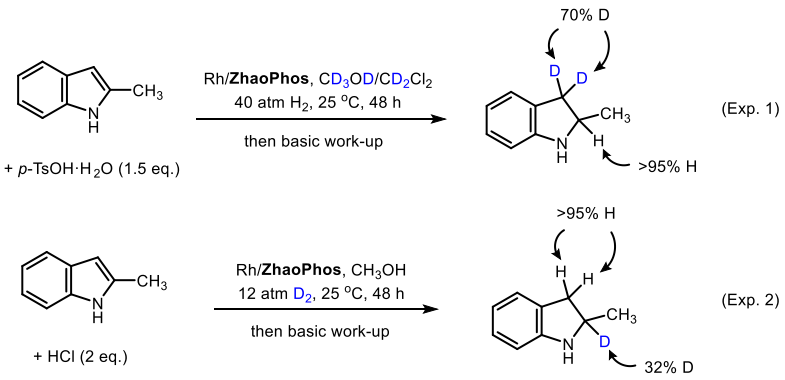

Figure 3.9 Deuterium labeling experiments.

3.4 Nonlinear effect

The hydrogen bonding between thiourea molecules in supramolecular chemistry prompted us to investigate the potential dimerization or high-order aggregation of this thiourea-containing catalyst. Quantitative nonlinear effect (NLE) experiment was carried out. An obvious positive NLE was observed in the hydrogenation of 2-methylindole with ZhaoPhos/Rh complex (Table 4.6).

Table 3.6 Nonlinear effect for asymmetric hydrogenation of indole. [a]

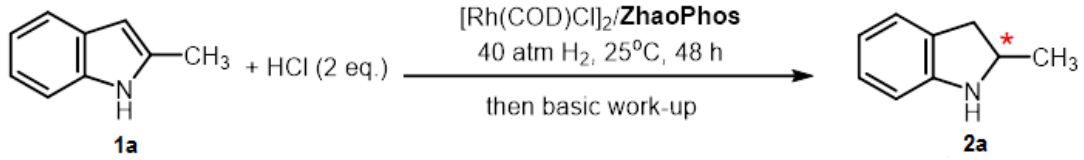

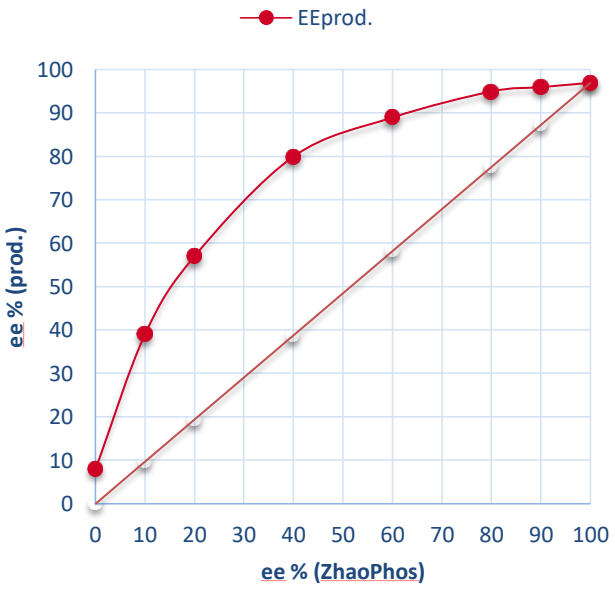

Entry	ee fo ZhaoPhos	conversion[b]	ee[c]
1	0	98%	8%
2	10%	98%	39%
3	20%	98%	57%
4	40%	98%	80%
5	60%	98%	89%
6	80%	98%	95%
7	90%	98%	96%
8	100%	98%	97%

[a] reaction condition: 1a (0.2 mmol) in 2.0 ml solvent, **1a**/[Rh(COD)Cl]$_2$/ligand ratio=100/0.50/1.0, 0.4 ml of HCl (1.0 M) in AcOH solution was added; [b] conversion was determined by ^{1}H NMR analysis, no side product was observed; [c] ee was determined by HPLC or GC with a chiral stationary phase.

A non-covalent interaction between thiourea ligands might be responsible for this phenomenon. The ZhaoPhos/rhodium complex, categorized as bidentate L-L/M system, is not suitable for Kagan's classic ML_1L_2 model or "Reservoir Model".[45] Another reasonable mechanism is thus needed to explain this phenomenon. When the Hayashi and coworkers studied the rhodium catalyzed 1,4-addition of phenylboronic acid to enones,[46] an strong negative NLE was observed. With kinetic and NMR studies, they proposed that a dimeric rhodium complex serves as the precursor of the catalytically active Rh complex. Similarly, Jacobsen and coworkers observed dimerization via anion binding play important roles in some organocatalytic reactions.[47] Based on Hayashi's and Jacobsen's studies, we proposed a similar dimer (Figure 3.10) which is responsible for the observed strong positive NLE. When treating the metal precursor [Rh(COD)Cl]$_2$ with enantiopure ZhaoPhos, a homochiral dimer is formed, which will sequentially dissociate to form a monomer. Once reacting with hydrogen gas, an oxidative addition will change this square planar monomer into a reactive octahedral complex. On the other hand, when the Rh precursor is treated with mixed enantiomers of ZhaoPhos, both homochiral and heterochiral dimers will form. The heterochiral dimer is more stable than the homochiral ones, resulting in an enantiomeric enrichment for the reactive

monomer rhodium dihydride complex. A positive NLE will be therefore observed in hydrogenation of 2-methylindole.

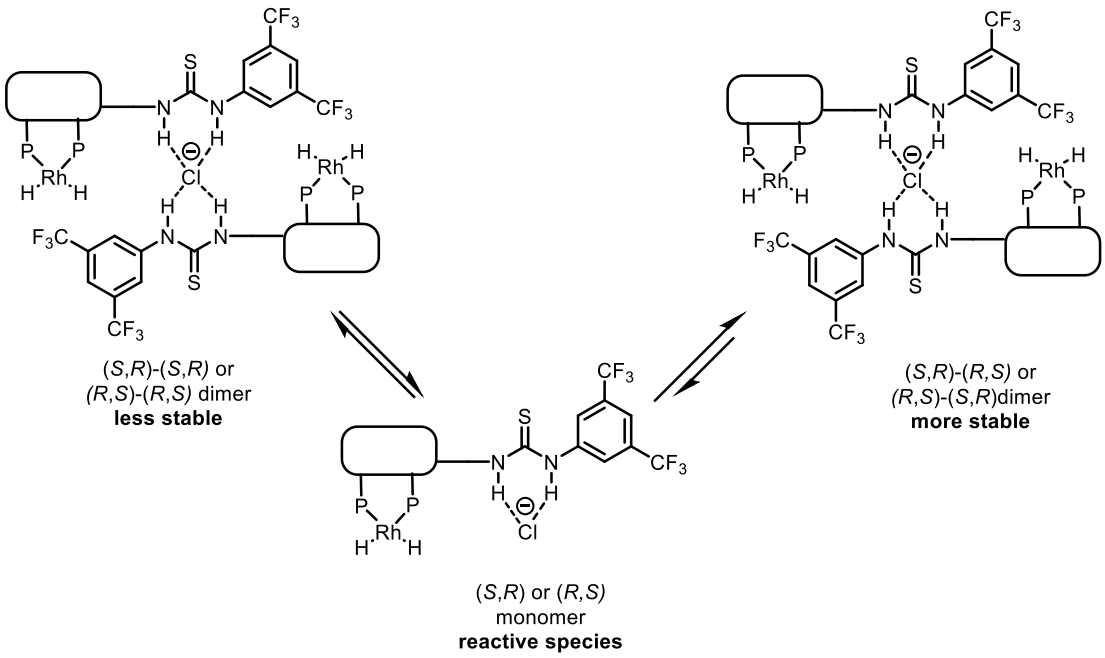

Figure 3.10 Equilibrium scheme for nonlinear effect.

3.5 Conclusion

In summary, we have developed an efficient methodology to synthesize chiral indolines. By employing a cooperative catalysis of transition metal, Brønsted acid and anion binding, prochiral indoles are successfully hydrogenated with excellent enantioselectivities. After introducing strong Brønsted acid HCl, protonation of indole leads to an enamine-imine tautomerization equilibrium. The resulting iminium was reduced by a rhodium-ZhaoPhos complex. Isotope labeling experiments supported this reaction sequence. Dimerization via anion binding was proposed to explain the observed positive nonlinear effect.

3.6 Experimental Section

3.6.1 Synthesis of indole substrates.

Method A

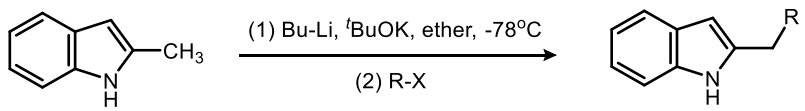

2-methylindole (10 mmol, 1.31 g) was dissolved in ether at room temperature, the mixture was under nitrogen protection. Butyllithium in hexane solution was added dropwise to the stirring mixture. Then potassium tert-butoxide was added in one portion. The color of the mixture became bright yellow. After stirring for 30 min, the mixture was cooled to -78°C, methyl iodide was added dropwise. After stirring for another 2 hours at -78°C, several drops of water was added to quench the reaction. Ammonium chloride solution was added to adjust the pH to neutral. After separation, the aqueous layer was washed with ether and the organic layer was combined. The ether solution was dried over anhydrous sodium sulfate and then the volatile was evaporated under reduced pressure. The crude product was purified by flash chromatography (hexanes/ethyl acetate).

Method B

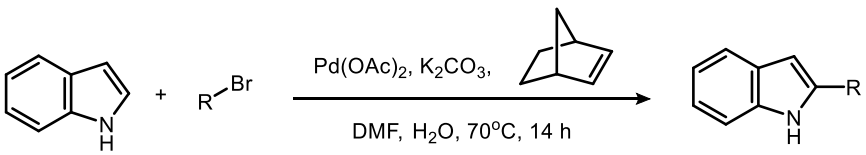

A Schlenk flask was charged with indole (5 mmol, 0.65 g), alkyl bromide, norbornene, potassium carbonate and palladium(II) acetate. Water (0.1 M) in DMF was added. The mixture was frozen at -78 ^{o}C and the flask was evacuated and backfilled with nitrogen for 3 times. The stoppered mixture was

stirred at 70°C for 14 hours. After cooled to room temperature, the mixture was diluted with ether and washed with water. The organic layer was dried over anhydrous sodium sulfate and the volatile was evaporated under reduced pressure. The crude product was purified by flash chromatography (hexanes/ethyl acetate).

Method C

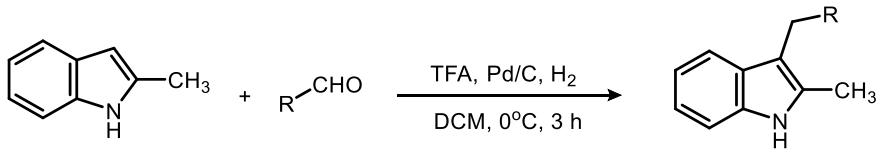

In a round bottom flask, a solution of 2-methylindole (5 mmol, 0.65 g) and aldehyde in dichloromethane was added to a stirring ice-cold mixture of trifluoroacetice acid and palladium on carbon in DCM. This flask was filled with hydrogen and the mixture was stirred at 0°C. After TCL monitoring showed the consumption of indole (approximately 3 h), the Pd/C was filtered and the solvent was concentrated under reduced pressure. The crude product was purified by chromatography (hexane/ethyl acetate).

Method D

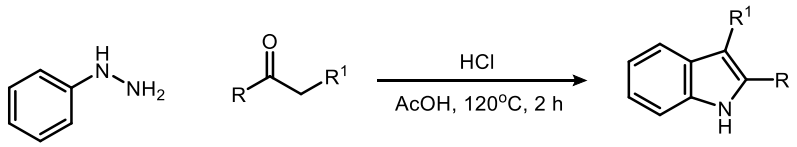

A round bottom flask was charged with 0.5 ml phenyl hydrazine, 0.78 ml cyclohexanone, 1ml of concentrate HCl and 20 ml of acetic acid. The mixture was heated at 120°C for 2 hours and cooled back to room temperature. 2M of NaOH solution was added. After the pH became 6-7, the mixture was cooled in ice. The aqueous layer was extracted with ether 3 times and the combined

mixture was dried over anhydrous sodium sulfate and concentrated under reduced pressure. The crude product was purified by chromatography (hexane/ethyl acetate).

Method A Method B Method C Method D

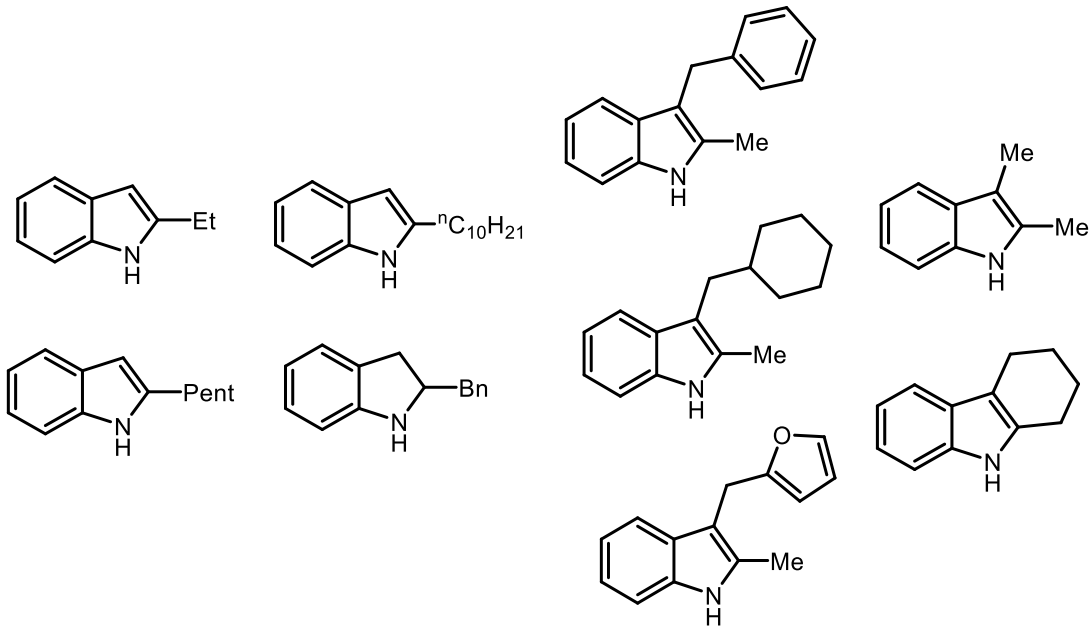

3.6.2 General procedure for asymmetric hydrogenation of indoles.

In the nitrogen-filled glovebox, solution of $[Rh(COD)Cl]_2$ (2.46 mg, 0.005 mmol) and ZhaoPhos (2.1 eq.) in 5.0 ml anhydrous solvent was stirred at room temperature for 20 min. A specified volume of the resulting solution (0.50 ml, 1% Rh catalyst) was transferred to a Score-Break ampule charged with substrate solution (0.1 mmol in 0.5 ml) by syringe. 0.2 ml of hydrogen chloride in acetic acid solution (1.0 M) was added by syringe. The ampule was placed into an autoclave, which was then charged with 40 atm H_2. The autoclave was stirred at desired temperature for the indicated period of time. After release of H_2,

saturated potassium carbonate solution and dichloromethane was added and the mixture was stirred for 30 min. The organic layer was dried with Na_2SO_4. After removal of solvent, the crude product was analyzed by 1H NMR to determine the conversion. The enantiomeric excess was determined by GC or HPLC analysis. The absolute configurations were assigned according to literature.

3.6.3 Deuterium labeling experiments.

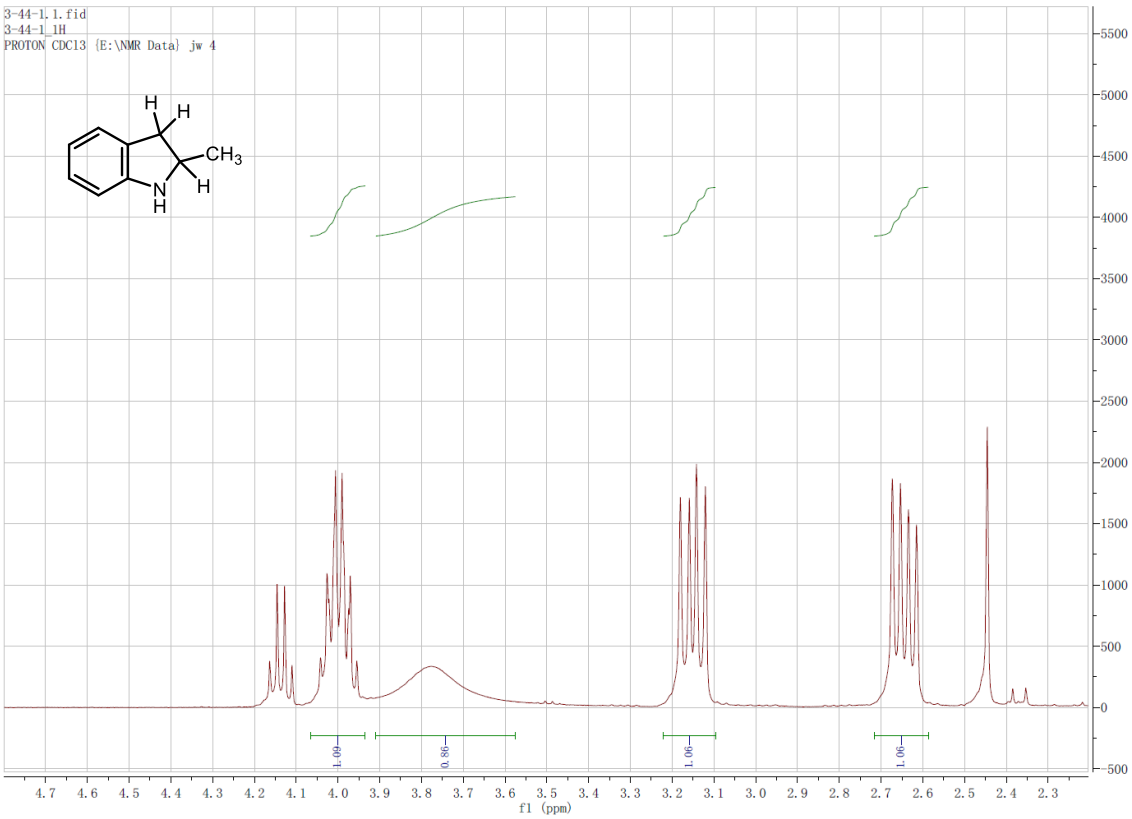

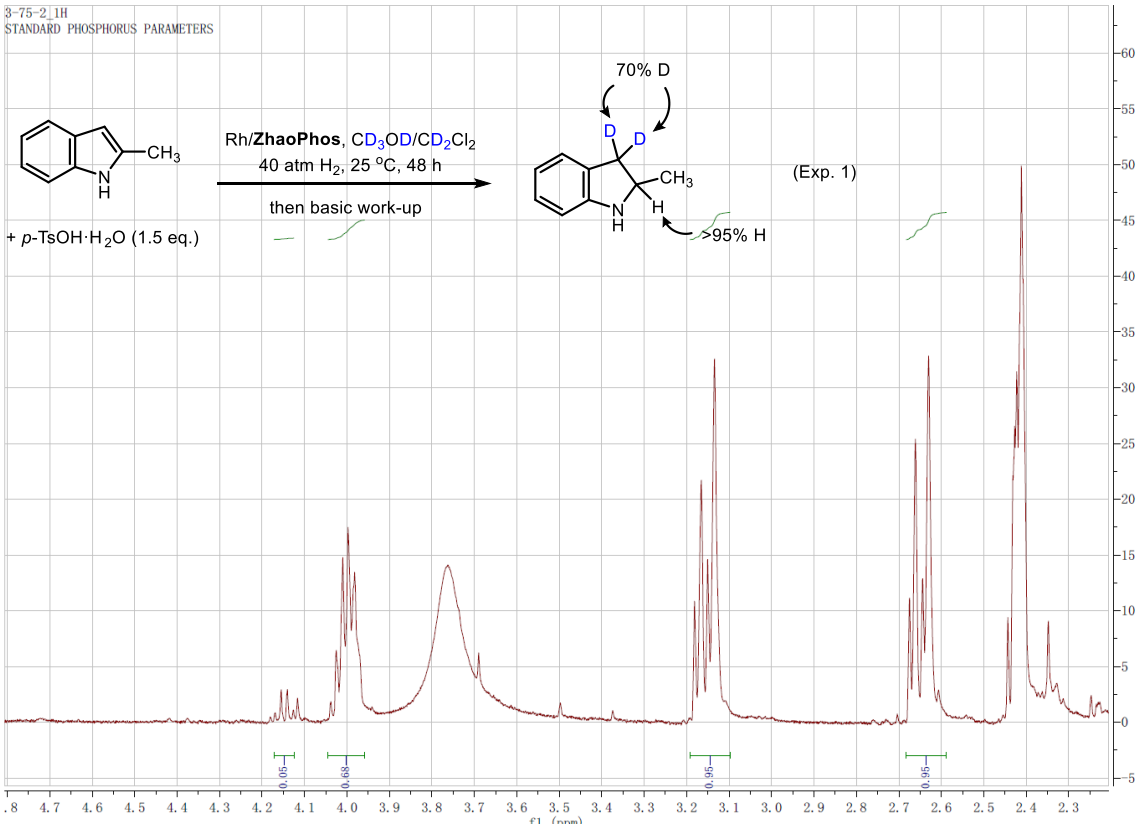

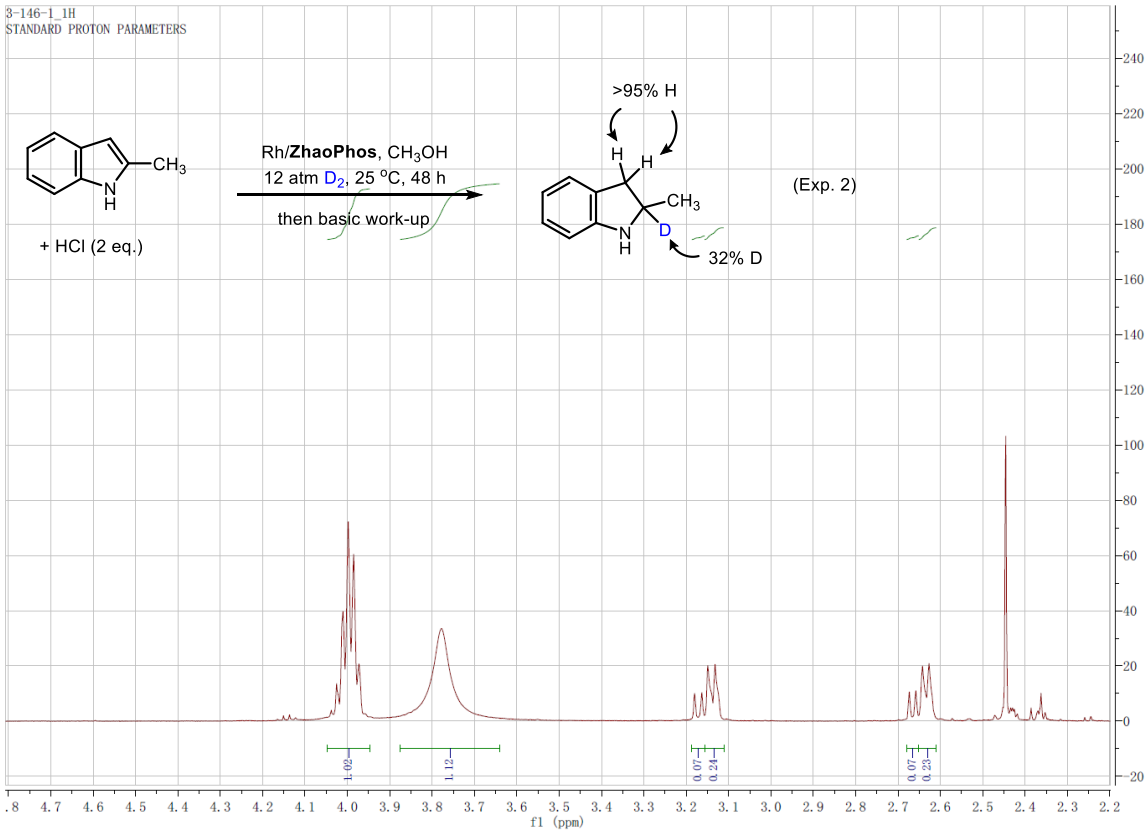

3.6.4 Characterization data for chiral indolines.

(S)-2-methylindoline (2a)

Colorless oil. ^{1}H NMR (400 MHz, $CDCl_3$) δ 7.09 (d, *J* = 7.3 Hz, 1H), 7.02 (t, *J* = 7.6 Hz, 1H), 6.70 (t, *J* = 7.4 Hz, 1H), 6.62 (d, *J* = 7.7 Hz, 1H), 4.00 (tq, *J* = 8.1, 6.2 Hz, 1H), 3.79 (br, 1H), 3.16 (dd, *J* = 15.4, 8.5 Hz, 1H), 2.65 (dd, *J* = 15.4, 7.8 Hz, 1H), 1.30 (d, *J* = 6.2 Hz, 3H). ^{13}C NMR (400 MHz, $CDCl_3$): δ 150.96, 128.89, 127.23, 124.72, 118.52, 109.16, 55.23, 37.78, 22.30. HPLC (Daicel Chiralpak OD-H, hexanes/i-PrOH = 97/3, Flow rate = 0.8 ml/min, UV = 254 nm): t_1 = 12.1 min, t_2 = 13.8 min.

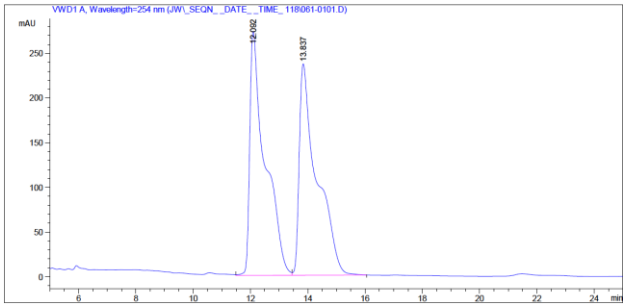

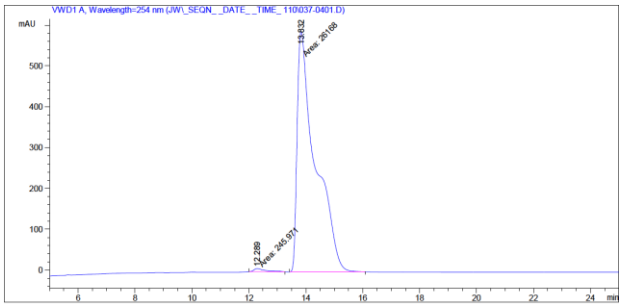

Peak #	RetTime [min]	Type	Width [min]	Area mAU *s	Height [mAU]	Area %
1	12.289	MM	0.5220	245.97058	7.85383	0.9312
2	13.832	MM	0.7410	2.61680e4	588.53992	99.0688
Totals :				2.64140e4	596.39375	

(S)-2-ethylindoline (2b)

Colorless oil. ^{1}H NMR (400 MHz, CDCl3) δ 7.07 (d, J = 7.2 Hz, 1H), 7.01 (t, J = 7.6 Hz, 1H), 6.68 (td, J = 7.4, 0.9 Hz, 1H), 6.60 (d, J = 7.7 Hz, 1H), 3.88 (br, 1H), 3.78 (tt, J = 8.5, 6.6 Hz, 1H), 3.13 (dd, J = 15.5, 8.6 Hz, 1H), 2.69 (dd, J = 15.5, 8.4 Hz, 1H), 1.64 (qd, J = 7.5, 4.0 Hz, 2H), 0.98 (t, J = 7.4 Hz, 3H). ^{13}C NMR (400 MHz, $CDCl_3$) δ 151.00, 128.86, 127.17, 124.62, 118.37, 108.99, 61.49, 35.72, 29.55, 10.69. HPLC (Daicel Chiralpak OD-H, hexanes/i-PrOH = 97/3, Flow rate = 0.8 ml/min, UV = 254 nm): t_1 = 9.5 min, t_2 = 11.3 min.

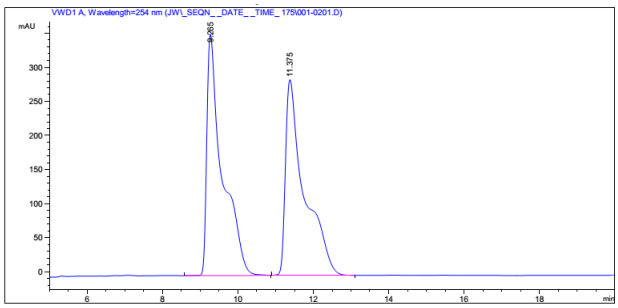

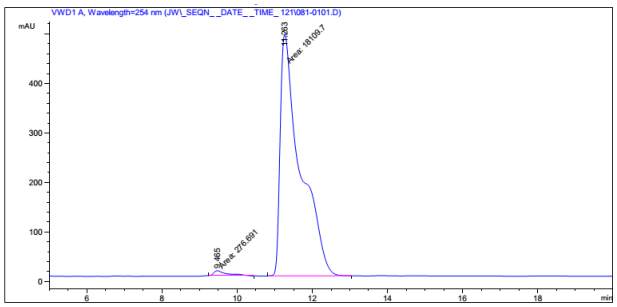

Peak #	RetTime [min]	Type	Width [min]	Area mAU *s	Height [mAU]	Area %
1	9.465	MM	0.4431	276.69092	10.40781	1.5049
2	11.263	MM	0.6176	1.81097e4	488.70456	98.4951
Totals :				1.83864e4	499.11237	

(S)-2-pentylindoline (2c)

Colorless oil. ^{1}H NMR (400 MHz, $CDCl_3$) δ 7.07 (d, *J* = 7.2 Hz, 1H), 7.00 (t, *J* = 7.6 Hz, 1H), 6.68 (td, *J* = 7.4, 0.7 Hz, 1H), 6.60 (d, *J* = 7.7 Hz, 1H), 3.84 (dq, *J* = 8.5, 6.7 Hz, 1H), 3.35 (br, 1H), 3.12 (dd, *J* = 15.5, 8.6 Hz, 1H), 2.68 (dd, *J* = 15.4, 8.4 Hz, 1H), 1.68 – 1.53 (m, 2H), 1.47 – 1.17 (m, 6H), 0.91 (dd, *J* = 8.9, 4.8 Hz, 3H). ^{13}C NMR (400 MHz, $CDCl_3$) δ 150.98, 128.91, 127.19, 124.63, 118.45, 109.08, 60.08, 36.81, 36.18, 31.87, 26.23, 22.62, 13.99. HPLC (Daicel Chiralpak OD-H, hexanes/i-PrOH = 97/3, Flow rate = 0.8 ml/min, UV = 254 nm): t_1 = 6.7 min, t_2 = 8.8 min.

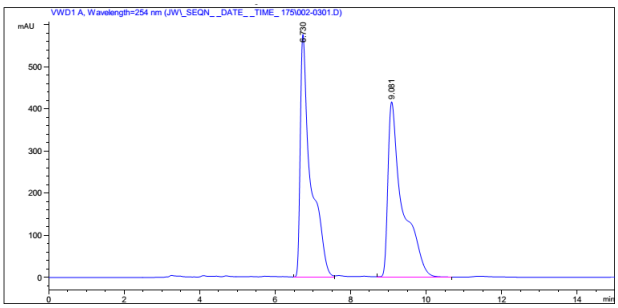

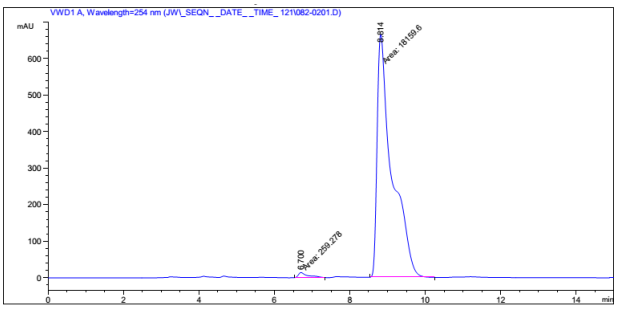

Peak #	RetTime [min]	Type	Width [min]	Area mAU *s	Height [mAU]	Area %
1	6.700	MM	0.3064	259.27817	14.10447	1.4077
2	8.814	MM	0.4549	1.81596e4	665.32605	98.5923
Totals :				1.84189e4	679.43052	

(S)-2-decylindoline (2d)

Colorless oil. ^{1}H NMR (400 MHz, $CDCl_3$) δ 7.07 (d, *J* = 7.2 Hz, 1H), 7.00 (t, *J* = 7.6 Hz, 1H), 6.68 (t, *J* = 7.4 Hz, 1H), 6.60 (d, *J* = 7.7 Hz, 1H), 3.83 (ddd, *J* = 15.2, 8.5, 6.7 Hz, 2H), 3.12 (dd, *J* = 15.4, 8.6 Hz, 1H), 2.67 (dd, *J* = 15.4, 8.5 Hz, 1H), 1.71 – 1.55 (m, 4H), 1.30 (d, *J* = 21.9 Hz, 14H), 0.89 (t, *J* = 6.8 Hz, 3H). ^{13}C NMR (400 MHz, $CDCl_3$) δ 150.99, 128.90, 127.17, 124.63, 118.40, 109.04, 60.09, 36.84, 36.16, 31.90, 29.63, 29.33, 26.58, 22.68, 14.10. HPLC (Daicel Chiralpak OD-H, hexanes/i-PrOH = 97/3, Flow rate = 0.8 ml/min, UV = 254 nm): t_1 = 6.0 min, t_2 = 8.2 min.

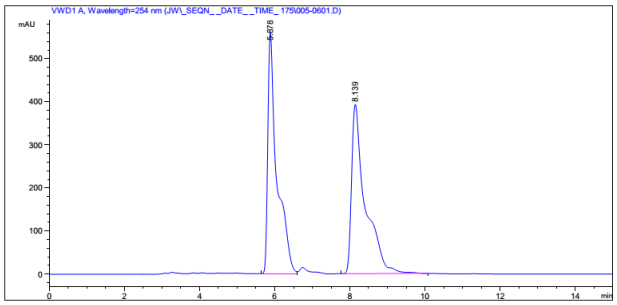

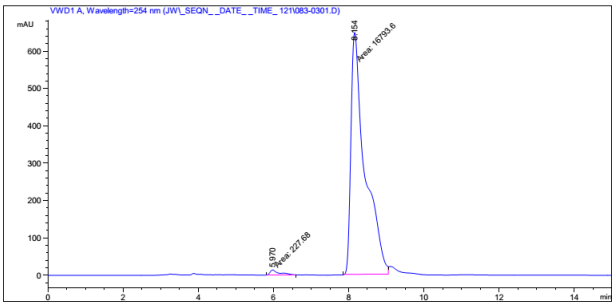

Peak #	RetTime [min]	Type	Width [min]	Area mAU *s	Height [mAU]	Area %
1	5.970	MM	0.2832	227.68025	13.40041	1.3376
2	8.154	MM	0.4317	1.67936e4	648.28119	98.6624
Totals :				1.70213e4	661.68159	

(S)-2-benzylindoline (2e)

Colorless oil. ^{1}H NMR (400 MHz, $CDCl_3$) δ 7.34 (t, *J* = 7.3 Hz, 3H), 7.25 (dd, *J* = 10.7, 7.6 Hz, 2H), 7.09 (d, *J* = 7.3 Hz, 1H), 7.02 (t, *J* = 7.6 Hz, 1H), 6.70 (t, *J* = 7.4 Hz, 1H), 6.58 (d, *J* = 7.7 Hz, 1H), 4.09 (ddd, *J* = 15.8, 8.4, 5.6 Hz, 1H), 3.81 (br, 1H), 3.15 (dd, *J* = 15.5, 8.5 Hz, 1H), 3.00 – 2.74 (m, 3H). ^{13}C NMR (400 MHz, $CDCl_3$) δ 150.53, 139.08, 129.11, 128.62, 128.35, 127.33, 126.43, 124.79, 118.51, 109.07, 60.96, 42.72, 35.94. HPLC (Daicel Chiralpak OD-H, hexanes/i-PrOH = 97/3, Flow rate = 0.8 ml/min, UV = 254 nm): t_1 = 9.8 min, t_2 = 11.1 min.

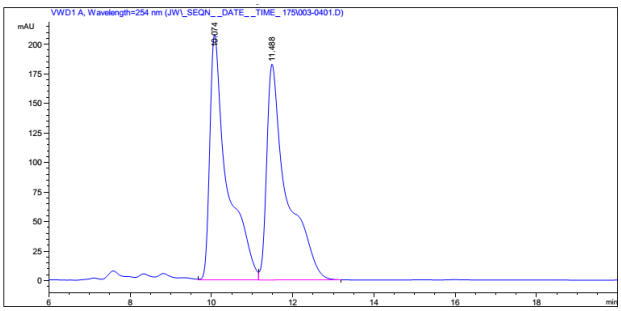

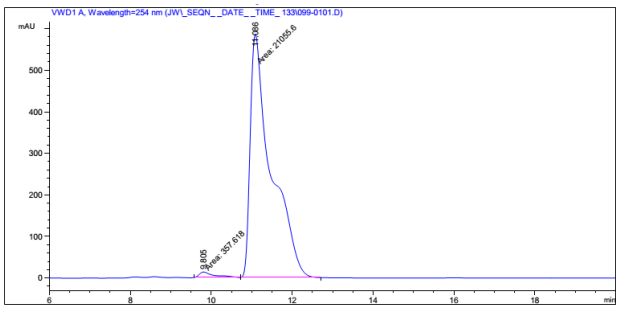

Peak #	RetTime [min]	Type	Width [min]	Area mAU *s	Height [mAU]	Area %
1	9.805	MM	0.4497	357.61798	13.25354	1.6701
2	11.086	MM	0.5992	2.10556e4	585.62494	98.3299
Totals :				2.14132e4	598.87847	

(S)-2,5-dimethylindoline (2g)

Colorless oil. ^{1}H NMR (400 MHz, $CDCl_3$) δ 6.91 (s, 1H), 6.82 (d, *J* = 7.7 Hz, 1H), 6.52 (d, *J* = 7.8 Hz, 1H), 4.09 – 3.77 (m, 1H), 3.44 (br, 1H), 3.10 (dd, *J* = 15.4, 8.4 Hz, 1H), 2.60 (dd, *J* = 15.4, 7.7 Hz, 1H), 2.25 (s, 3H), 1.28 (d, *J* = 6.2 Hz, 3H). ^{13}C NMR (400 MHz, $CDCl_3$) δ 148.56, 129.23, 127.89, 127.48, 125.49, 109.14, 55.37, 37.85, 22.22, 20.74. HPLC (Daicel Chiralpak OD-H, hexanes/i-PrOH = 97/3, Flow rate = 0.8 ml/min, UV = 254 nm): t_1 = 7.2 min, t_2 = 9.1 min.

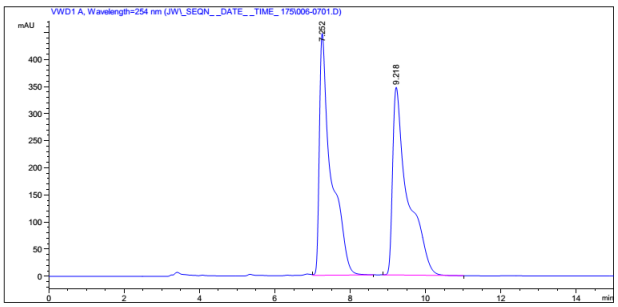

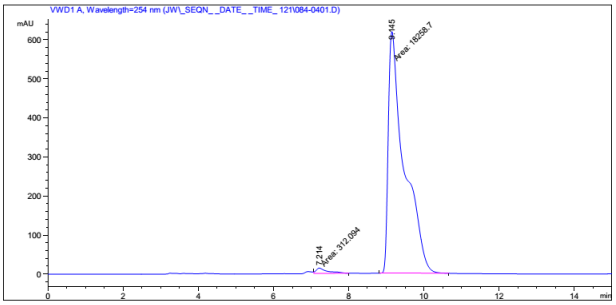

Peak #	RetTime [min]	Type	Width [min]	Area mAU *s	Height [mAU]	Area %
1	7.214	MM	0.3670	312.09412	14.17488	1.6806
2	9.145	MM	0.4916	1.82587e4	619.00964	98.3194
Totals :				1.85708e4	633.18452	

(S)-5-methoxy-2-methylindoline (2h)

Colorless oil. ^{1}H NMR (400 MHz, $CDCl_3$) δ 6.74 (dd, *J* = 5.5, 4.3 Hz, 1H), 6.60 (dd, *J* = 8.3, 2.4 Hz, 1H), 6.55 (d, *J* = 8.4 Hz, 1H), 4.04 – 3.94 (m, 1H), 3.75 (s, 3H), 3.40 (br, 1H), 3.12 (dd, *J* = 15.5, 8.3 Hz, 1H), 2.63 (dd, *J* = 15.5, 7.9 Hz, 1H), 1.30 (d, *J* = 6.2 Hz, 3H). ^{13}C NMR (400 MHz, $CDCl_3$) δ 153.47, 144.77, 130.66, 112.13, 111.71, 109.79, 55.95, 55.65, 38.29, 22.17. HPLC (Daicel Chiralpak OD-H, hexanes/i-PrOH = 97/3, Flow rate = 0.8 ml/min, UV = 254 nm): t_1 = 12.1 min, t_2 = 25.1 min.

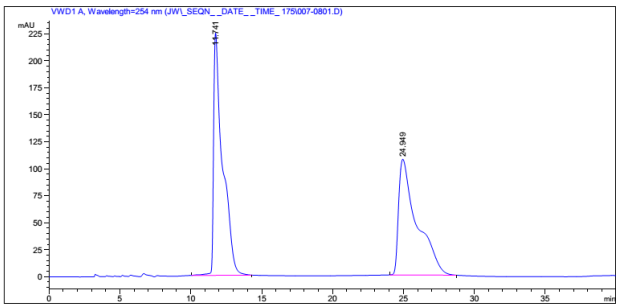

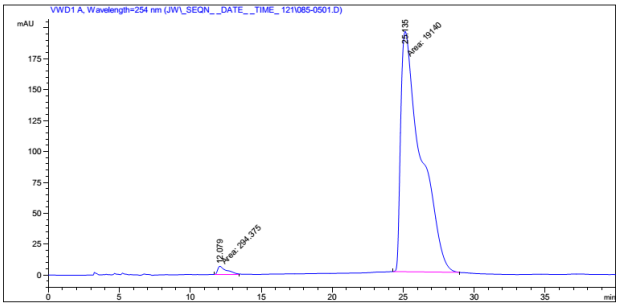

Peak #	RetTime [min]	Type	Width [min]	Area mAU *s	Height [mAU]	Area %
1	12.079	MM	0.7445	294.37491	6.58973	1.5147
2	25.135	MM	1.6384	1.91400e4	194.70343	98.4853
Totals :				1.94343e4	201.29316	

(S)-5-fluoro-2-methylindoline (2i)

Colorless oil. ^{1}H NMR (400 MHz, $CDCl_3$) δ 6.87 – 6.77 (m, 1H), 6.74 – 6.66 (m, 1H), 6.50 (dd, *J* = 8.4, 4.4 Hz, 1H), 4.06 – 3.96 (m, 1H), 3.33 (br, 1H), 3.12 (dd, *J* = 15.7, 8.5 Hz, 1H), 2.62 (ddd, *J* = 15.7, 7.8, 0.7 Hz, 1H), 1.29 (d, *J* = 6.2 Hz, 3H). ^{13}C NMR (400 MHz, $CDCl_3$) δ 156.97 (d, *J* = 234.7 Hz), 146.92 (s), 130.64 (d, *J* = 8.2 Hz), 113.09 (d, *J* = 23.2 Hz), 112.11 (d, *J* = 23.7 Hz), 109.28 (d, *J* = 8.2 Hz), 55.89, 38.02, 22.16. HPLC (Daicel Chiralpak OD-H, hexanes/i-PrOH = 97/3, Flow rate = 0.8 ml/min, UV = 254 nm): t_1 = 7.3 min, t_2 = 10.7 min.

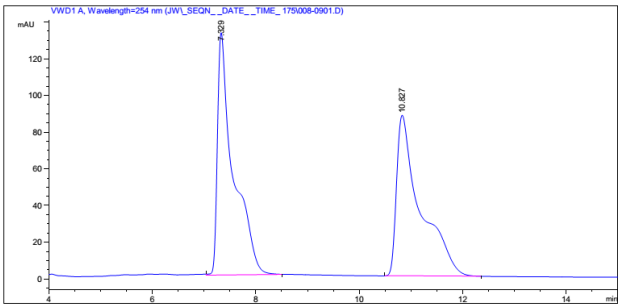

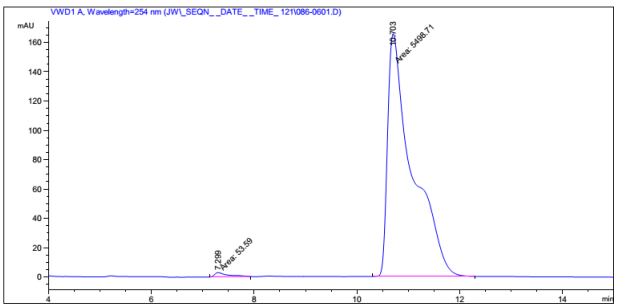

Peak #	RetTime [min]	Type	Width [min]	Area mAU *s	Height [mAU]	Area %
1	7.299	MM	0.3069	53.58995	2.91006	0.9652
2	10.703	MM	0.5535	5498.71191	165.58165	99.0348
Totals :				5552.30187	168.49171	

(S)-5-chloro-2-methylindoline (2j)

Colorless oil. ^{1}H NMR (400 MHz, $CDCl_3$) δ 7.02 (s, 1H), 6.95 (dd, *J* = 8.2, 1.8 Hz, 1H), 6.49 (d, *J* = 8.2 Hz, 1H), 4.01 (tt, *J* = 14.4, 6.2 Hz, 1H), 3.76 (br, 1H), 3.12 (dd, *J* = 15.7, 8.6 Hz, 1H), 2.61 (dd, *J* = 15.7, 7.6 Hz, 1H), 1.28 (d, *J* = 6.2 Hz, 3H). ^{13}C NMR (400 MHz, $CDCl_3$) δ 149.50, 130.75, 126.94, 124.86, 122.93, 109.69, 55.61, 37.60, 22.16. HPLC (Daicel Chiralpak OD-H, hexanes/i-PrOH = 97/3, Flow rate = 0.8 ml/min, UV = 254 nm): t_1 = 8.1 min, t_2 = 14.5 min.

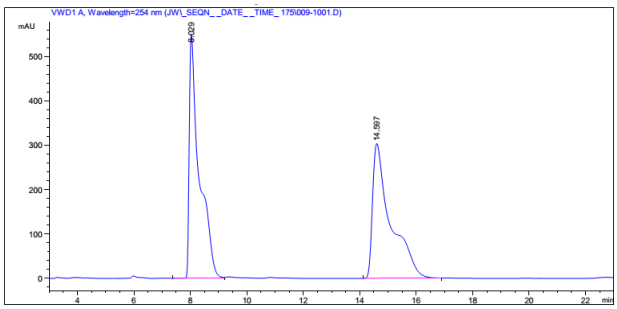

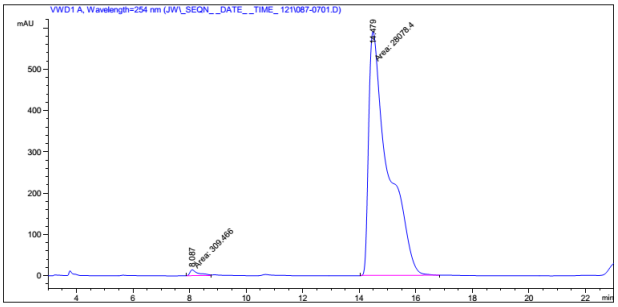

Peak #	RetTime [min]	Type	Width [min]	Area mAU *s	Height [mAU]	Area %
1	8.087	MM	0.3608	309.46597	14.29349	1.0901
2	14.479	MM	0.7926	2.80784e4	590.45758	98.9099

Totals : 2.83879e4 604.75107

(S)-5-bromo-2-methylindoline (2k)

Colorless oil. ^{1}H NMR (400 MHz, $CDCl_3$) δ 7.17 – 7.14 (m, 1H), 7.09 (dd, *J* = 8.2, 2.0 Hz, 1H), 6.45 (d, *J* = 8.2 Hz, 1H), 4.10 – 3.91 (m, 1H), 3.76 (br, 1H), 3.12 (dd, *J* = 15.7, 8.5 Hz, 1H), 2.62 (dd, *J* = 15.7, 7.6 Hz, 1H), 1.27 (d, *J* = 6.2 Hz, 3H). ^{13}C NMR (400 MHz, $CDCl_3$) δ 149.95, 131.23, 129.82, 127.65, 110.25, 109.90, 55.53, 37.51, 22.15. HPLC (Daicel Chiralpak OD-H, hexanes/i-PrOH = 97/3, Flow rate = 0.8 ml/min, UV = 254 nm): t_1 = 8.6 min, t_2 = 15.4 min.

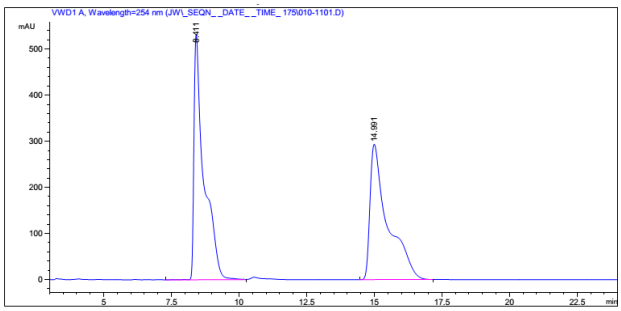

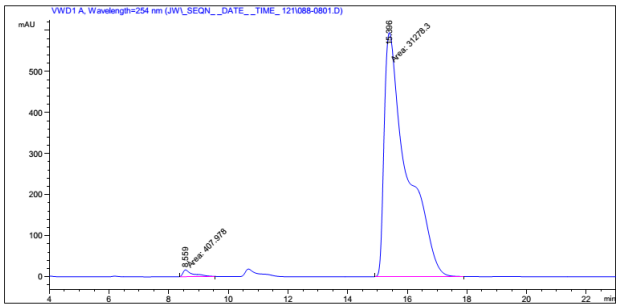

Peak #	RetTime [min]	Type	Width [min]	Area mAU *s	Height [mAU]	Area %
1	8.559	MM	0.4066	407.97836	16.72300	1.2876
2	15.396	MM	0.8760	3.12783e4	595.09326	98.7124
Totals :				3.16862e4	611.81626	

(S,S)-2,3-dimethylindoline (2l)

Colorless oil. ^{1}H NMR (400 MHz, $CDCl_3$) δ 7.12 – 6.98 (m, 2H), 6.73 (t, *J* = 7.4 Hz, 1H), 6.62 (d, *J* = 7.7 Hz, 1H), 4.01 – 3.89 (m, 1H), 3.64 (br, 1H), 3.33 – 3.22 (m, 1H), 1.18 (d, *J* = 7.2 Hz, 3H), 1.14 (d, *J* = 6.5 Hz, 3H). ^{13}C NMR (400 MHz, $CDCl_3$) δ 150.09, 134.24, 127.21, 123.75, 118.67, 109.28, 58.34, 39.43, 16.28, 13.60. HPLC (Daicel Chiralpak OD-H, hexanes/i-PrOH = 97/3, Flow rate = 0.8 ml/min, UV = 254 nm): t_1 = 31.1 min, t_2 = 36.0 min.

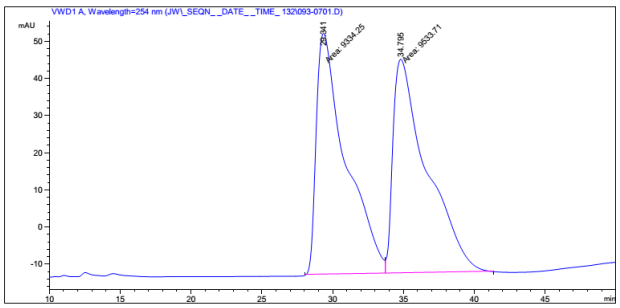

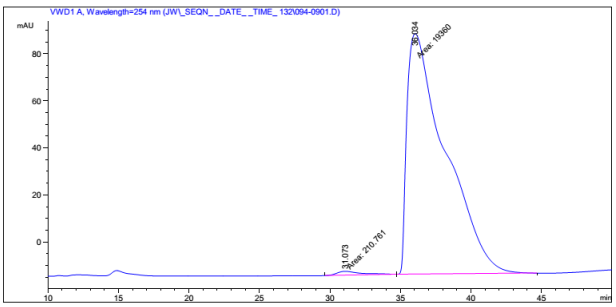

Peak #	RetTime [min]	Type	Width [min]	Area mAU *s	Height [mAU]	Area %
1	31.073	MM	1.4677	210.76115	1.69098	1.0769
2	36.034	MM	3.1541	1.93600e4	102.29957	98.9231
Totals :				1.95708e4	103.99055	

(S,S)-3-benzyl-2-methylindoline (2m)

Colorless oil. ^{1}H NMR (400 MHz, $CDCl_3$) δ 7.31 (t, *J* = 7.2 Hz, 2H), 7.27 – 7.22 (m, 1H), 7.20 (t, *J* = 6.8 Hz, 2H), 7.07 – 6.97 (m, 1H), 6.65 (d, *J* = 7.7 Hz, 1H), 6.59 (q, *J* = 7.5 Hz, 2H), 4.06 – 3.97 (m, 1H), 3.69 (br, 1H), 3.54 (dd, *J* = 15.9, 7.8 Hz, 1H), 2.93 (ddd, *J* = 22.8, 13.9, 8.1 Hz, 2H), 1.24 (d, *J* = 6.5 Hz, 3H).

^{13}C NMR (400 MHz, $CDCl_3$) δ 150.37, 140.32, 131.90, 129.13, 128.23, 127.42, 125.96, 124.82, 118.23, 109.36, 58.43, 45.94, 34.23, 16.46. HPLC (Daicel Chiralpak OD-H, hexanes/i-PrOH = 97/3, Flow rate = 0.8 ml/min, UV = 254 nm): t_1 = 14.6 min, t_2 = 21.3 min.

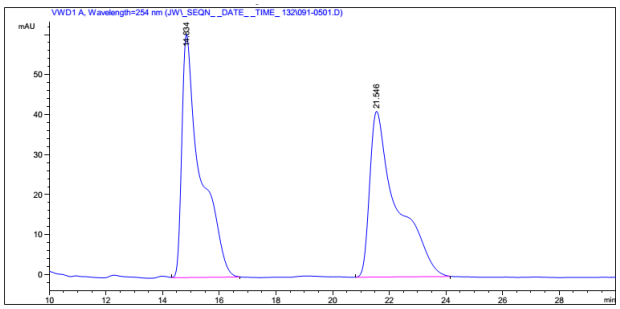

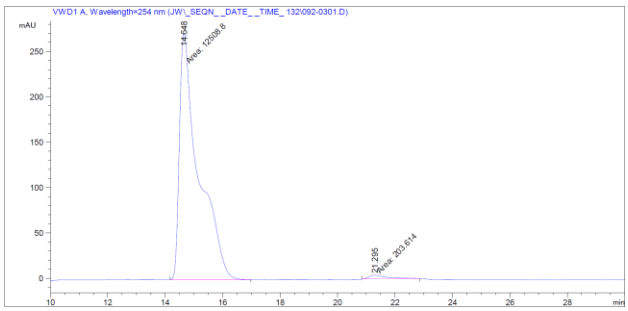

Peak #	RetTime [min]	Type	Width [min]	Area mAU *s	Height [mAU]	Area %
1	14.648	MM	0.7682	1.25088e4	271.38623	98.3983
2	21.295	MM	0.8002	203.61430	4.24083	1.6017
Totals :				1.27124e4	275.62706	

(S,S)-3-(cyclohexylmethyl)-2-methylindoline (2n)

Colorless oil. ^{1}H NMR (400 MHz, $CDCl_3$) δ 7.09 – 6.95 (m, 2H), 6.72 (td, *J* = 7.4, 0.9 Hz, 1H), 6.62 (d, *J* = 7.7 Hz, 1H), 3.94 (dq, *J* = 13.1, 6.5 Hz, 1H), 3.59 (br, 1H), 3.26 (dd, *J* = 15.1, 7.5 Hz, 1H), 1.94 – 1.82 (m, 1H), 1.82 – 1.61 (m, 4H), 1.61 – 1.48 (m, 1H), 1.50 – 1.32 (m, 2H), 1.34 – 1.15 (m, 3H), 1.13 (dd, *J* = 13.7, 4.8 Hz, 3H), 0.96 (ddd, *J* = 19.8, 9.7, 3.6 Hz, 2H). ^{13}C NMR (400 MHz, $CDCl_3$) δ 150.40, 132.91, 127.12, 124.16, 118.43, 109.41, 58.57, 41.55, 35.28, 33.59, 26.71, 26.35, 16.27. HPLC (Daicel Chiralpak OD-H, hexanes/i-PrOH = 97/3, Flow rate = 0.8 ml/min, UV = 254 nm): t_1 = 8.4 min, t_2 = 9.6 min.

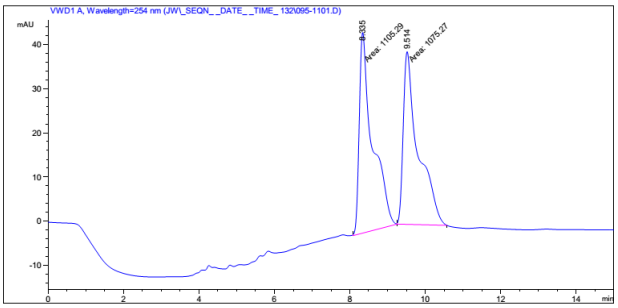

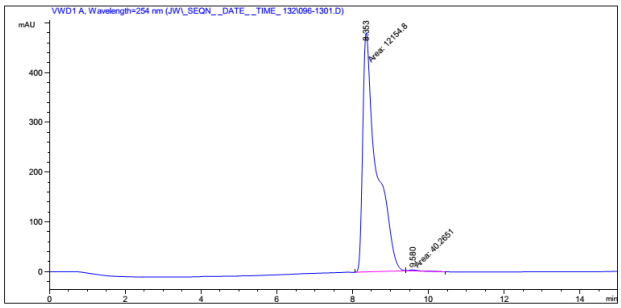

Peak #	RetTime [min]	Type	Width [min]	Area mAU *s	Height [mAU]	Area %
1	8.353	MM	0.4212	1.21548e4	480.94183	99.6698
2	9.580	MM	0.3124	40.26510	2.14804	0.3302
Totals :				1.21950e4	483.08987	

(S,S)-3-(furan-2-ylmethyl)-2-methylindoline (2o)

Colorless oil. ^{1}H NMR (400 MHz, $CDCl_3$) δ 7.38 – 7.36 (m, 1H), 7.03 (t, *J* = 7.6 Hz, 1H), 6.74 (d, *J* = 7.2 Hz, 1H), 6.69 – 6.61 (m, 2H), 6.32 (dd, *J* = 2.9, 2.0 Hz, 1H), 6.01 (d, *J* = 3.1 Hz, 1H), 4.10 – 3.99 (m, 1H), 3.68 (br, 1H), 3.60 (dd, *J* = 15.7, 7.8 Hz, 1H), 3.03 – 2.83 (m, 2H), 1.21 (d, *J* = 6.5 Hz, 3H). ^{13}C NMR (400 MHz, $CDCl_3$) δ 154.33, 150.27, 140.89, 131.49, 127.58, 124.48, 118.49, 110.22, 109.36, 106.32, 58.12, 43.55, 27.04, 16.30. HPLC (Daicel Chiralpak OD-H, hexanes/i-PrOH = 97/3, Flow rate = 0.8 ml/min, UV = 254 nm): t_1 = 17.1 min, t_2 = 21.8 min.

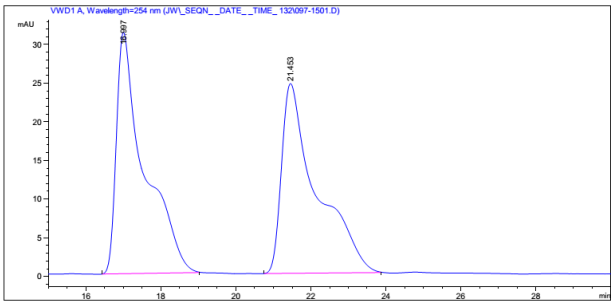

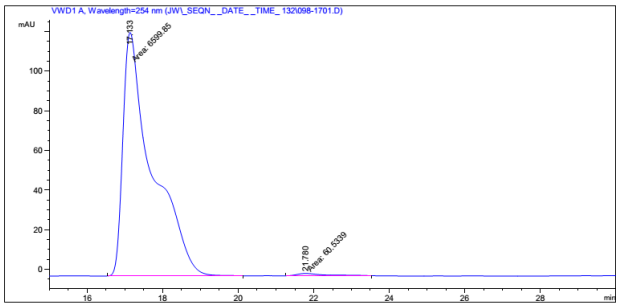

Peak #	RetTime [min]	Type	Width [min]	Area mAU *s	Height [mAU]	Area %
1	17.133	MM	0.8961	6599.84961	122.75162	99.0911
2	21.780	MM	0.8642	60.53390	1.16744	0.9089
Totals :				6660.38351	123.91906	

(S,S)-2,3,4,4a,9,9a-hexahydro-1H-carbazole (2p)

White solid. ^{1}H NMR (400 MHz, $CDCl_3$) δ 7.09 (d, *J* = 7.2 Hz, 1H), 7.03 (t, *J* = 7.6 Hz, 1H), 6.75 (t, *J* = 7.4 Hz, 1H), 6.68 (d, *J* = 7.7 Hz, 1H), 3.74 (dd, *J* = 11.7, 6.6 Hz, 1H), 3.65 (br, 1H), 3.11 (q, *J* = 6.6 Hz, 1H), 1.78 (dd, *J* = 12.1, 6.2 Hz, 2H), 1.70 – 1.63 (m, 1H), 1.57 (tt, *J* = 6.7, 4.4 Hz, 2H), 1.48 – 1.29 (m, 3H). ^{13}C NMR (400 MHz, $CDCl_3$) δ 150.73, 133.50, 126.96, 123.11, 118.75, 110.12, 59.61, 40.91, 29.17, 26.95, 22.50, 21.65. Chiral GC (Supelco γ-Dex225, 140°C, Flow rate = 1.0 ml/min): t_1 = 37.7 min, t_2 = 38.9 min.

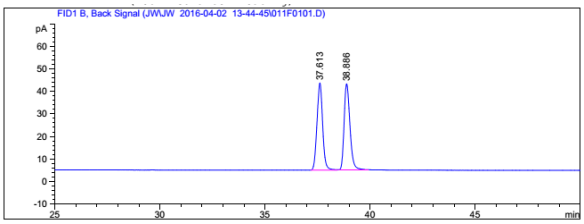

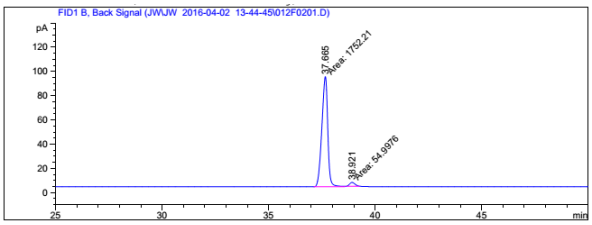

Peak #	RetTime [min]	Type	Width [min]	Area [pA*s]	Height [pA]	Area %
1	37.665	MM	0.3213	1752.20508	90.89358	96.95675
2	38.921	MM	0.2880	54.99761	3.18315	3.04325
Totals :				1807.20269	94.07672	

3.7 References

1. Rueping, M.; Koenigs, R. M.; Atodiresei, I. *Chem. Eur. J.* **2010,** *16*, 9350.
2. Allen, A. E.; MacMillan, D. W. C. *Chem. Sci.* **2012,** *3*, 633.
3. Meeuwissen, J.; Reek, J. N. H. *Nat. Chem.* **2010,** *2*, 615.
4. (a) Du, Z.; Shao, Z. *Chem. Soc. Rev.* **2013,** *42*, 1337. (b) Shao, Z.; Zhang, H. *Chem. Soc. Rev.* **2009,** *38*, 2745.
5. Xu, H.; Zuend, S. J.; Woll, M. G.; Tao, Y.; Jacobsen, E. N. *Science* **2010,** *327*, 986.
6. Wieland, J.; Breit, B. *Nat. Chem.* **2010**, *2*, 832.
7. Breit, B.; Seiche, W. *J. Am. Chem. Soc.***2003,** *125*, 6608.
8. Diab, L.; Šmejkal, T.; Geier, J.; Breit, B. *Angew. Chem. Int. Ed.* **2009,** *48*, 8022.
9. Šmejkal, T.; Breit, B. *Angew. Chem. Int. Ed.* **2008,** *47*, 311.
10. Gatzenmeier, T.; van Gemmeren, M.; Xie, Y.; Höfler, D.; Leutzsch, M.; List, B. *Science* **2016,** *351* , 949.
11. Doyle, A. G.; Jacobsen, E. N. *Chem. Rev.* **2007,** *107*, 5713.
12. Zhang, Z.; Schreiner, P. R. *Chem. Soc. Rev.* **2009,** *38*, 1187.
13. Takemoto, Y. *Chemical and Pharmaceutical Bulletin* **2010,** *58*, 593.
14. Taylor, M. S.; Jacobsen, E. N. *Angew. Chem. Int. Ed.* **2006,** *45*, 1520.
15. Brak, K.; Jacobsen, E. N. *Angew. Chem. Int. Ed.* **2013,** *52*, 534.
16. Du, Z.; Shao, Z. *Chem. Soc. Rev.* **2013,** *42*, 1337.
17. Shao, Z.; Zhang, H. *Chem. Soc. Rev.* **2009,** *38* , 2745.
18. Knowles, R. R.; Jacobsen, E. N. *PNAS* **2010,** *107*, 20678.
19. Zhao, Q.; Li, S.; Huang, K.; Wang, R.; Zhang, X. *Organic Letters* **2013,** *15*, 4014.
20. Akiyama, T. *Chem. Rev.* **2007,** *107*, 5744.
21. Akiyama, T.; Mori, K. *Chem. Rev.* **2015,** *115*, 9277.
22. Parmar, D.; Sugiono, E.; Raja, S.; Rueping, M. *Chem. Rev.* **2014,** *114*, 9047.
23. Rueping, M.; Nachtsheim, B. J.; Ieawsuwan, W.; Atodiresei, I. *Angew. Chem. Int. Ed.* **2011,** *50*, 6706.
24. James, T.; van Gemmeren, M.; List, B. *Chem. Rev.* **2015,** *115*, 9388.
25. Pihko, P. M. *Hydrogen Bonding in Organic Synthesis*. Wiley: **2009**.
26. Pihko, P. M. *Angew. Chem. Int. Ed.* **2004,** *43*, 2062.
27. Taylor, M. S.; Jacobsen, E. N. *Angew. Chem. Int. Ed.* **2006,** *45*, 1520.
28. Doyle, A. G.; Jacobsen, E. N. *Chem. Rev.* **2007,** *107*, 5713.
29. Phipps, R. J.; Hamilton, G. L.; Toste, F. D. *Nat. Chem.* **2012,** *4*, 603.
30. Mahlau, M.; List, B. *Angew. Chem. Int. Ed.* **2013,** *52*, 518.
31. Fattorusso, E.; Taglialatela-Scafati, O. *Modern Alkaloids: Structure, Isolation, Synthesis, and Biology*. Wiley: **2008**.
32. Kochanowska-Karamyan, A. J.; Hamann, M. T. *Chem. Rev.* **2010,** *110*, 4489.
33. Ishikura, M.; Abe, T.; Choshi, T.; Hibino, S. *Natural Product Reports* **2013,** *30*, 694.
34. Wang, D.-S.; Chen, Q.-A.; Lu, S.-M.; Zhou, Y.-G. *Chem. Rev.* **2012,** *112*, 2557.
35. Zhou, Y.-G.*Acc. Chem. Res.* **2007,** *40*, 1357.
36. Wang, D.-S.; Chen, Q.-A.; Li, W.; Yu, C.-B.; Zhou, Y.-G.; Zhang, X. *J. Am. Chem. Soc.***2010,** *132*, 8909.
37. Duan, Y.; Li, L.; Chen, M.-W.; Yu, C.-B.; Fan, H.-J.; Zhou, Y.-G., *J. Am. Chem. Soc.* **2014,**

136, 7688.

38. Zhao, Q.; Li, S.; Huang, K.; Wang, R.; Zhang, X. *Organic Letters* **2013,** *15*, 4014.
39. Zhao, Q.; Wen, J.; Tan, R.; Huang, K.; Metola, P.; Wang, R.; Anslyn, E. V.; Zhang, X. *Angew. Chem. Int. Ed.* **2014,** *53*, 8467.
40. Kelly, T. R.; Kim, M. H. *J. Am. Chem. Soc.***1994,** *116*, 7072.
41. All pka's are data measured in water, for qualitative analysis.
42. ^{31}P NMR study of ligand shows a significant change in chemical shift (from -25.1 and -17.9 ppm to +1.9 and +7.6 ppm). This change suggests protonation on phosphorus.
43. 1.0 eq. of HCl gives 95% conversion and 5.0 eq. HCl give 98% conversion, 97% ee was observed for both cases.
44. Wen, J.; Tan, R.; Liu, S.; Zhao, Q.; Zhang, X. *Chem. Sci.* **2016**, *7*, 3047.
45. Guillaneux, D.; Zhao, S.-H.; Samuel, O.; Rainford, D.; Kagan, H. B. *J. Am. Chem. Soc.***1994,** *116*, 9430.
46. Kina, A.; Iwamura, H.; Hayashi, T. *J. Am. Chem. Soc.* **2006,** *128*, 3904.
47. Ford, D.; Lehnherr, D.; Kennedy, C. R.; Jacobsen, E. N. *J. Am. Chem. Soc.* **2016,** *138*, 7860.